

**Dottorato di Ricerca in Bioingegneria - XIX Ciclo**

Sede amministrativa: Università degli Studi di Bologna

---

Sede consorziata: Università degli Studi di Bologna

Dipartimento di Elettronica, Informatica e Sistemistica

ING/IND34

**Primary stability in cementless total hip replacement:  
measurement techniques and aided-surgery**

*Stabilità primaria di protesi d'anca non cementata:  
tecniche di valutazione ed assistenza in sala operatoria*

Tesi di Dottorato dell'Ing. Elena Varini

Supervisore:

Controrelatore:

Chiar.mo Prof. Luca Cristofolini  
Cappozzo

Chiar.mo Prof. Aurelio

Co-Supervisore:

Chiar.mo Prof. Angelo Cappello

---

Bologna, Marzo 2007



# CONTENTS

<b>SUMMARY</b> .....	<b>1</b>
<b>INTRODUCTION</b> .....	<b>5</b>
<b>CHAPTER 1: BONE, HIP JOINT AND TOTAL HIP ARTHROPLASTY</b> .....	<b>9</b>
<b>1.1 Bone and Bones</b> .....	<b>11</b>
1.1.1 The human skeleton. ....	11
1.1.2 Bone morphology and macro structure. ....	12
1.1.3 Micro-structure of bone. ....	14
1.1.4 Bone cells. ....	16
1.1.5 Bone turnover and development .....	18
<b>1.2 Hip Joint</b> .....	<b>22</b>
<b>1.3 Total Hip Arthroplasty (THA)</b> .....	<b>23</b>
1.3.1 Overview of the THA procedure .....	23
1.3.2 Mechanical consideration on the effect of THA .....	25
1.3.3 State of the art in THA .....	27
<b>1.4 Primary stability of uncemented hip stems</b> .....	<b>28</b>
1.4.1 The uncemented hip prosthesis .....	28
1.4.2 Bone-cement interface: considerations .....	31
1.4.3 Evaluation of cementless hip implant stability: state of the art. ....	32
<b>References</b> .....	<b>34</b>
<b>CHAPTER 2: INTRA-OPERATIVE EVALUATION OF PRIMARY STABILITY OF CEMENTLESS HIP STEMS: A DEVICE BASED ON THE DIRECT MICROMOTION ASSESSMENT</b> .....	<b>39</b>
<b>2.1 Introduction</b> .....	<b>41</b>
<b>2.2 Materials and Methods</b> .....	<b>43</b>
2.2.1 Feasibility study. ....	43
2.2.2 Description of the final device .....	45
2.2.3 Operation of the device .....	47
2.2.4 Validation. ....	48
2.2.5 Calibration .....	48
<b>2.3 Results</b> .....	<b>50</b>
2.3.1 Noise and drift of the final device .....	50
2.3.2 Stiffness of the final device. ....	50
2.3.3 Repeatability .....	51
2.3.4 Calibration. ....	51

<b>2.4 Discussion</b> .....	<b>54</b>
<b>References</b> .....	<b>58</b>

<b>CHAPTER 3: CAN THE RASP BE USED TO PREDICT INTRA-OPERATIVELY THE PRIMARY STABILITY THAT CAN BE ACHIEVED BY PRESS-FITTING THE STEM IN CEMENTLESS HIP ARTHROPLASTY? .....</b>	<b>61</b>
<b>3.1 Introduction</b> .....	<b>63</b>
<b>3.2 Materials and Methods</b> .....	<b>64</b>
3.2.1 The intra-operative device. ....	64
3.2.2 In vitro validation. ....	65
3.2.3 Preliminary in vivo verification. ....	67
3.2.4 Data processing and statistical analysis .....	67
<b>3.3 Results</b> .....	<b>68</b>
<b>3.4 Discussion</b> .....	<b>70</b>
<b>References</b> .....	<b>73</b>

<b>CHAPTER 4: INTRA-OPERATIVE EVALUATION OF CEMENTLESS HIP IMPLANT STABILITY: A PROTOTYPE DEVICE BASED ON VIBRATION ANALYSIS</b> .....	<b>75</b>
<b>4.1 Introduction</b> .....	<b>77</b>
<b>4.2 Materials and Methods</b> .....	<b>77</b>
4.2.1 Description of the prototype device. ....	79
4.2.2 Setting the software parameters. ....	83
4.2.3 In vitro validation. ....	85
<b>4.3 Results</b> .....	<b>86</b>
4.3.1 Parameter setting .....	86
4.3.2 In vitro validation .....	87
<b>4.4 Discussion</b> .....	<b>89</b>
<b>References</b> .....	<b>93</b>

<b>CHAPTER 5: IN VITRO MEASUREMENT OF THE FREQUENCY RESPONSE FUNCTION OF STEM-BONE SYSTEMS FOR THE EVALUATION OF IMPLANT STABILITY</b> .....	<b>97</b>
<b>5.1 Introduction</b> .....	<b>99</b>
<b>5.2 Simplified model of the system</b> .....	<b>100</b>
<b>5.3 In vitro testing</b> .....	<b>102</b>
5.3.1 The measurement device. ....	102
5.3.2 In vitro testing protocol. ....	103
<b>5.3 Results</b> .....	<b>104</b>
<b>5.4 Discussion</b> .....	<b>106</b>

<b>References</b> .....	<b>108</b>
-------------------------	------------

<b>CHAPTER 6: PROPOSAL FOR AN IN VITRO METHOD FOR ASSESSING IMPLANT-BONE MICROMOTIONS IN RESURFACING IMPLANTS UNDER DIFFERENT LOADING CONDITIONS</b> .....	<b>111</b>
--	------------

<b>6.1 Introduction</b> .....	<b>113</b>
-------------------------------	------------

<b>6.2 Materials and Methods</b> .....	<b>114</b>
--	------------

6.2.1 Micromotion measurements .....	114
--------------------------------------	-----

6.2.2 Mechanical in vitro testing .....	116
---	-----

6.2.3 Specimens .....	117
-----------------------	-----

6.2.4 Statistics .....	118
------------------------	-----

<b>6.3 Results</b> .....	<b>119</b>
--------------------------	------------

6.3.1 Micromotion during non destructive testing .....	119
--	-----

6.3.2 Micromotion during destructive testing .....	120
--	-----

<b>6.4 Discussion</b> .....	<b>121</b>
-----------------------------	------------

<b>References</b> .....	<b>123</b>
-------------------------	------------

<b>CONCLUSION</b> .....	<b>127</b>
-------------------------	------------

<b>Acknowledgements</b> .....	<b>129</b>
-------------------------------	------------

<b>APPENDIX A: STEM DAMAGE DURING IMPLANTATION OF MODULAR HIP PROSTHESIS</b> .....	<b>131</b>
--	------------

<b>APPENDIX B: ON THE BIOMECHANICAL STABILITY OF STRAIGHT CONICAL HIP STEM</b> .....	<b>141</b>
--	------------

<b>APPENDIX C: PREDICTING THE SUBJECT-SPECIFIC PRIMARY STABILITY OF CEMENTLESS IMPLANTS DURING PRE-OPERATIVE PLANNING: PRELIMINARY VALIDATION OF SUBJECT-SPECIFIC FINITE ELEMENT MODELS</b> .....	<b>151</b>
---	------------



## Summary

Primary stability of stems in cementless total hip replacements is recognized to play a critical role for long-term survival and thus for the success of the overall surgical procedure. In Literature, several studies addressed this important issue. Different approaches have been explored aiming to evaluate the extent of stability achieved during surgery. Some of these are *in-vitro* protocols while other tools are conceived for the post-operative assessment of prosthesis migration relative to the host bone. *In vitro* protocols reported in the literature are not exportable to the operating room. Anyway most of them show a good overall accuracy. The RSA, EBRA and the radiographic analysis are currently used to check the healing process of the implanted femur at different follow-ups, evaluating implant migration, occurrence of bone resorption or osteolysis at the interface. These methods are important for follow up and clinical study but do not assist the surgeon during implantation.

At the time I started my Ph.D Study in Bioengineering, only one study had been undertaken to measure stability intra-operatively. No follow-up was presented to describe further results obtained with that device.

In this scenario, it was believed that an instrument that could measure intra-operatively the stability achieved by an implanted stem would consistently improve the rate of success. This instrument should be accurate and should give to the surgeon during implantation a quick answer concerning the stability of the implanted stem. With this aim, an intra-operative device was designed, developed and validated. The device is meant to help the surgeon to decide how much to press-fit the implant. It is essentially made of a torsional load cell, able to measure the extent of torque applied by the surgeon to test primary stability, an angular sensor that measure the relative angular displacement between stem and femur, a rigid connector that enable connecting the device to the stem, and all the electronics for signals conditioning. The device was successfully validated *in-vitro*, showing a good overall accuracy in discriminating stable from unstable implants. Repeatability tests showed that the device was reliable. A calibration procedure was then performed in order to convert the angular readout into a linear displacement measurement, which is an information clinically relevant and simple to read in real-time by the surgeon.

The second study reported in my thesis, concerns the evaluation of the possibility to have predictive information regarding the primary stability of a cementless stem, by measuring the micromotion of the last rasp used by the surgeon to prepare the femoral canal. This information would be really useful to the surgeon, who could check prior to the implantation process if the planned stem size can achieve a sufficient degree of primary stability, under optimal press fitting conditions. An intra-operative tool was developed to this aim. It was derived from a previously validated device, which was adapted for the specific purpose. The device is able to measure the relative micromotion between the femur and the rasp, when a torsional load is applied. An in-vitro protocol was developed and validated on both composite and cadaveric specimens. High correlation was observed between one of the parameters extracted from the acquisitions made on the rasp and the stability of the corresponding stem, when optimally press-fitted by the surgeon. After tuning in-vitro the protocol as in a closed loop, verification was made on two hip patients, confirming the results obtained in-vitro and highlighting the independence of the rasp indicator from the bone quality, anatomy and preserving conditions of the tested specimens, and from the sharpening of the rasp blades.

The third study is related to an approach that have been recently explored in the orthopaedic community, but that was already in use in other scientific fields. It is based on the vibration analysis technique. This method has been successfully used to investigate the mechanical properties of the bone and its application to evaluate the extent of fixation of dental implants has been explored, even if its validity in this field is still under discussion. Several studies have been published recently on the stability assessment of hip implants by vibration analysis.

The aim of the reported study was to develop and validate a prototype device based on the vibration analysis technique to measure intra-operatively the extent of implant stability. The expected advantages of a vibration-based device are easier clinical use, smaller dimensions and minor overall cost with respect to other devices based on direct micromotion measurement. The prototype developed consists of a piezoelectric exciter connected to the stem and an accelerometer attached to the femur. Preliminary tests were performed on four composite femurs implanted with a conventional stem. The results showed that the input signal was repeatable and the output could be recorded accurately.

The fourth study concerns the application of the device based on the vibration analysis technique to several cases, considering both composite and cadaveric specimens. Different degrees of bone quality were tested, as well as different femur anatomies and several levels of

press-fitting were considered. The aim of the study was to verify if it is possible to discriminate between stable and quasi-stable implants, because this is the most challenging detection for the surgeon in the operation room. Moreover, it was possible to validate the measurement protocol by comparing the results of the acquisitions made with the vibration-based tool to two reference measurements made by means of a validated technique, and a validated device. The results highlighted that the most sensitive parameter to stability is the shift in resonance frequency of the stem-bone system, showing high correlation with residual micromotion on all the tested specimens. Thus, it seems possible to discriminate between many levels of stability, from the grossly loosened implant, through the quasi-stable implants, to the definitely stable one.

Finally, an additional study was performed on a different type of hip prosthesis, which has recently gained great interest thus becoming fairly popular in some countries in the last few years: the hip resurfacing prosthesis.

The study was motivated by the following rationale: although bone-prosthesis micromotion is known to influence the stability of total hip replacement, its effect on the outcome of resurfacing implants has not been investigated *in-vitro* yet, but only clinically. Thus the work was aimed at verifying if it was possible to apply to the resurfacing prosthesis one of the intra-operative devices just validated for the measurement of the micromotion in the resurfacing implants. To do that, a preliminary study was performed in order to evaluate the extent of migration and the typical elastic movement for an epiphyseal prosthesis. An *in-vitro* procedure was developed to measure micromotions of resurfacing implants. This included a set of *in-vitro* loading scenarios that covers the range of directions covered by hip resultant forces in the most typical motor-tasks. The applicability of the protocol was assessed on two different commercial designs and on different head sizes. The repeatability and reproducibility were excellent (comparable to the best previously published protocols for standard cemented hip stems). Results showed that the procedure is accurate enough to detect micromotions of the order of few microns. The protocol proposed was thus completely validated. The results of the study demonstrated that the application of an intra-operative device to the resurfacing implants is not necessary, as the typical micromovement associated to this type of prosthesis could be considered negligible and thus not critical for the stabilization process.

Concluding, four intra-operative tools have been developed and fully validated during these three years of research activity. The use in the clinical setting was tested for one of the devices,

which could be used right now by the surgeon to evaluate the degree of stability achieved through the press-fitting procedure. The tool adapted to be used on the rasp was a good predictor of the stability of the stem. Thus it could be useful for the surgeon while checking if the pre-operative planning was correct. The device based on the vibration technique showed great accuracy, small dimensions, and thus has a great potential to become an instrument appreciated by the surgeon. It still need a clinical evaluation, and must be industrialized as well. The in-vitro tool worked very well, and can be applied for assessing resurfacing implants pre-clinically.

## ***Introduction***

Total hip replacement is a very successful procedure to solve the effects of degenerative pathologies of the human hip joint. Young, active patients are frequently treated with cementless prostheses. These implants are mechanically stabilised in the host bone at surgery time through a press-fitting procedure. The primary mechanical stability achieved by these implants is critical for the long-term outcomes of the operation.

Surgeon's experience in planning the kind and the size of stem to be implanted is fundamental for achieving good fixation. But, even assuming a theoretically perfect choice, there is still the practical problem of correct positioning of the stem in the femur during surgery. In particular the level of press-fitting during stem insertion is critical. If the surgeon does not press-fit enough the stem, the stem is not stable, which leads to aseptic loosening of the implant (fibrous tissue layer formation). If the press-fit is excessive, femoral intra-operative fractures may occur. Intra-operative fractures are not a negligible problem, and reported rates of periprosthetic fractures can be as high as 4% - 28%. Surgeons are guided only by their experience in finding the optimal compromise of press-fitting.

Common methods to measure the primary stability of cementless prostheses are conceived for *in vitro* tests. These studies have shown that the main values of micromovement at the stem/femur interface are found when the torsional moment around the femur axis prevails (15–29Nm). A limit value of interface micromotion may be inferred from the literature and the concept of stability threshold introduced: *an implant is stable if, under a torque of 15–20Nm, the micromotion is smaller than 100 micron* (see Chapter 1).

The direct intra-operative measurement of the stem-bone micromotion under a torsional load and its comparison with a stability threshold is a possible approach to solve the problem of stability assessment and assist the surgeon in achieving the optimal compromise. A device based on the direct assessment of implant stability was developed first by Harris *et al.* in 1991. In that study the accuracy and the repeatability of the method were not clearly assessed. To the authors' knowledge no follow-up was presented to describe further results obtained with that device (see Chapter 2).

Recently, a new approach has been explored for assessing stem stability intra-operatively. It is based on the study of the frequency pattern of the implant-bone system, by using vibration analysis. This method has been successfully used to investigate the mechanical properties of

the bone and its application to evaluate the extent of fixation of dental implants has been explored, even if its validity in this field is still under discussion (see Chapter 4).

*In vitro* protocols reported in the literature are not exportable to the operating room. Anyway most of them show a good overall accuracy. The method of Harris *et al.* can be used intra-operatively, but its accuracy in measuring the displacements is not comparable to the *in vitro* methods. Moreover no existing system makes a real-time comparison between the actual readout and a stability threshold. The vibration analysis technique has been introduced into the orthopaedic field, it seems to be sensitive enough to detect stability, but its reliability must be demonstrated. An instrument that could measure intra-operatively the stability achieved by an implanted stem would consistently improve the rate of success. This instrument should be accurate and should give to the surgeon during implantation a quick answer concerning the stability.

The research work described in the present thesis was aimed at investigating on the initial stabilization process of cementless prosthesis and at the development of intra-operative techniques to help the surgeon evaluating the extent of stability achieved through the press-fitting procedure.

The work was carried out at the 'Laboratorio di Tecnologia Medica' (Rizzoli Orthopaedic Institutes, Bologna, Italy) in collaboration with the 'Laboratorio di Bioingegneria' of the University of Bologna. Some of this work formed part of a project financed by the European Commission: ISAC project (Intra-operative Stability Assessment Console) IST-1999-20226.

To this purpose, the studies performed during the three years Ph.D Course in Bioengineering, were focused to develop different solutions to the problem of intra-operative stem stability assessment.

The first approach was focused on the design, development and validation of a device based on the direct measurement of the stability of the stem achieved with the press-fitting performed by the surgeon. Basically, the device proposed measures the torque applied by the surgeon to an implanted stem while estimating the shear displacement at the stem/femur interface, by using two separate transducers. The data are processed and compared with a pre-set stability threshold, providing the surgeon with real-time clinical relevant information concerning stability (see Chapter 2).

With the same assumptions, the second study was aimed at studying whether it was possible to predict the prosthesis stability based on an assessment made prior to the stem implantation. This kind of real-time information would be very helpful for the surgeon while operating. In fact, especially for unclear cases, the pre-operative planning may result unsuitable. In these cases, intra-operative complications may occur, generating firstly higher risks for the patient, and secondly a possible increase in terms of costs and time for surgery. To avoid that sort of problems, an intra-operative tool was developed to be applied on the rasp. The active purpose of the study was to determine a parameter relative to the rasp stability that could be a good indicator of the stability of the stem, when optimally press-fitted by the surgeon. An *in-vitro* protocol was validated and a preliminary verification was performed by replicating the protocol on two hip patients (see Chapter 3).

The third part of the thesis concerns the study of the possibility to address the problem of stem stability assessment by means of the vibration analysis technique. This different approach should guarantee an intra-operative device featuring smaller dimensions, lower cost, and an overall procedure more simple and fast. The first part of the investigation was aimed at the understanding of the principles of the stem-bone system and the exploration of its vibration modes. A measurement device was developed and a preliminary *in-vitro* trial was performed to validate the protocol (see Chapter 4). A more complete validation was performed *in-vitro* on both composite and cadaveric specimens. The device was tested on specimens characterized by different bone quality and anatomy and by considering different levels of press-fitting. The device was validated by comparing its output to the one obtained through a validated procedure applied on the same specimen with the same degree of press-fitting (see Chapter 5).

Finally, an additional study is reported on a proposal for an *in-vitro* method for assessing implant-bone micromotions in resurfacing implants under different loading conditions. This method should include a set of *in-vitro* loading scenarios that covers the range of directions covered by hip resultant forces in the most typical motor-tasks. Gap-opening and shear-sliding micromotions were measured in the locations where they reach the maximum value by means of high-precision LVDT. The applicability of the protocol was assessed on two different commercial designs and on different head sizes (see Chapter 6).



# **CHAPTER 1**

## **BONE, HIP JOINT AND TOTAL HIP ARTHROPLASTY**





## 1.1 Bone and Bones

### 1.1.1 The human skeleton

The skeletal tissues, cartilage and bone, are a highly specialized type of connective tissue which have the primary role of supporting structure [1, 2]. The main constituent of the skeleton is bone (Fig. 1.1), which differs from other connective tissues (i.e. cartilage, ligaments and tendons) for the high mineralization of the extra cellular matrix. Thus, the main features of this type of human tissue are rigidity and hardness that enable the skeleton to maintain the shape of the body, to transmit muscular forces from one part of the body to another during movement, to protect the soft tissues of the cranial, thoracic and pelvic cavities, to supply the framework for the bone marrow.

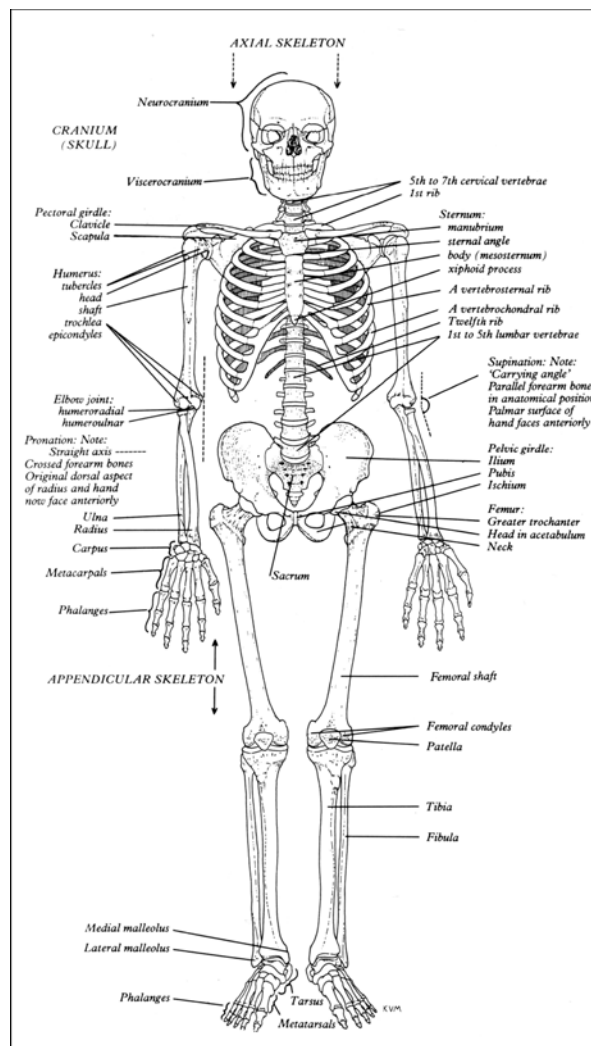


Fig. 1.1 A human adult male skeleton: anterior view

### 1.1.2 Bone morphology and macro structure

By considering their morphology, bones can be grouped into different families [2]:

- Long bones: e.g. femur, tibia, humerus
- Short bones: e.g. carpus, tarsus
- Flat bones: e.g. cranial vault, scapulae
- Irregular bones: any element not easily assigned to the foreign groups

As for the interest of the present thesis on the coxo-femoral articulation, the morphology of the femur is described. As all long bones, the femur consists of a cylindrical shaft (or diaphysis) and two wider and roughly spherical ends, the epiphyses. Conical regions, called metaphases, connect the diaphysis with the epiphysis (Fig.1.2). Most bones have the ends wider than their central part, with the joints covered by articular cartilage.

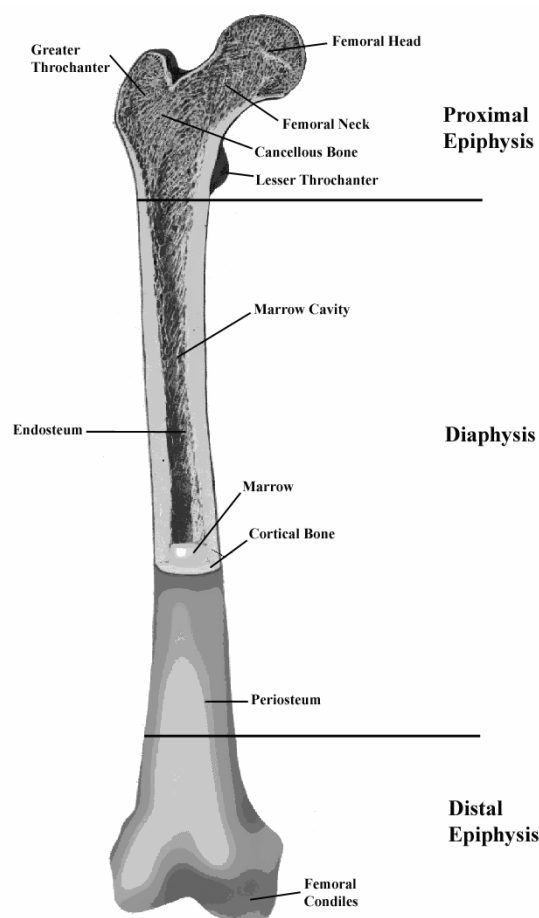


*Fig. 1.2 Schematic representation of a human femur*

All bones are composed by two basic structures [1]:

- Cortical bone (Compact bone)
- Trabecular bone (Cancellous bone)

Cortical bone is a dense, solid mass, with the exception of microscopic channels. Approximately 80% of the skeletal mass in the adult skeleton is cortical bone. It forms the outer wall of all bones, being largely responsible for the supportive and protective function of the skeleton. The remaining 20% of the bone mass is cancellous bone, a lattice of plates, rods and arches named trabeculae (Fig. 1.3)

The diaphysis is composed mainly of cortical bone. The epiphysis and metaphysis contain mostly cancellous bone, with a thin outer shell of cortical bone. During growing, the epiphysis is separated from the metaphysis by a plate of hyaline cartilage, known as the epiphyseal plate or growth plate. The growth plate and the adjacent cancellous bone of the metaphysis constitute a region where cancellous bone production and elongation of the cortex occurs. In the adult, the cartilaginous growth plate is replaced by cancellous bone, which causes the epiphysis to become fused to the metaphysis.

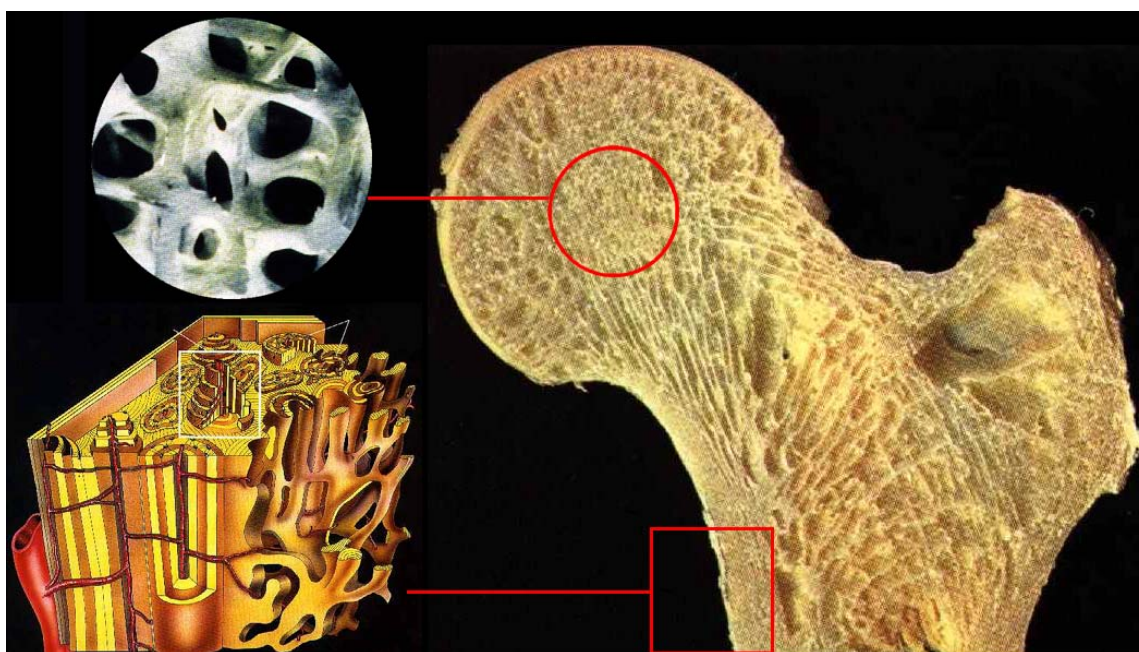


*Fig. 1.3 Schematic showing trabecular and cancellous bone, respectively*

Bone is restricted to appositional growth because of the non expandable nature of mineralized bone tissue; thus, all bone activities occur at bone surfaces. Bone tissue has two major surfaces:

periosteal and endosteal (fig. 1.2). The periosteum covers the outer bone surface, being composed of a sheet of fibrous connective tissue and an inner layer of undifferentiated cells. It has the potential to form bone during growth and fracture healing. The periosteum is absent in areas where tendons or ligaments insert in bone, on bone ends covered with articular cartilage, in subscapular areas and in the neck of the femur.

The endosteum is a thin cellular layer which covers the marrow cavity of the diaphysis and the cavities of cortical and cancellous bone. It is a thin layer of bone surface cells (osteoclasts, osteoblasts, and bone lining cells).

Bone consists of 65% mineral, 35% organic matrix, cells and water. The bone mineral, in form of small crystals, is placed between collagen fibres. The mineral is largely impure hydroxyapatite,  $\text{Ca}_6(\text{PO}_4)_6(\text{OH})_2$ , containing carbonate, citrate, fluoride and strontium. The organic matrix consists of 90% collagen and about 10% non collagenous proteins. From a mechanical point of view, the bone matrix is comparable to a composite material: the organic matrix is responsible to give toughness to the bone, while the inorganic matrix has the function to stiffen and strengthen the bone [1].

### **1.1.3 Micro-structure of bone**

Mammalian cortical and cancellous bone is of two main types: woven or lamellar. In the developing embryo, the bone tissue is of the woven type. It is a matrix of interwoven coarse collagen fibres, containing osteocytes distributed approximately at random. Woven bone can be seen as a provisional material, eventually resorbed and replaced by lamellar bone.

Adult bone is composed of lamellar bone, which is built up of 3- to 7- $\mu\text{m}$ -thick unit layers (lamellae) which contain collagen fibres that run parallel to each other [1]. In histological preparations, under polarized light, the lamellae appear as alternating light and dark levels, which is the result of differing orientations of collagen fibres within adjacent lamellae (fig. 1.4).

The main structural unit of cortical bone is given by the osteon or the Haversian system (Fig. 1.4). A typical osteon is a cylinder about 200  $\mu\text{m}$  in diameter, consisting of a central canal (Haversian canal) surrounded by about 20-30 concentric lamellae. The circumference of the shaft of long bones is surrounded by several layers of lamellae, immediately underneath the periosteum and on the internal surface adjacent to the endosteum. These lamellae are called

circumferential lamellae. In the gaps between Haversian systems can be found interstitial lamellae, as angular fragments of previous concentric and circumferential lamellae. Within the Haversian canals run blood vessels, lymphatics, nerves.

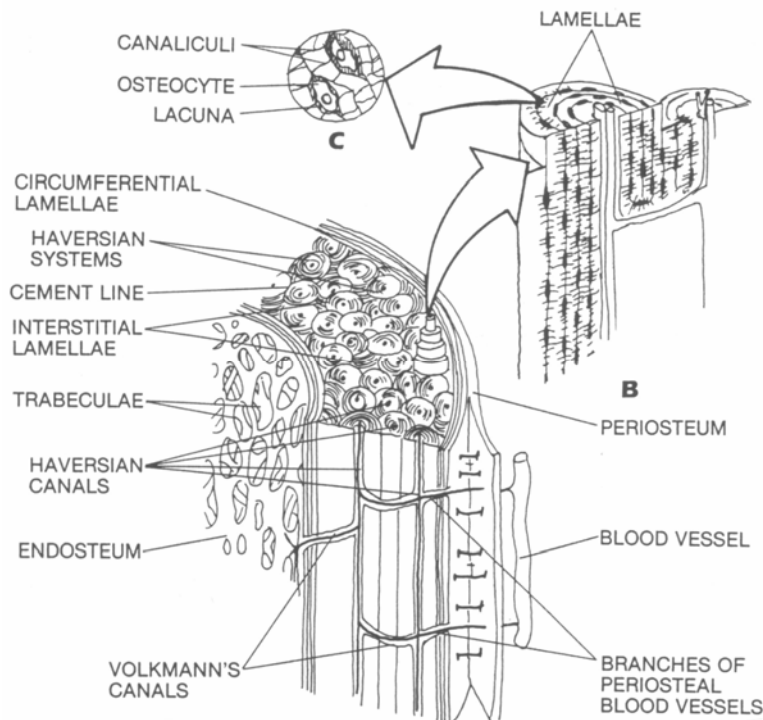


*Fig. 1.4 The fine structure of bone is illustrated schematically in a section of the shaft of a long bone depicted without inner marrow.*

The Haversian canals are interconnected by transverse canals, also called the Volkmann canals, which also allow the communication with the periosteum and bone marrow. The outer border of each osteon is surrounded by a cement line, which is a 1- to 2- $\mu\text{m}$ -thick layer of mineralized matrix, deficient in collagen fibres. Throughout the bone, small cavities (lacunae) containing entrapped bone cells (osteocytes) are found. Microscopic tubular canals (canaliculi) connect the lacunae to each other and to the Haversian canal.

The structural unit of trabecular bone is the trabecular packet, a hemiosteon. Ideally, it is shaped like a shallow crescent with a radius of 600  $\mu\text{m}$ , 50  $\mu\text{m}$  thick and 1 mm long. As with cortical bone, cement lines hold the trabecular packets together.

### 1.1.4 Bone cells

Bone cells are usually grouped as follows [1,3,4]:

- osteoprogenitor cells
- osteoclasts
- osteoblasts
- osteocytes
- bone-lining cells

#### Osteoprogenitor cells:

These kinds of cells have the capacity of mitosis and further differentiation and specialization into mature bone cell. They could be divided in two sub-groups: one type gives rise to bone forming osteoblasts, the other type gives rise to bone resorbing osteoclasts. Both types are commonly found near bone surface [3].

#### Osteoclasts:

Osteoclasts are bone-resorbing cells, which contain one to more than 50 nuclei and range in diameter from 20 to over 100  $\mu\text{m}$ . Their role is to resorb bone, by solubilizing both the mineral and the organic component of the matrix. The signals for the selection of sites to be resorbed are unknown. Biphosphonates, calcitonin and estrogen are commonly used to inhibit resorption. These are believed to act by inhibiting the formation and activity of osteoclasts and promoting osteoclasts apoptosis.

#### Osteoblasts:

Osteoblasts are bone-forming cells that synthesize and secrete unmineralized bone matrix (the osteoid). They seem to participate in the calcification and resorption of bone and to regulate the flux of calcium and phosphate in and out of bone. Osteoblasts occur as a layer of contiguous cells which in their active state are cuboidal (15 to 30  $\mu\text{m}$  thick). Bone formation occurs in two stages: matrix formation followed by mineralization, denoted by deposition of crystals of hydroxyapatite.

Their life cycle can be summarized as follows [1,3,4]:

- the birth from a progenitor cell

- the differentiation from stem cells to osteoblasts and participation in elaborating matrix and calcifying units
- either returning to the pre-osteoblast pool, transform into bone-lining cell and burial as osteocytes, or death.

The development of osteoblasts and osteoclasts are inseparably linked on a molecular basis. Both are derived from precursor cells originating in bone marrow (with osteoblasts from multipotent mesenchymal stem cells, while osteoclasts from hemaiopoietic cells of the monocyte/macrophage lineage), and osteoblast differentiation is a prerequisite for osteoclast development [1].

### Osteocytes

During bone formation, some osteoblasts are left behind in the newly formed osteoid as osteocytes when the bone formation moves on. The osteoblasts embedded in lacunae differentiate into osteocytes. In mature bone osteocytes are the most abundant cell type. They are found to be about ten times more than osteoblasts in normal human bone. Mature osteocytes possess a cell body that has the shape of an ellipsoid, with the longest axis (25  $\mu\text{m}$ ) parallel to the surrounding bone lamella. The osteocytes are thought to be the cells best placed to sense the magnitude and distribution of strains. They are thought both to respond to changes in mechanical strain and to disseminate fluid flow to transduce information to surface cells, via the canalicular processes and the communicating gap junctions. Osteocytes play a key role in homeostatic, morphogenetic and restructuring process of bone mass that constitute the regulation of mineral and architecture [1].

### Bone-lining cells

Bone-lining cells are believed to be derived from osteoblasts that have become inactive, or osteoblast precursors that have ceased activity or differentiated and flattened out on bone surfaces. Bone-lining cells occupy the majority of the adult bone surface. They serve as an ion barrier separating fluids percolating through the osteocyte and lacunar canalicular system from the interstitial fluids. Bone-lining cells are also involved in osteoclastic bone resorption, by digesting the surface osteoid and subsequently allow the osteoclast access to mineralized tissue. Furthermore, it has been postulated that the 3D-networks of bone-lining cells and osteocytes are

able to sense the shape of the bone, together with its reaction to stress and strain, and to transmit these sensations as signals to the bone surface for new bone formation/resorption.

### **1.1.5 Bone turnover and development**

In normal conditions, bone is characterized by a balanced coexistence of resorptive and appositional process.

#### Bone resorption

The actual mechanism for the activation of osteoclast bone resorption is still unclear. Where osteoclasts come in contact with the surface of bone, these begin to erode the bone forming cavities (Howship's lacunae) in cancellous bone, and forming cutting cones or resorption cavities in cortical bone. The resorption process occurs in two steps, which occur essentially simultaneously: dissolution of mineral and enzymic digestion of organic macromolecules.

#### Bone formation

Bone formation occurs in two phases: matrix synthesis followed by extra cellular mineralization. The building of bone as a functional organ is an important process, as bone constantly enlarges, renews and develops itself in time. In the same time it adapts itself to support protection, mechanical needs and numerous metabolic and hematopoietic activities [2,5,6]. The formation of a functionally competent bone is the result of a combination of several processes:

- intramembraneous ossification
- endochondral ossification
- growth
- modeling into a desired shape
- constant replacement of “old” with “new” bone.

The intramembraneous ossification (membrane bone formation) forms the bulk of the future cortical bone shell. This gives origin to many of the bones of the facial skeleton, of the vault of the skull, of the sense organs and parts of the mandible and of the clavicle.

The endochondral ossification (cartilage bone formation) forms the bulk of the future cancellous bones, giving origin to most of the bones at the base of the skull, the vertebral column, the pelvis and the extremities. Cartilage cells (chondrocytes) proliferate and deposit matrix until a cartilage model of the future bone is built. The cartilage cells mature, grow, followed by the calcification of the matrix. Osteoblasts appose woven bone on the substrate of unresorbed calcified cartilage cores, forming the primary spongiosa. This will later be replaced by a lamellar trabecular packet building the secondary spongiosa, i.e. the future adult spongiosa.

### Modelling

In general, growth and modeling are linked together [1]. Modeling allows the development of normal architecture during growth, controlling the shape, size, strength and anatomy of bones and joints (Fig.1.5). It increases the outside cortex and marrow cavity diameters, gives shape to the ends of long bones, drifts trabeculae and cortices, enlarges the cranial vault and changes the cranial curvature. During normal growth, periosteal bone is added faster by formation drifts than endosteal bone is removed by resorption drifts. This process is regulated so that the cylindrical shaft markedly expands in diameter, whereas the thickness of the wall and the marrow cavity slowly increase.

Modeling controls also the modulation of the bone architecture and mass when the mechanical condition changes [7]. For example, bone surfaces can be moved to respond to mechanical requirements. A coordinate action of bone resorption and formation of one side of the periosteal and endosteal surfaces can move the entire shaft to the right or left, allowing some bones to grow eccentrically [8].

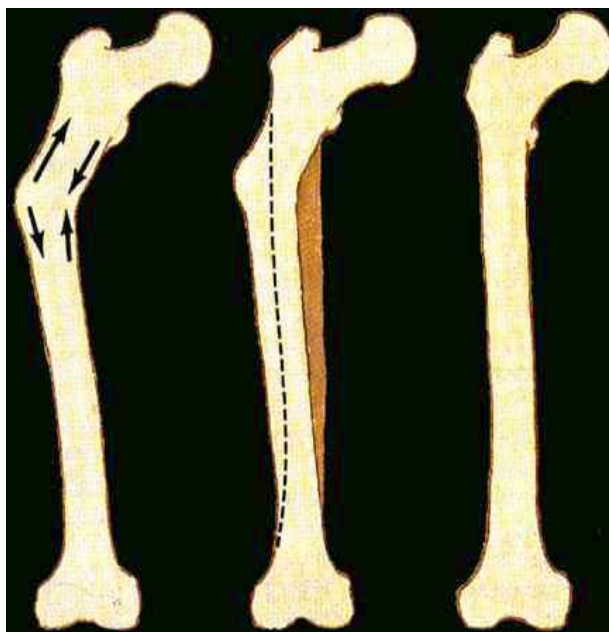


*Fig.1.5 Example of the modeling process. In this case bone remodelling is induced by a traumatic event. The trauma has deformed the femur, which gradually models towards a shape that is similar to the original one.*

### Remodelling

Remodeling can be defined as a process that produces and maintains bone that is biomechanically and metabolically competent [1]. At infancy, the immature (woven) bone at the metaphysis is structurally inferior to mature bone. In adult bone, the quality (e.g. mechanical properties) of bone deteriorates with time. Thus, as many other tissues, bone must replace or renew itself. This replacement of immature and old bone occurs by a process called remodeling, which is a sequence of resorption followed by formation of new lamellar bone [7] (Fig.1.6). The remodeling characterizes the whole life of bones. For normal rates of periodic bone replacement (bone turnover), cancellous bone has a mean age of 1 to 4 years, while cortical bone about 20 years.

## Bone Remodeling Cycle

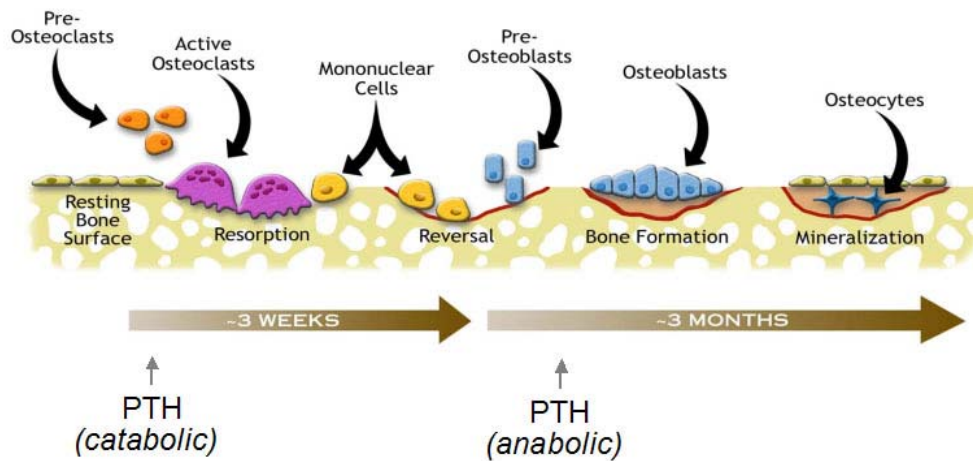


*Fig. 1.6 The remodelling process*

### Mechanical usage

During the last decades, it has been common belief that the bone turnover processes were mostly governed by homeostasis, ignoring or underestimating the role of mechanical functions [8].

The mechanostat hypothesis was introduced by Frost [10,11] to explain how mechanical usage regulates bone mass and architecture. According to this new vision, depending on the mechanical usage of the bone, signals are transmitted to the modelling and remodelling system, which actively alter bone mass and shape.

## 1.2 Hip Joint

The hip is one of the human joints that allow the greatest mobility. It is characterized by intrinsic stability too, thanks to the concave shape of the acetabulum and to the presence of a bony rim in the superior, posterior and anterior aspects [9].

The femoral head has a spherical shape, slightly flattened both anteriorly and posteriorly. The femoral head is covered of articular cartilage, with the exception of the fovea. On the acetabular face, fovea covers a horseshoe shaped zone and it is set in the central region. The fovea is thick, not articulated and it is filled with some fat, the sinusoidal membrane and the ligamentum rotundum [12,13].

The articular capsule is inserted on the acetabular edge proximally and on the femur distally. The dense fibrous tissue of the capsule is reinforced anteriorly and inferiorly, and only slightly in the posterior aspect. A single thick layer called orbicularis zone surrounds the femoral head, increasing the stabilizing function of the fibrous cartilaginous head ring.

The retinaculi are fibrous pedicles of the articular capsule that bend down towards the femoral neck. The blood vessel that run on the retinaculi supply the principal blood irroration to the femoral head. There are principally three lines:

- vessels running along the retinaculi
- vessels running in the ligamentum rotundum
- vessels running internally in the femoral neck

If one or more of these lines are damaged/interrupted, vessels of the other lines develop and grow, so as to counterbalance the reduced blood supply to the femoral head.

The femur is the longest bone in the human body. It is composed by the following basic structures:

- femoral head
- neck
- greater and lesser trochanter
- femoral shaft
- distal condiles

## **1.3 Total Hip Arthroplasty**

### **1.3.1 Overview of the THA procedure**

Over the last decades, total hip arthroplasty (THA) has become one of the most successful surgical operations. Symptoms such as pain and loss of function indicate THA as the solution. These symptoms can appear in different forms, as rigidity, deformity, limb shortening or movement reduction. THA is the solution preferred also in case of osteoarthritis, rheumatoid arthritis, psoriatic arthritis, avascular necrosis, trauma and tumours.

Today, a large variety of solutions are available: from the use of ultra high molecular weight polyethylene for the hemispherical socket, which is fixed onto the acetabulum, to the ceramic one and the metallic or ceramic head. Most of the implant is nowadays modular (Fig.1.7). Modularity assures the possibility of adapting the geometry of the prosthesis to the joint morphology of the patient. This solution provides more flexibility during primary surgery and simplified revision procedures [14,15]. This is particularly useful when the hip anatomy is badly affected as in DDH or in post-traumatic arthritis [16] and when a mini approach is used [17].

Usually, this type of prosthesis features a modular head to be inserted into a neck, which is on its turn fixed to a stem. The stem is inserted in the medullary canal of the femur. The metallic head, neck and stem, can be either of stainless steel, titanium alloy or chrome cobalt alloy. Both socket and stem can be fixed using methyl-methacrylate cement or by press-fit and direct bone ingrowth into the metallic surface.

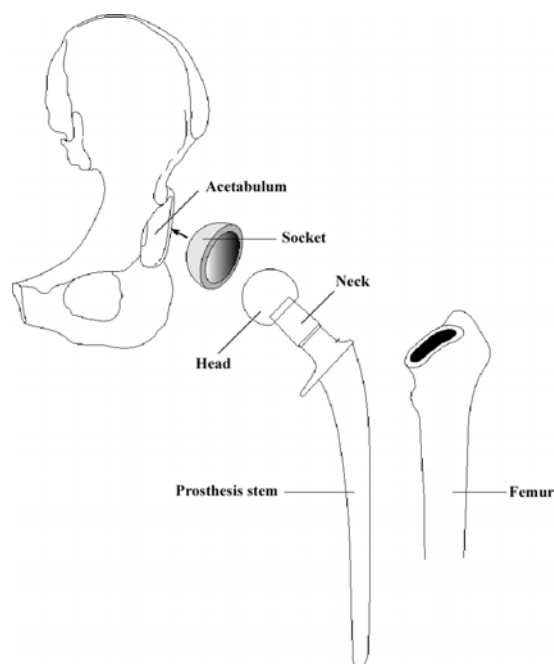


**Fig.1.7** Typical components of a modular prosthesis

Bioactive and bio inductive coatings (such as hydroxyapatite) are today normally used to facilitate and encourage the bone ingrowth process. This process has been demonstrated being highly dependent from the interface between prosthesis and bone. On a microscopic level, that means that the bone surrounding the prosthesis ingrowths into the porosity of the surface of the metallic alloy composing the prosthesis. Alloys as the titanium-aluminium-vanadium one, facilitates osteointegration of the prosthesis into the bone and thus allows the stabilization of the prosthesis.

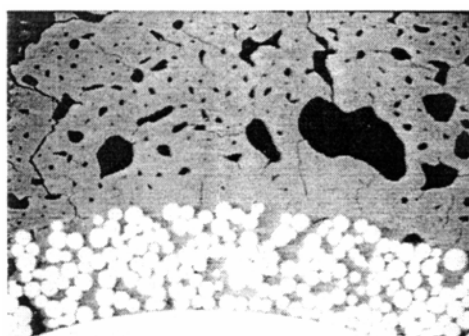


**Fig 1.** Scanning electron microscopy shows areas of bone penetrating into the depth of the porous coating (bone ingrowth).

**Fig.1.8** Example of bone ingrowth into a porous coated surface of a prosthesis

On a macroscopic level, the stabilization process of a cementless prosthesis depends on the geometry of the prosthesis as compared to the bone anatomy, depends on the stiffness of the prosthesis and finally on the strength of the interface, intended as capability to transfer loads and to avoid relative micromotion between stem and bone.

Hip replacement requires surgical access to the upper femur. Different surgical approaches have been developed and are in clinical practice. Each of them have advantages and disadvantages, but all of them include the neck resection, giving this way an access to both the acetabulum and the femoral intramedullary canal.

### **1.3.2 Mechanical considerations on the effect of THA**

The aim of THA is to reproduce in the hip and in the femur the same load transfer and the same stress distributions of the healthy femur.

The forces normally applied to the femur across the hip joint are transmitted via the cancellous bone of the pelvis to the acetabular subchondral bone [9,18]. These forces can have resultants being in magnitude several times the body weight. The forces are shared by the complex network of cancellous bone of the femoral head and of the femoral neck, and are then conveyed to the femoral shaft. We have already highlighted how the wall head and shaft architecture is functional to the load the hip joint and the femur are designed to bear. It is obvious that the drastic modification in shape, mass and mechanical characteristics of the structures after total hip arthroplasty deeply alters the equilibrium between form and functions of the hip. After uncemented total hip arthroplasty, a material having uniform stiffness and strength replaces the complex subchondral plate of the acetabulum [18]. In the femur, the proximal shaft is filled by a large, stiff piece of metal, having dimensions and mechanical characteristics that respond to the needs of having a highly strong filling (to prevent femur fracture) and a strong bone-implant interface.

The presence of a stiff, heavy filling results in a drastic increase of the overall stiffness of the proximal femur. If the material is too stiff and the proximal fit produced during surgery by press-fit is not quasi-perfect, then the risk of stress shielding increases. Stress shielding is due to the fact that the higher stiffness of the metal leads the stem to uptake the most of the load transferred to the femur through the hip joint [19]. Because the proximal femur is no more loaded as before,

it remodels, losing a significant mass of cortical bone. At the same time, the stem transfers the load uptake proximally to the bone of the femoral shaft, in correspondence of its distal tip (Fig.1.9)



*Fig.1.9 The remodelling process as a consequence of the introduction of a device that alter the physiologic load transfer*

The consequence is an evident hypertrophy of the femoral shaft, at the level just distal to the tip of the stem. If the proximal resorption is massive, the process yields mobilization, strength reduction and on the long term gross loosening [19].

The stems used in THAs are generally less bulky and less stiff than the ones used in uncemented implants.

The advantage of cemented hip arthroplasty is that the primary stability is ensured by the presence of a cement layer at the interface between the implant and the bone. This layer ensures immediate bone-metal bonding, thus primary stability, and solves all superficial irregularities of the bone rasped during surgery by filling all the empty spaces in between.

The main problem with cemented hip implants is the mechanical deterioration of the cement layer. Even if it guarantees immediate implant stability and a higher proximal load transfer with respect to uncemented stems, the cement can debond from the metal and defects can generate on the external surface of inside its bulk. The micro cracks so generated can aggregate in large cracks, cement debris leading to inflammatory reactions of living tissues, while the rupture of the cement layer would reduce implant stability. This way, the loosening process would be fired and self-sustained, thank to cyclic loading and immuno-inflammatoty processes.

### **1.3.3 State of the art in THA**

Almost five decades have elapsed since Charnley firstly introduced THA in clinical practice, and at the same time presented to the orthopaedic community one of the most durable and complex procedures ever developed. The evolution of surgical techniques, implant materials and implant designs has led at today to excellent long-term results in older and more inactive patients, with survival rates reaching 90% or more at 10 years.

Since younger patients have been encouraged by the successful results, indications have been widened, so that today the number of primary THA performed in young and middle aged patients has significantly increased.

Infection and implant fracture were the two main causes of THA failure for the first generation of hip implants clinically adopted. During the first five decades the infection rate has been reduced to well below 1%, while improved materials have almost completely annihilated implant fracture rates.

Today aseptic loosening and bone lyses secondary to particulate debris are the first cause for implant failure.

The incidence of this failure mechanism is higher in younger patients, while 30% of implant failure within the first 10 years has been reported in young, male subjects. These results has confirmed the prediction of Charnely, who stated that the true challenge in THA practice came when 45-50-year old patients were considered for operation, as every innovation must have a reasonable chance to provide the patient with at least 20 years of trouble-free activity.

Now the question is whether it is possible to create an implant that lasts a lifetime even in relatively young patients. The challenge for the orthopaedic research in the present decade is to study deeply the variables that play a crucial role in the success of the THA procedure.

For the scope of present thesis, the issues concerning uncemented THA will be addressed.

## 1.4 Primary stability of uncemented hip stems

### 1.4.1 The uncemented hip prosthesis

Historically, THA was firstly designed and applied in orthopaedics without the use of cement [20].

Cementless implants are based on a simple concept. Firstly the press-fit guarantees that both the stem and the prosthetic cup are steadily anchored to the bone in the immediate post-operative period (primary stability). Meanwhile, the bone ingrowth into the metallic surfaces guarantees the long-term bonding and the mechanical stability of the whole prosthesis to the surrounding bony layers (secondary stability). This way, the prosthetic hip can accomplish the same mechanical and physical functions of the normal joint, after appropriate rehabilitation.

Unfortunately, many factors can jeopardise the outcome of an implant, by acting not only in the short, but also in the long term.

Complication of cementless prostheses consists essentially in those causing the failure of the osteointegration process, those annihilating the mechanical stability of the implant. When the bony fixation fails, even low loads can cause high relative motions between the implant and the bone. These high interfacial motions further discourage bone ingrowth, and lead to tissue inflammatory processes, which often results in fibrous tissue formation. Fibrous tissue creates a sort of friction bearing surface, which increases interfacial motion, thus leading to implant gross loosening [21].

Implant loosening maybe partial or total, and it can involve one or both the components (stem and cup), thus different degrees of loosening are possible. The bony fixation is often difficult to assess. A localized radiolucent line is always a bad indication, but not always conventional radiograph arrives to detect the debonding between the two surfaces [21].

Then, even when loosening can be detected by X-Ray and RSA, there is not a strictly and direct correspondence between failure (needing revision) and loosening. The revision of an implant is decided on the base of many factors among them, the degree of pain the patient feels, the loss of mobility, septic evidences. In some particular cases, the removal of cementless stem can be even more difficult than the removal of cemented stems. For example, when:

- Loosening is limited to specific areas (thus the bone ingrowth interfacial regions mechanically impede the stem extraction);

- The distal tip of the stem breaks (thus its retrievals becomes surgically complex) is much more difficult than for the cemented ones, as even partial bone ingrowth impedes stem extraction.

Cemented and cementless fixations are both in clinical practice today [21]. The surgeon, on the base of the peculiar situation, makes the choice between the two techniques. For example, cementless fixation is to be preferred to cemented one in the case of young patient, for whom the bony tissue is usually in good conditions, increasing the possibilities of an active bone ingrowth that stabilizes the implant. In young patients cement would mean problems due to cement damage in the long term [22].

Hereinafter are illustrated the principal factors that contribute to the outcome of a cementless implant.

- Stem material: the good compromise between compliance and stiffness of the material is crucial for implant success. If the implant is too stiff, stress shielding is the direct consequence. If the material is too elastic, high interfacial motions discourage bone ingrowth [23].
- Stem design: the shape of the stem must be well chosen. Edges and sharp changes of geometry and section should be avoided, as they generate stress concentrations. Peak stress is then transferred to the adjacent bone, causing localized bone hypertrophy. The shape of the stem should also encourage primary fixation with the help of press-fit, thus in particular rotational stability, which is the most difficult to be achieved. When the stem has a sufficient taper, the loads applied to the head tends to stabilize the stem by mechanical interlocking, wedging it into the femoral canal [24].
- Cup insert material: the wide use of polyethylene in the cup insert has determined a high rate of revision on an entire generation of implants. Polyethylene is a material that is highly subjected to wear products and particles release. Those particles cause the inflammation of the bony tissue, stimulating the concentration of macrophages and osteoclasts and the production of fibrous tissue. In failed particles of polyethylene have been found in the cytoplasm of the macrophage and giant cells surrounding the cup, but also in those around the stem. That means that these particles migrate from the cup region, through the interface, to the stem one, thus endangering the stability of the whole implant [25].
- Stem superficial texture: especially for uncemented implants, the superficial texture is essential for stimulating bone ingrowth and stability, both primary and secondary. Many

investigations have analyzed this aspect. A brief literature review will be illustrated in the next paragraph. The superficial texture of an implant can be characterized by many parameters, and the investigation usually aim to find the optimal range of one or more of such parameters for the stability of the implant. Unfortunately, there are only rare cases in which the authors try to make an exhaustive analysis, by taking into consideration the variation of the minimum set of parameters that describes the superficial texture of the implant. Anyway, thank to the research efforts, the implant designs have been ameliorated in the recent years.

- Coating: the positive role played by osteoinductive and osteoconductive materials, such as hydroxiapatite has been already assessed by the literature. A stem design coated with one of such materials gives significantly better results of the same stem design, non-coated. With the term, “better results” we here mean: higher rate of bone ingrowth, especially in the first post-operative period, both in the osteopenic and in normal patients; higher osteoconductivity (bone can bridge wider gaps), even if usually equal, when not lower, bone mineral density [26,27,28].
- Load and load peaks: the loads applied to an implant are fundamental for its stability. Especially in the first post-operative period, high load peaks can inhibit bone ingrowth, disrupting the bone bridges that start to growth into the stem. Many studies were performed in order to determine the ranges and directions of loads applied to the head of either the femur or the prosthesis, during normal activities. Those analyses allowed determining what physical activities have to be avoided after surgery, during rehabilitation. They also gave the load ranges to be used for in-vitro testing on new implant prototypes [29,30].
- Quality of surrounding bone: the quality of the surrounding bone cannot be varied depending on the needs. Nevertheless, it is a physiological variable that must be taken into account by the surgeon in order to evaluate the best implant design and characteristics for the patient. For this reason, in presence of osteopenic and/or osteoporotic bone the surgeon performs a careful analysis before intervention. The quality of the surrounding bone is strongly dependent on the age and gender of the patient: the younger the patient, the higher the quality of the bony tissues; a female subject has usually higher rates of osteoporosis, especially after menopause [31].

### **1.4.2 The bone-stem interface: considerations**

The bone-metal interface is the most delicate site of an uncemented implant, where the living tissue and the non living material meet each other. Even if the bone is a living material, while the prosthesis is a non living one, these two systems exchange chemical and mechanical signals across the interface. Such signals generate then reactions on both the bone and the implant. It is then obvious that actions and reactions occurring at the interface level are crucial for the outcome of the hip replacement.

After stem implantation, the wounded bone comes in contact with the implant. If the surgery was well performed, the stem is pressed towards the cortical bone on a uniform way along its length and around its sections. The direct contact between the stem and the cortical bone is guaranteed during surgery, when spongy bone is rasped away. Marrow is a soft tissue that cannot support load; neither transmits it to the stem. Moreover it prevents spongy bone to directly growth into the stem.

Thanks to this press-fit achieved during surgery, the stem stability is guarantee in the immediate post-operative period (primary stability), while the bone layers immediately adjacent to the stem are preloaded, thus encouraged to grow.

During the first post-operative days the patient is prevented from moving, then gradually higher loads are applied to the operated limb.

Time has actually to be given to the wounded bone to overcome the traumatic surgical event: the damaged trabeculae and Haversian systems are removed by the osteoclasts and macrophages and new woven bone is formed by the osteoblasts.

The woven bone gradually replaces the bone clot formed around the stem, growing on it and tightly ensuring it in its position (secondary stability).

Progressive loading is a key-factor for secondary healing. If not loaded the bone is not stimulated to grow. In fact, bone resorbs and reduces its mineral content. Load allows bone to model and remodel around the stem in a way that best accommodates the new conditions, which were generated after THA.

After THA then, the proportions between the filling material and the outside wall one are inverted with respect to the pre-operative situation. It is obvious that such a “revolution” in the structure and in the physiology of the femur will inevitably need considerable changes to develop a new quasi-steady state.

### 1.4.3 Evaluation of cementless hip implant stability: state of the art

As already mentioned, cementless implants are mechanically stabilised in the host bone at surgery time through a press-fitting procedure. The primary mechanical stability achieved by these implants is critical for the long-term outcomes of the operation [32-35]. As already explained in previous sections, various factors affect long-term stability and finally the outcome. It is commonly accepted that one of these is the achievement of a good level of osteointegration between bone tissue and stem surface [36,37]. Osteointegration is possible if the relative stem/bone micromotion is below a certain threshold. In the literature different ranges can be found, from 30 to 150 micron [36,38]. Surgeon's experience in planning the kind and the size of stem to be implanted is fundamental for achieving good fixation. But, even assuming a theoretically perfect choice, there is still the practical problem of correct positioning of the stem in the femur during surgery. In particular the level of press-fitting during stem insertion is critical. If the surgeon does not press-fit enough the stem, the stem is not stable, which leads to aseptic loosening of the implant (fibrous tissue layer formation) [39-40]. If the press-fit is excessive, femoral intra-operative fractures may occur. Intra-operative fractures are not a negligible problem [41], and reported rates of periprosthetic fractures can be as high as 4% - 28% [42-44]. Surgeons are guided only by their experience in finding the optimal compromise of press-fitting.

*In vitro* studies have shown that the largest values of shear micromovement at the stem/femur interface are measured when the torsional moment around the femur axis prevails [35,45-47]. Daily activities like stair climbing or rising from a seated position produce the highest torsional moments. Typical values of physiological torsional moment vary from 15 to 29 Nm [29,48-50]. A limit value of interface micromotion may be inferred from the literature [36,38] and the concept of stability threshold can be introduced: ***for instance, an implant can be defined as stable if, under a torque of 20 Nm, the micromotion is smaller than 100 micron.*** This torque is slightly smaller than the maximum values in the literature, taking into account that patients apply reduced loads in the immediate post-operative demanding period, when most activities are avoided [34,45,51,52]. Commonly used methods to measure primary stability of cementless prostheses are conceived for *in vitro* tests [45,51,53]. Only one study has been undertaken to measure stability intra-operatively [37]. The method consisted of a torque wrench able to

measure the torque applied by the surgeon to an implanted stem. The surgeon could also evaluate the displacement between stem and femur, by judging visually the indication of a micrometer dial gauge in contact with the femur and fixed to the stem. In that study the accuracy and the repeatability of the method were not clearly assessed. To the authors' knowledge no follow-up was presented to describe further results obtained with that device.

In the second and third chapters an intra-operative device is described. It was validated and a first introduction in the operating room was performed with really good results.

An alternative approach has been recently investigated. It concerns the use of the vibration analysis technique to evaluate the extent of stability achieved during surgery. This method has been successfully used to investigate the mechanical properties of the bone and its application to evaluate the extent of fixation of dental implants has been explored [54-57], even if its validity in this field is still under discussion [58]. Several studies have been published recently on the stability assessment of hip implants by mechanical vibration analysis. Li *et al.* [59], in 1996, demonstrated the usefulness of vibration in the diagnosis of implant loosening by considering the amplitude response at all frequencies (within a certain range) and the spectral analysis of particular waveforms. Georgiou and Cunningham [60] performed a comparison of vibration testing and radiographs in patients with total hip replacement and found that the vibration testing method was 20% more sensitive with respect to radiographs and was able to diagnose 13% more patients. They used vibrations up to 1000Hz and discriminated successfully grossly unstable implants from highly stable ones. However, to detect early loosening the method seemed to have insufficient diagnostic sensitivity. Thus, more advanced techniques of excitation and signal analysis seem to be necessary to improve the sensitivity of the technique. Qi *et al.* [61] suggested exciting the implant-bone system with higher harmonics (at least 1000Hz or higher) being more sensitive to implant stability and indicative of interface failure. Confirmation of these results came from Jacques *et al.* [62], who combined experimental testing and simulated modal analysis. Their study demonstrated that the resonance frequency shift of the higher vibration modes of the implant-bone system was the most sensitive parameter to detect the stability of the prosthesis in the femur.

In the fourth and fifth chapters, an application of this technique to the prosthesis stability assessment is reported

## References

1. Cowin, S. (2001) Bone Mechanics Handbook. Second edition, CRC Press, Boca Raton, USA.
2. Williams, P. L. (1995) Gray's anatomy. 38th edition, Churchill Livingstone, London, UK.
3. Weiss, L. (1990) Cell and tissue biology, Urban & Schwarzenberg, Baltimore.
4. Malluche, H. H. & Faugere, M. C. (1986) Atlas of mineralized bone histology, Karger AG, Basel, Switzerland
5. Frost HM, (1984) Intermediary organization of skeleton. Vol.I-II, Boca Raton CRC Press Inc, USA.
6. Hacnox NM. (1972) The biology of bone. Cambridge, Cambridge University Press.
7. Currey, J. D. (2003) The many adaptations of bone. J Biomech 36, 1487-1495.
8. Currey, J. D. (1984) What should bones be designed to do? Calcif. Tissue Int. 36 Suppl 1, S7-10.
9. Currey J. D. (1998) Mechanical properties of vertebrate hard tissues. Proc. Inst. Mech. Eng. [H], 212:6, 399-411.
10. Frost, H. M. (1987) Bone "mass" and the "mechanostat": a proposal. Anat Rec 219, 1-9.
11. Frost, H. M. (1995) Introduction to a new skeletal physiology, Pajaro Group, Pueblo Vol. I and II.
12. Alexander R McN (1993) Optimization of structure and movement of the legs of animals, Cambridge, Cambridge University Press.
13. Alexander R McN (1982) Optima for animals. London, Edward Arnold.
14. Bobyn JD, Tanzer M, Krygier JJ, Dujovne AR, Brooks CE, (1994) Concerns with modularity in total hip arthroplasty. Clin Orthop Relat Res; 298: 27-36.
15. Cameron HU, (2003) Orthopaedic crossfire--Stem modularity is unnecessary in revision total hip arthroplasty: In opposition. J Arthroplasty; 18(3 suppl 1): 101-103.
16. Noble PC, Kamaric E, Sugano N, Matsubara M, Harada Y, Ohzono K, Paravic V, (2003) Three-dimensional shape of the dysplastic femur: implications for THR. Clin Orthop Relat Res; 417: 27-40.
17. Kennon RE, Keggi JM, Wetmore RS, Zatorski LE, Huo MH, Keggi KJ, (2003) Total hip arthroplasty through a minimally invasive anterior surgical approach. J Bone Joint Surg Am; 85-A(suppl 4): 39-48

18. Blackburn J., Hodgkinson R., Currey J.D., Mason J.E. (1992) Mechanical properties of microcallus in human cancellous bone. *J Orthop Res*, 10:2, 237-46.
19. Hodgkinson R, Currey J.D. (1990) The effect of variation in structure on the Young's Modulus of cancellous bone: a comparison of human and non-human material. *Proc Inst Mech Eng [H]*, 204:2, 115-21.
20. Charnley J (1982) Faltin Lecture: evolution of total hip replacement. *Ann Chir Gynaecol* 71:103.
21. Engh CA, O'Connor D., Jasty M., McGovern TF, Bobynd JD, Harris WH (1992) Quantification of implant micromotion, strain shielding, and bone resorption with porous coated anatomic medullary locking femoral prosthesis. *Clin Orthop*, 250:13-29.
22. Malchau H, Snorrason F, Herberts P, Karrholm J (1994) Micromotion of femoral stems in total hip arthroplasty. A randomized study of cemented, hydroxyapatite-coated and porous-coated stems with roentgen stereophotogrammetric analysis. *J Bone Joint Surg [Am]*, 76:1692-1705.
23. Otani T, Whiteside LA, White SE, McCarthy DS (1993) Effect of femoral component material properties on cementless fixation in total hip arthroplasty. A comparison study between carbon composite, titanium alloy, and stainless steel. *J Arthrop* 8:67.
24. Whiteside LA, McCarthy DS, White SE (1996) Rotational stability of noncemented total hip femoral components. *J Orthop* 25:276.
25. Bobynd JD, Jacobs JJ, Tanzer M (1995) The susceptibility of smooth implant surfaces to periimplant fibrosis and migration of polyethylene wear debris. *Clin Orthop* 21.
26. Søballe K, Hansen ES, Brockstedt-Rasmussen H, Pedersen CM, Bunger C (1990) Hydroxyapatite coating enhances fixation of porous coated implants. A comparison in dogs between press-fit and noninterference fit. *Acta Orthop Scand* 61:299.
27. Søballe K, Hansen ES, Rasmussen H, Jorgensen PH, Bunger C (1992) Tissue ingrowth into titanium and hydroxyapatite-coated implants during stable and unstable mechanical conditions. *J Orthop Res* 10:285.
28. Søballe K, Brockstedt-Rasmussen H, Hansen ES, Bunger C (1992) Hydroxyapatite coating modifies implant membrane formation. Controlled micromotion studied in dogs. *Acta Orhtop Scand* 63:128.
29. Bergmann G, Graichen F, Rohlmann A (1995) Is staircase walking a risk for the fixation of hip implants) *J Biomech* 28:535-553.

30. Bergmann, G., Deuretzbacher, G., Heller, M., Graichen, F., Rohlmann, A., Strauss, J., and Duda, G. N., (2001) Hip contact forces and gait patterns from routine activities, *J Biomech*, 34: 859-71.
31. Søballe K, Hansen ES, Brockstedt-Rasmussen H (1991) Fixation of titanium and hydroxyapatite-coated implants in arthritic osteopenic bone. *J Arthrop* 6:307.
32. Kapandji A. (1982) Physiologie articulaire. In La Hanche, Librerie Maloine SA, Fascicule II.I
33. Rydell NW. (1966) Forces acting on the femoral head prosthesis. *Acta Orthopaedica Scand*, 37 Suppl 88: 96-125.
34. Maloney WJ, Jasty M, Burke DW, O'Connor DO, Zalenski EB, Bragdon CR, Harris WH. (1989) Biomechanical and histologic investigation of uncemented total hip arthroplasties: A study of autopsy-retrieved femurs after in vivo cycling. *Clin Orthop Rel Res*, 249:129-40
35. Schneider E, Kinast C, Eulenberger J, Wyder D, Eskilsson G, Perren SM. (1989) A comparative study of the initial stability of cementless hip prostheses. *Clin Orthop Rel Res*, 248: 200-9
36. Søballe K. (1993) Hydroxyapatite ceramic coating for bone implant fixation: Mechanical and histological studies in dogs. *Acta Orthop Scand, Suppl* 255: 1-58
37. Harris WH, Mulroy RD, Maloney WJ, Burke DW, Chandler HP, Zalenski EB. (1991) Intraoperative measurement of rotational stability of femoral components of total hip arthroplasty. *Clin Orthop*, 266:119-126
38. Pilliar RM, Lee JM, (1986) Maniopoulos C. Observations on the effect of movement on bone ingrowth into porous-surfaced implants. *Clin Orthop Rel Res*, 208: 108-113.
39. Goodman SB. (1994) The effects of micromotion and particulate materials on tissue differentiation: Bone chamber studies in rabbits. *Acta Orthop Scand, Suppl*.258: 1-43
40. Ishiguro N, Kojima T, Ito T, Saga S, Anma H, Kurokouchi K, Iwahori Y, Iwase T, Iwata H. (1997) Macrophage activation and migration in interface tissue around loosening total hip arthroplasty components. *J Biomed Mater Res*, 35: 399-406
41. Schutzer SF, Grady-Beson J, Jasty M, O'Connor DO, Bragdon C, Harris WH. (1995) Influence of intraoperative femoral fractures and cerclage wiring on bone ingrowth into canine porous coated femoral components. *J Arthrop*, 10: 823-829
42. Schwartz JJJ, Mayer JG, Engh CA. (1989) Femoral fractures during non-cemented total hip arthroplasty. *J Bone Joint Surg [Am]*,71:8 1135-1142

43. Otani T, Witheside LA. (1992) Failure of cementless fixation of the femoral component in total hip arthroplasty. *Ortho Clin North Am*,23: 335-346
44. Schmidt AH, Kyle RF.(2002) Periprosthetic fractures of the femur. *Ortho Clin North Am*,33:143-152.
45. Harman MK, Toni A, Cristofolini L, Viceconti M. (1995) Initial stability of uncemented hip stems: an in vitro protocol to measure torsional interface motion. *Medical Eng and Physics*,17: 163-171
46. Callaghan JJ, Fulghum CS, Lsisson RR, Stranne SK. (1992) The effect of femoral stem geometry on interface motion in uncemented porous-coated total hip prostheses: Comparison of straight-stem and curved-stem designs. *J Bone Joint Surg Am*, 74: 839-848
47. Nunn D, Freeman MA, Tanner KE, Bonfield W. (1989) Torsional stability of the femoral component of total hip arthroplasty: Response to an anteriorly applied load. *J Bone Joint Surg Am*,71: 452-5
48. Heller MO, Bergmann G, Deuretzbacher G, Claes L, Haas NP, Duda GN. (2001) Influence of femoral anteversion on proximal femoral loading: measurement and simulation in four patients. *Clin Biomech*, 16: 644-649
49. Hodge WA, Carlson KL, Fijan RS, Burgess RG, Riley PO, Harris WH, Mann RW. (1989) Contact pressures from an instrumented hip endoprosthesis. *J Bone Joint Surg*, 71-A: 1378-86
50. Kotzar GM, Davy DT, Goldberg WM, Heiple KG, Berilla J, Brown RH, Burnstein AH. (1991) Telemeterized in vivo hip joint force data: a report on two patients after total hip surgery. *J Orthop Res*,9: 621-33
51. Monti L, Cristofolini L, Viceconti M. (1999) Methods for quantitative analysis of the primary stability in uncemented hip prostheses. *Art Org*, 23: 851-859
52. Phillips TW, Nguyen LT, Munro SD. (1991) Loosening of cementless femoral stems: a biomechanical analysis of immediate fixation with loading vertical, femur horizontal. *J Biomech*, 24: 37-48
53. Baleani M, Cristofolini L, Toni A. (2000) Initial stability of a new hybrid fixation hip stem experimental measurement of implant-bone micromotion under torsional load in comparison with cemented and cementless stems. *J Biomed Mater Res*, 50: 605-615

54. Lowet, G, Van Audekercke, R, Van der Perre, G, Geusens, P, Dequeker, J, Lammens, J., (1993) The relation between resonant frequencies and torsional stiffness of long bones in vitro. Validation of a simple beam model., *J Biomech*, 26(6), 689-96.
55. Van Der Perre, G, Lowet, G. (1996) In vivo assessment of bone mechanical properties by vibration and ultrasonic wave propagation analysis, *Bone*, 18(1 Suppl), 29S-35S.
56. Meredith, N., Shagaldi, F., Alleyne, D., Sennerby, L., Cawley, P. (1997) The application of resonance frequency measurements to study the stability of titanium implants during healing in the rabbit tibia, *Clin. Oral. Impl. Res.*, 8(3), 234-243.
57. Friberg, B., Sennerby, L., Linden, B., Gröndahl, K., Lekholm, U., (1999) Stability measurements of one-stage Brånemark implants during healing in mandibles. A clinical resonance frequency analysis study, *Int. J. Oral Maxillofac. Surg.* 28, 266-272.
58. Koka, S., Commentary on resonance frequency analysis, *Int J Prosthodont*, 19(1), p.84
59. Li, P.L.S., Jones, N.B., Gregg, P.J., (1996) Vibration analysis in the detection of total hip prosthetic loosening, *Med.Eng.Phys.*, 18(7), 596-600
60. Georgiou, A.P., Cunningham J.L., (2001) Accurate diagnosis of hip prosthetic loosening using a vibrational technique, *Clin Biomech*, 16, 315-323
61. Qi, G., Mouchon, W.P., Tan, T.E., (2003) How much can a vibrational diagnostic tool reveal in total hip arthroplasty loosening?, *Clin Biomech*, 18, pp. 444-458
62. Jaecques, S.V.N., Pastrav, C., Zahariuc, A., Van der Perre, G., (2004) Analysis of the fixation quality of cementless hip prostheses using a vibrational technique, *Proc. International Conference on Noise and Vibration Engineering*, 443-456

## **CHAPTER 2**

# **INTRA-OPERATIVE EVALUATION OF PRIMARY STABILITY OF CEMENTLESS HIP STEMS: A DEVICE BASED ON THE DIRECT MICROMOTION ASSESSMENT**



This chapter is part of a manuscript which was published on Medical Engineering and Physics, 2006 Jun; 28(5):475-82. It concerns the development and validation of an intra-operative device based on the direct measurement of the primary stability of cementless stem.

## 2.1 Introduction

Total hip replacement is a very successful procedure to solve the effects of degenerative pathologies of the human hip joint. Young, active patients are frequently treated with cementless prostheses. These implants are mechanically stabilised in the host bone at surgery time through a press-fitting procedure. The primary mechanical stability achieved by these implants is critical for the long-term outcomes of the operation (1-4). Various factors affect long-term stability and finally the outcome. It is commonly accepted that one of these is the achievement of a good level of osteointegration between bone tissue and stem surface (5,6). Osteointegration is possible if the relative stem/bone micromotion is below a certain threshold. In the literature different ranges can be found, from 30 to 150 micron (5,7). Surgeon's experience in planning the kind and the size of stem to be implanted is fundamental for achieving good fixation. But, even assuming a theoretically perfect choice, there is still the practical problem of correct positioning of the stem in the femur during surgery. In particular the level of press-fitting during stem insertion is critical. If the surgeon does not press-fit enough the stem, the stem is not stable, which leads to aseptic loosening of the implant (fibrous tissue layer formation) (8,9). If the press-fit is excessive, femoral intra-operative fractures may occur. Intra-operative fractures are not a negligible problem (10), and reported rates of periprosthetic fractures can be as high as 4% - 28% (11-13). Surgeons are guided only by their experience in finding the optimal compromise of press-fitting.

*In vitro* studies have shown that the largest values of shear micromovement at the stem/femur interface are measured when the torsional moment around the femur axis prevails (4,14-16). Daily activities like stair climbing or rising from a seated position produce the highest torsional moments. Typical values of physiological torsional moment vary from 15 to 29 Nm (17-20). A limit value of interface micromotion may be inferred from the literature (5,7) and the concept of stability threshold can be introduced: for instance, an implant can be defined as stable if, under a torque of 20 Nm, the micromotion is smaller than 100 micron. This torque is slightly smaller than the maximum values in the literature, taking into account that

patients apply reduced loads in the immediate post-operative demanding period, when most activities are avoided (3,15,21,22). Commonly used methods to measure primary stability of cementless prostheses are conceived for *in vitro* tests (14,21,23). Only one study has been undertaken to measure stability intra-operatively (6). The method consisted of a torque wrench able to measure the torque applied by the surgeon to an implanted stem. The surgeon could also evaluate the displacement between stem and femur, by judging visually the indication of a micrometer dial gauge in contact with the femur and fixed to the stem. In that study the accuracy and the repeatability of the method were not clearly assessed. To the authors' knowledge no follow-up was presented to describe further results obtained with that device.

*In vitro* protocols reported in the literature are not exportable to the operating room. Anyway most of them show a good overall accuracy. The method of Harris *et al.* (6) can be used intra-operatively, but its accuracy in measuring the displacements is not comparable to the *in vitro* methods. Moreover no existing system makes a real-time comparison between the actual readout and a stability threshold. It is believed that an instrument that could measure intra-operatively the stability achieved by an implanted stem would consistently improve the rate of success (24). This instrument should be accurate and should give to the surgeon during implantation a quick answer concerning the stability.

The aim of the present study was to design, validate, and test *in vitro* a new device to be used intra-operatively to assess primary stability. The device is meant to help the surgeon to decide how much to press-fit the implant. It must have the following features:

- (i) The transducer accuracy and range must be adequate to discriminate stability. In particular the resolution on the shear micromotion must be of the order of few micron.
- (ii) Its use in the operating room should be easy and safe. This involves dimensional limitations, selected materials, and compatibility with any object, person and action in the surgical theatre.
- (iii) It must withstand sterilization, considering one of the common procedures (e.g. autoclave cycle used for rubber equipment: 121°C for 20-40 min; 2.1 bar; saturated steam atmosphere), so all the sensor and the electronics must be selected to resist to that conditions.

(iv) The information provided should be clear and unequivocal. A simple and user-friendly interface for the surgeon is needed.

(v) The data should be recorded and saved in a file downloaded after the operation.

(vi) The device should be suitable for patients of every size, both for the right and left limb.

(vii) The device must be programmable. This feature provides to change the pre-set threshold or the internal parameter concerning calibration (see Calibration, below).

Basically, the device proposed measures the torque applied by the surgeon to an implanted stem while estimating the shear displacement at the stem/femur interface, by using two separate transducers. The data are processed and compared with a pre-set stability threshold, providing the surgeon with real-time clinical relevant information concerning stability.

## 2.2 Materials and Methods

### 2.2.1 Feasibility study

A feasibility study was undertaken in order to evaluate if it was possible to build a measurement system:

(i) sufficiently accurate to predict instability;

(ii) geometrically compatible with the patient's body and with the surgeon's manoeuvres.

For the first purpose a pilot prototype (Fig.2.1) was built and tested *in vitro*. It hosted two independent transducers measuring the torque applied and the corresponding rotation. The prototype was subjected to two different kinds of tests. Repeated tests were performed to evaluate the intrinsic accuracy of the device (stiffness and maximum oscillation of the signals). Then the measured displacements were assessed by comparison against a validated procedure for stability assessment (14,21,23). Thus the correlation between the device displacement readout and the reference measurements was calculated. The overall accuracy of the prototype was estimated by repeated tests on seven specimens, four embalmed re-hydrated (left; length: 400-450 mm; bone quality: from mildly to severely osteoporotic) and 3 composite (Mod 3103, Pacific Res. Labs. Inc., Vashon Island, WA) (23,25). The same kind

of stem (Mod. AnCAFit 14 left, cementless, Wright Medical Technology, Arlington, TN, USA) was implanted with different degrees of press-fitting.

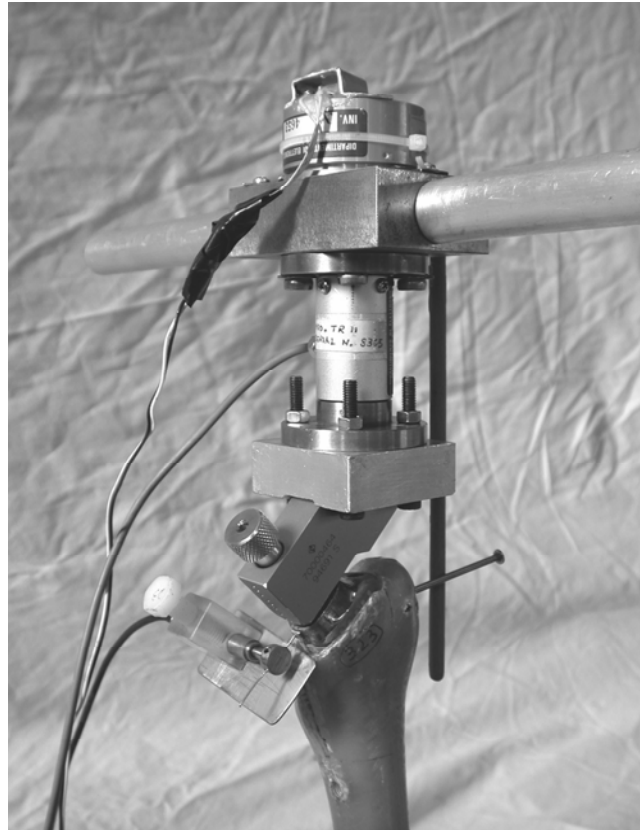


**Fig.2.1** Pilot prototype for the feasibility study. It hosted a rotation sensor (on top) and a torsional load cell (below the handles for applying the torque manually). It was tested *in vitro* to evaluate the sensitivity of the method. The LVDT for the additional reference micromotion measurement is visible bonded to the calcar. A reference pin is inserted on the lateral aspect of the greater trochanter for the angular probe.

For the second purpose a mock-up (Fig. 2.2) of the same dimension and shape of the planned final device was manufactured and tested intra-operatively in the surgical theatre by an experienced surgeon. After inserting the mock up, the surgeon verified the geometrical compatibility in relation to the patient tissues. He indicated:

- (i) that the dimensions of the base part (connector) and the upper part (sensors) were acceptable;
- (ii) that height could be increased if necessary;
- (iii) which was the optimal position for the reference pin (anterior-proximal).

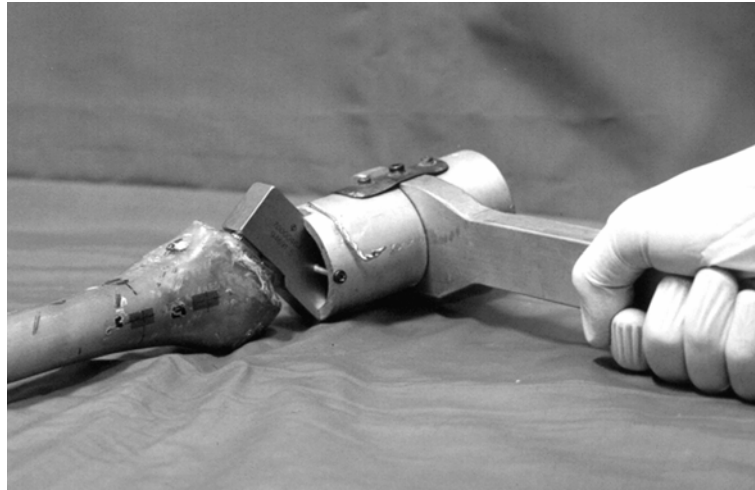


**Fig. 2.2** Mock-up for the geometrical compatibility test. The mock-up had the same geometry and the same conical connection to the stem as the final device.

Taking into consideration the suggestions of the surgeon and from the indications of the pilot study, the final device was designed.

### **2.2.2 Description of the final device**

The final device (Fig.2.3) incorporates two transducers with the desired accuracy, and it is able to withstand the environmental conditions of an autoclave cycle for rubber equipment sterilization:

- (i) To accommodate possible different patient geometries, a total excursion of  $\pm 7.5$  mm was designed. Thus the angular sensor selected was characterized by technology RVDT (Mod. RV1KX, Sentech Inc., USA) with a non-linearity of  $\pm 0.243\%$  FS in the range of  $\pm 30^\circ$  (corresponding to about  $\pm 7.5$ mm), sensitivity 3.3mV/V/deg, maximum storage temperature of 137°C;
- (ii) The torque level chosen to test stability (20Nm) is typical of stair climbing activity (14,17,18,21,23). Thus it was decided for a torsional load cell (Mod. TSP-07, Leane, Parma, Italy – range  $\pm 25$  Nm) with a non-linearity of  $\pm 0.2\%$  F.S. and maximum storage temperature of 140°C.

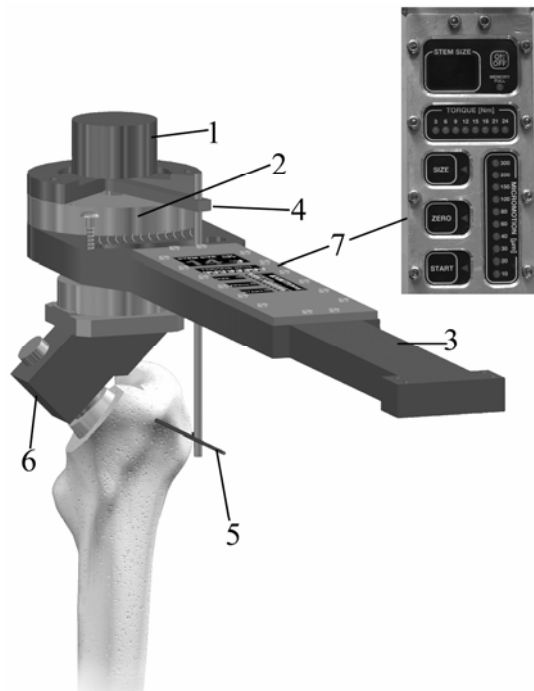


**Fig. 2.3** Sketch of the device. The RVDT angular sensor (1) and the torsional load cell (2) are connected to the handle (3). The angular probe (4), jointed with the shaft, is in contact with the Kirschner nail (5). The probe (4) can move within an angular range of about 70° and is kept into contact with the nail by means of a returning spring. A precision conical tapered connector (6) provides a rigid connection with the stem. It is possible to set the device to right or left simply by unscrewing four screws and rotating the stem connector 180°. The electronics are hosted inside the handle. The surgeon interface (7) is visible on the handle top: the four buttons, the display and the two bi-coloured series of LEDs.

All the components are rigidly connected so as to avoid movements between each part.. A custom designed connector allows an easy and safe insertion of the device exploiting the stem neck modularity. The RVDT angular probe needs a reference point connected to the host bone. For this purpose a Kirschner nail (2.5 mm of diameter) is driven anteriorly on the greater trochanter prior to the insertion of the device. This procedure is little invasive: the patient's soft tissues are not damaged by the Kirschner.

All the electronics are hosted in a cavity machined inside the handle and covered by a thin layer of a special varnish for high temperatures. The analogue signals of the torsional load cell and the RVDT are acquired (sampling frequency: 200Hz), AD converted and processed by a microprocessor (Mod. Atmega128, Atmel, San Jose, California, USA). The surgeon interface (Fig. 2.3), located in the upper side of the handle and clearly visible during the operation, is composed by:

- (i) a two-digit display for the visualization of the stem size set and the residual battery charge;
- (ii) four buttons to select a function of the device;
- (iii) two bi-coloured series of LEDs, indicating the amount of torque applied and the extent of micromotion achieved.

The microprocessor manages the real-time lighting of the LEDs. Moreover data are recorded in a separate memory (Mod. DATAFLASH AT45DB011B, 512Kbyte, Atmel, San Jose, California, USA) for post-operative evaluation. The device is fed by a rechargeable battery (8V), with an autonomy of about 1 hour-recording.

### 2.2.3 Operation of the device

The surgeon turns on and inserts the device; after that he/she sets the stem size by using one button: a corresponding number is visualised on the display. Another button allows the ‘zero-reading’ of the sensors; then, after starting the acquisition by means of another button, it is possible to handle and load the wrench. Following the application of the torque, the device will rotate with respect to the femur together with the stem, and a stem/femur shear motion will occur. The current value of the angle and the torque level achieved yield direct information about the stem/femur shear motion and the extent of implant stability. The device measures an angle and, since the stability threshold is referred to a linear displacement limit, the angular readout must be converted onto a linear displacement (see Calibration, below). When the surgeon applies an increasing torque, the two series of LED turn on, indicating the level of torque and micromovement. Two cases are possible:

- (i) Stable stem: the LEDs light all green indicating the torque and motion levels achieved, with values below the threshold. When the last light LED of the torque-series turns red, it means that the level of torque useful to verify the stem stability is achieved.
- (ii) Unstable stem: the last light LED of the micromotion series turns red at an indicated motion level, which corresponds to the motion threshold being exceeded.

The surgeon can extract the device, and in the first case terminates the stem insertion phase, while in the second he can press harder and repeat the measurement protocol.

## 2.2.4 Validation

The measurement system was validated *in vitro*. In each test the signals from the transducers were recorded and subsequently analysed.

(i) The stability and drift of the signals were quantified. Every part of the system was rigidly fixed, so as to avoid further noise due to possible mechanical vibrations. Then the device was powered and the signals were acquired over 120 seconds. For each acquisition the maximum difference between the values was calculated.

(ii) The mechanical compliance of the device was tested. The angular displacement readout is the sum of the actual angular displacement and the deformation of the device under torsion. The latter one is an artefact that needs to be subtracted from the transducer readout. The aim of these tests was to estimate the stiffness of the device in order to obtain the real angular displacement between stem and femur. For this purpose, the typical torque/angle curve was determined and the angular readout corrected. The device was clamped in a vice and the angular probe was held in contact with the vice. An operator applied to the wrench an increasing load up to 20 Nm (eight replicates). This was needed to exclude possible sensitivity of the angular readout to other spurious load components inadvertently applied by the surgeon when manually loading. During the test, the torque and the angular displacement were recorded.

(iii) The degree of repeatability of the device measurement was evaluated *in vitro*. Two composite femurs were implanted with the same stem (Mod. Ancafit). Composite femurs were used to reduce other sources of variability than the device itself. The device was inserted in the stem and the angular probe put into contact with the Kirschner nail. An increasing load was then manually applied. On the same specimen six repetitions were performed, in the same conditions of press-fitting of the stem. The device was dismantled after each test and the angular probe was detached and then reset into contact with the nail between repetitions. The angular displacement at 10 Nm was analysed.

## 2.2.5 Calibration

The device measures the stem/femur relative rotation angle. Since the stability threshold is referred to a stem/femur linear micromotion, the angular readouts must be converted into

linear displacement values. This is possible by multiplying the measured angle with a radius equivalent of rotation (coefficient of calibration).

This coefficient must account for all the variability due to bone quality, femur morphology and different degree of press fitting of the implanted stem. For this reason, five embalmed re-hydrated femurs were selected by X-ray analysis, so as to host three different sizes of the same kind of stem (Mod. AnCAFit, sizes 13, 14, 16). Additionally, three composite femur models (Mod. 3103, Pacific Res. Labs. Inc., all hosting size 14) were used to represent femurs with an ideal bone quality. An experienced surgeon prepared the femurs to be implanted, in a single session and following the standard surgical protocol.

The calibration was achieved *in vitro* (fig. 2.4) by applying a torque to the device, previously inserted in the implanted femur. The angle values were compared with a reference micromotion on the proximal medial region in the neck resection plane, obtained by a validated *in vitro* protocol. The reference signal from two external LVDT sensors (D5/40G8, RDP Electronics, Wolverhampton, UK) was acquired to measure the linear interface micromotion in parallel with the angular readout. This system allowed the stem/femur shear micro-motion to be measured in a range of  $\pm 1$ mm, with an overall accuracy better than one micron (21,23). The LVDTs were mounted onto metal frames previously glued onto the neck resection cut. A pin connected to the LVDT mobile core was inserted in a  $\varnothing 1$  mm hole drilled on a  $2 \times 2$  mm slab, made of aluminium, glued on the stem neck. The data from the medial LVDT were always used for the calibration, consistently with previous method (14,21,23). The data from the second LVDT were never used for the calibration, but they were useful to interpret stem-bone micromovement.

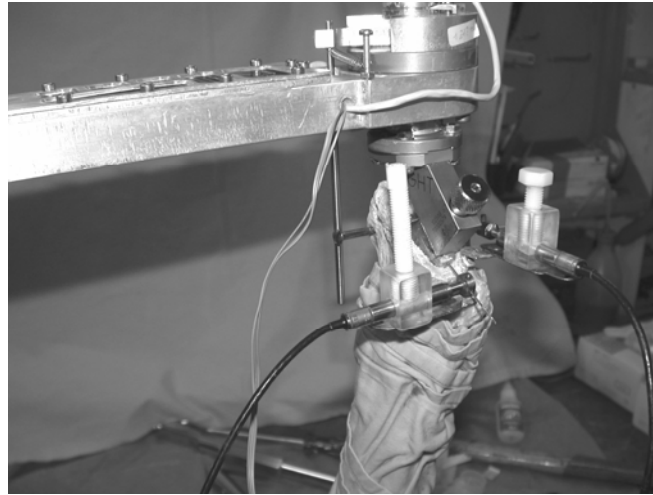


**Fig. 2.4** *Experimental set up for calibration. The device was mounted on the press-fitted stem and the torque was manually applied. The reference LVDTs are visible, mounted on the neck resection.*

The instrumented femur was clamped distally in a vice and the stem was press-fitted, with the help of the standard surgical tools. The device was inserted on the stem and the LVDT in its frame. The angular probe was brought in contact with the Kirschner nail. A torque was manually applied to the handle. Depending on the implant stability, the maximum torque applied reached 15 to 25 Nm (it was reduced for loose implants in order to prevent bone specimen damage). This was made in order to simulate the real surgical technique. Torque, angle and linear shear displacement were recorded. The procedure was repeated six times with the same degree of press-fitting. The device was then removed. The stem was press-fitted further inside the femoral cavity, using the surgical standard instruments. Stability was re-assessed following the procedure above. For each femur two or three degrees of press-fitting were tested (low-medium-good), depending on the bone quality.

The final coefficient of calibration was calculated as the average of the coefficient of calibrations previously found for the single femurs, hosting a stem of the same size. Different coefficients were obtained for the different stem sizes.

## 2.3 Results

### 2.3.1 Noise and drift of the final device

The total fluctuation of the signals from the two transducers were 0.02 Nm for the torque and 0.009° for the angle (equivalent to about 2 micron, considering an average radius of 14mm). These were about two orders of magnitude lower than the expected readout, showing a very stable signal.

### 2.3.2 Stiffness of the final device

The torsional deflection under load was significant, corresponding to about 70 micron of artefactual micromotion with a torque applied of about 22 Nm (Fig.2.5).

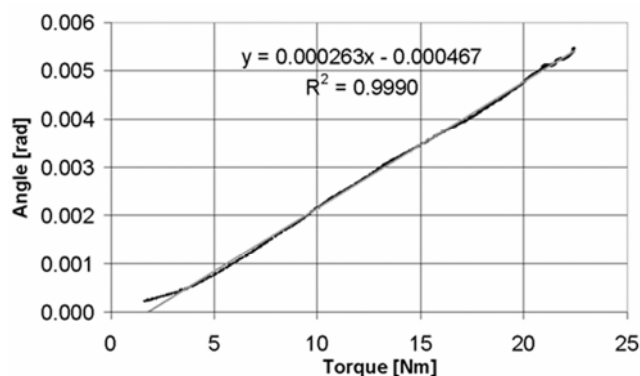


*Fig. 2.5 Typical correlation graph obtained during the validation of the device: torque vs angle. The regression line and  $R^2$  coefficient of an experimental test are reported.*

The artefactual angular readout was almost linear with the torque applied. Linear regression analysis was performed; the RVDT reading must be corrected as follows:

$$angle_{correct} = angle_{readout} - ( A * torque_{readout} + B ) \quad (1)$$

where  $A = (25.8 \pm 0.6) * 10^{-5}$  rad/Nm and  $B = (-58.5 \pm 18.9) * 10^{-5}$  rad, with  $R^2 = 0.99$  and  $RMSE = 0.00007$  rad. This curve is valid only for the loading ramp. The results excluded any significant effect of other load components than the torque applied. The small offset is probably due to hysteresis of the angular transducer. This correction allows eliminating an

artefact of the order of 70 micron (corresponding to a torque of about 22 Nm), leaving an uncertainty of about 1 micron (with the same torque applied).

### 2.3.3 Repeatability

The angular displacement value, corresponding to a 10 Nm torque, was analysed in the six repetitions. The errors were due to the measurement chain on the whole, including the variability in setting the angular probe. The difference among the six values was always less than 10 micron.

### 2.3.4 Calibration

A strong linear correlation ( $R^2 > 0.98$ ) between the angle and the linear displacement values was found in each test (Fig. 2.6). The regression slope of a no-intercept straight angle-linear micromotion line was calculated, along with the  $R^2$  coefficient, the root mean squared error (RMSE) and the peak error between the actual interface motion, measured by the external LVDT, and the predicted one.

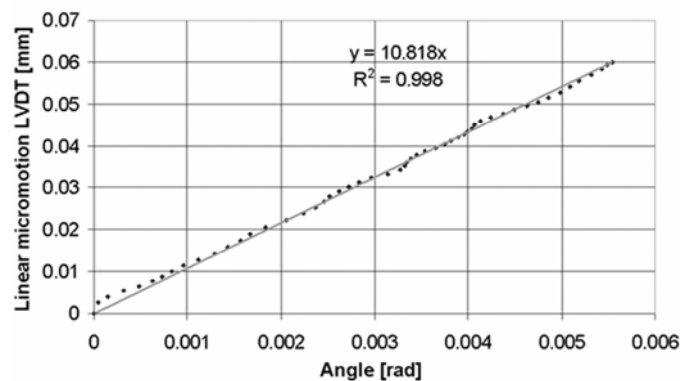


*Fig. 2.6 Typical correlation graph obtained for one test repetition during the calibration of the device: reference interface shear motion vs rotation angle. The regression line and  $R^2$  coefficient of an experimental test are reported*

Some runs were discarded so as to compute a calibration coefficient that was based on clinically relevant cases. First, grossly loose implants were discarded when showing

micromotions greater than 500 micron with a torque of 5 Nm. Then, the Chauvenet criterion was applied to discard outliers (26). 6 runs out of 88 were discarded.

For each stem size, the calibration coefficient was calculated as the average of the angular coefficient for the six repetitions, on the specimen considered (Tab.2.1). The uncertainty of this coefficient was estimated as the CoV over the six repetitions of all the specimens tested of the same stem size. The CoV was computed over the composite sample, the cadaveric sample, and pooling all specimens together.

**Tab.2.1.** Calibration coefficients for each size

Stem size	Calibration coefficient (mean $\pm$ std.dev) (mm/rad)	CoV% Composite femurs	CoV% Cadaveric femurs	CoV% Total
13	11.96 $\pm$ 2.73	-	23	23
14	14.29 $\pm$ 2.95	20	0.5	21
16	17.83 $\pm$ 4.09	-	23	23

Such range of variability (ranging from 21% to 23%) not only includes the repeatability of the device, but also the variability between patients (bone density, morphology, etc.), the variability associated with the stem press-fitting within a given femur, and the variability of the entire measurement procedure (including the position of the Kirschner nail). Therefore, this is the maximum uncertainty that can be expected to affect micromotion measurements in real use, taking into account all possible sources of variation.

The calibration coefficients showed an highly linear correlation ( $R^2 > 0.99$ ) when plotted against the stem sizes.

## 2.4 Discussion

The purpose of this work was to develop a device to test intra-operatively the primary stability of an implanted cementless stem. The final prototype was designed following the initial guidelines and the suggestions from a pilot study. By means of *in vitro* tests it was

verified that the measurement system could provide significant information concerning primary stability. Data processing allowed the real-time comparison between the measured stem/femur displacement and a pre-set micromotion threshold of a 100 micron, together with the indication of the torque level achieved.

Special attention was paid to the accuracy of the signals. All possible error sources were considered and quantified:

(i) The fluctuations of the displacement and the torque signals (2 micron and 0.02 Nm, respectively) are negligible with respect to expected readouts (micromotion threshold of 100 micron with 20 Nm of torque applied)

(ii) The angular displacement readout is the sum of the nominal angular displacement and the deformation of the device under torsion. The *in-vitro* tests demonstrated that such effect is not negligible. With the angular correction, the error with 22 Nm of torque is decreased from about 70 micron to less than 1 micron.

(iii) The repeatability in measuring the angular displacements was investigated. All the possible errors (internal to the device or due to the experimental set up) affecting the measurement were considered. The errors (max 10 micron) are one order of magnitude lower than the expected signal (100 micron threshold) for discriminating stable/unstable implants.

As stated above, the coefficient of calibration provided to convert the angular value measured by the device into a linear shear displacement at the stem/femur interface. The angle and the shear motion can be well described with a linear regression. Data was highly linear, confirming the correctness of linearly converting the angle into a linear displacement. An average coefficient of calibration was subsequently computed for each stem size, which in a way summarises all the single tests coefficients. The coefficient of variation (21%-23%) of this parameter represents the overall accuracy of the measurement method, taking into account:

(i) The overall intrinsic error of the measurement system (including the variability in positioning the Kirschner nail);

(ii) The errors associated with the variability of the motion pattern of the stem within the femoral cavity, due to the differences in stem position inside the canal between press-fitting

repetitions, and to the different position of the microrotation axis. Even if a quantification of these phenomena was not the objective of this study, it is clear that this may have direct consequences on the angular readout, on the linear displacement readout and on their relationship;

(iii) The inter-femur variability. Bone tissue quality of the four cadaveric specimens varied from mildly to severely osteoporotic. Overall femur length was variable from 400 to 450 mm. The composite femurs added to this study (to simulate femurs with a better bone quality) showed a behaviour comparable with human femurs (25). Therefore, it is possible to state that the device was tested and calibrated considering a wide variability of bone quality and geometry.

*In-vitro* protocols with loading conditions similar to this study (14,21,23,27) can measure micromotions up to 600 micron (permanent migration), as well as in a narrower range of 5-50 micron (elastic motions) (14,23,27), exploiting sensors with an accuracy ranging from a fraction of a micron to several micron. The final device presented here has an inherent accuracy of about 1 micron on the full range of interface stem/femur micromotion, for which it was validated and calibrated. Thus it is in line with the typical values just mentioned.

Published *in vitro* protocols that measure repetitive stem micromotion when a torsional load is applied (alone or with axial components) reveal a wide range of experimental variability. When cadaveric femurs are used, the coefficient of variation estimated varies from less than 10% to greater than 100% depending on the test protocol (14,28). This number lowers to 15-50% when composite femurs are tested in similar biomechanical conditions (14,28). The overall accuracy of the measurement protocol here presented (21%-23%) is affected by all these factors, and falls in the typical ranges just quoted. When the device indicates the nominal threshold limit (100 micron), the real interface micromotion could be within 77 to 123 micron. These values are within the ranges indicating critical micromotion (5,7). For all these considerations the overall accuracy appears sufficient to discriminate between definitely stable (few tens of micron) and unstable implants (> 100 micron).

It is acknowledged that the method of this study simplifies the physiological loading conditions: only the torsional moment is applied. This is the most common approach in the literature (4,14,21,22,23,27). Moreover, this was needed to make the intra-operative test simple. The maximum torque level chosen (25 Nm) is comparable with the maximum torque

level found in the *in vitro* literature (4,14,21,22,27) and is basically in agreement with telemetric data from *in vivo* patients (17,18), even if it is lightly reduced. The reduction follows the consideration that the physical activities generating high interface motions, like stair climbing, should be strictly limited in the immediate postoperative period (3,15,22).

The only method directly comparable to the present one is the study of Harris *et al.* (6). The paper of Harris *et al.* does not quantify the overall accuracy. From the description it seems that the contact between the probe and the bone is not always in the same point, changing from anterior to posterior side, depending on the surgical procedure. It is acknowledged that in the present study the position of the Kirschner wire can be slightly changed depending on the anatomy, but this variability is already included in the overall uncertainty (21%-23%). Nevertheless, in the paper of Harris, the contact system, that works as a reference for the displacements, has the advantage of being not invasive. Moreover no quantitative threshold was applied in assessing the stability. To the authors' knowledge no follow up was presented describing a development or the experimental results of this promising idea.

Some limitations of the presented device must be underlined.

(i) The device was tested only with one model of stem (Mod. AncaFit). Generally speaking every kind and/or size of stem has its coefficient of calibration. Using a different prostheses design or a size which is different from the tested ones, the coefficients provided in this study must be adapted before being inserted in the on-board software. Adaptation is possible either with *in vitro* calibration tests or with theoretical considerations. An highly linear correlation ( $R^2 > 0.99$ ) was observed plotting the calibration coefficients against the stem sizes; thus a prediction of the coefficients corresponding to other stem sizes is possible. An *in-vitro* calibration could confirm this theoretical finding.

(ii) The set up of the device depends directly on the operating room constraints. For example, time limitations between any step of a surgical operation restricted the field of solutions concerning the kind of reference on the bone for the angular measurement. The choice of a moderately invasive reference, a Kirschner nail, seemed to the authors a good compromise. It allows a rapid insertion on the greater trochanter, while it provides a rigid fixation in the cortical bone.

This study presented a device to evaluate intra-operatively cementless stem primary stability. The final prototype was successfully designed, validated and calibrated. The overall accuracy

(21%-23%) was considered sufficient to discriminate between a stable and an unstable implant. Data was actually managed in real-time, and the surgeon interface provided clear information concerning stability. The device is ready for clinical trial in the operating room, which is now in progress.

## References

1. Kapandji A. Physiologie articulaire. In La Hanche, Librerie Maloine SA, 1982, Fascicule II.I
2. Rydell NW. Forces acting on the femoral head prosthesis. *Acta Orthopaedica Scand*, 1966, Vol.37 Suppl 88: 96-125
3. Maloney WJ, Jasty M, Burke DW, O'Connor DO, Zalenski EB, Bragdon CR, Harris WH. Biomechanical and histologic investigation of uncemented total hip arthroplasties: A study of autopsy-retrieved femurs after in vivo cycling. *Clin Orthop Rel Res*, 1989, Vol.249:129-40
4. Schneider E, Kinast C, Eulenberger J, Wyder D, Eskilsson G, Perren SM. A comparative study of the initial stability of cementless hip prostheses. *Clin Orthop Rel Res*, 1989, Vol.248: 200-9
5. Søballe K. Hydroxyapatite ceramic coating for bone implant fixation: Mechanical and histological studies in dogs. *Acta Orthop Scand*, 1993, Suppl 255: 1-58
6. Harris WH, Mulroy RD, Maloney WJ, Burke DW, Chandler HP, Zalenski EB. Intraoperative measurement of rotational stability of femoral components of total hip arthroplasty. *Clin Orthop*, 1991, Vol.266: 119-126
7. Pilliar RM, Lee JM, Maniopoulos C. Observations on the effect of movement on bone ingrowth into porous-surfaced implants. *Clin Orthop Rel Res*, 1986, Vol.208: 108-113
8. Goodman SB. The effects of micromotion and particulate materials on tissue differentiation: Bone chamber studies in rabbits. *Acta Orthop Scand*, 1994, Suppl.258: 1-43
9. Ishiguro N, Kojima T, Ito T, Saga S, Anma H, Kurokouchi K, Iwahori Y, Iwase T, Iwata H. Macrophage activation and migration in interface tissue around loosening total hip arthroplasty components. *J Biomed Mater Res*, 1997, Vol.35: 399-406
10. Schutzer SF, Grady-Beson J, Jasty M, O'Connor DO, Bragdon C, Harris WH. Influence of intraoperative femoral fractures and cerclage wiring on bone ingrowth into canine porous coated femoral components. *J Arthroplasty*, 1995, Vol.10: 823-829
11. Schwartz JTJ, Mayer JG, Engh CA. Femoral fractures during non-cemented total hip arthroplasty. *J Bone Joint Surg [Am]*, 1989, Vol.71:8 1135-1142
12. Otani T, Witheside LA. Failure of cementless fixation of the femoral component in total hip arthroplasty. *Ortho Clin North Am*, 1992, Vol.23: 335-346

13. Schmidt AH, Kyle RF. Periprosthetic fractures of the femur. *Ortho Clin North Am*, 2002, Vol.33: 143-152
14. Harman MK, Toni A, Cristofolini L, Viceconti M. Initial stability of uncemented hip stems: an in vitro protocol to measure torsional interface motion. *Medical Eng and Physics*, 1995, Vol.17: 163-171
15. Callaghan JJ, Fulghum CS, Lsisson RR, Stranne SK. The effect of femoral stem geometry on interface motion in uncemented porous-coated total hip prostheses: Comparison of straight-stem and curved-stem designs. *J Bone Joint Surg Am*, 1992, Vol.74: 839-848
16. Nunn D, Freeman MA, Tanner KE, Bonfield W. Torsional stability of the femoral component of total hip arthroplasty: Response to an anteriorly applied load. *J Bone Joint Surg Am*, 1989, Vol.71: 452-5
17. Heller MO, Bergmann G, Deuretzbacher G, Claes L, Haas NP, Duda GN. Influence of femoral anteversion on proximal femoral loading: measurement and simulation in four patients. *Clin Biomech*, 2001, Vol.16: 644-649
18. Bergmann G, Graichen F, Rohlmann A. Is staircase walking a risk for the fixation of hip implants? *J Biomech*, 1995, Vol.28: 535-53
19. Hodge WA, Carlson KL, Fijan RS, Burgess RG, Riley PO, Harris WH, Mann RW. Contact pressures from an instrumented hip endoprosthesis. *J Bone Joint Surg*, 1989, Vol.71-A: 1378-86
20. Kotzar GM, Davy DT, Goldberg WM, Heiple KG, Berilla J, Brown RH, Burnstein AH. Telemeterized in vivo hip joint force data: a report on two patients after total hip surgery. *J Orthop Res*, 1991, Vol.9: 621-33
21. Monti L, Cristofolini L, Viceconti M. Methods for quantitative analysis of the primary stability in uncemented hip prostheses. *Art Org*, 1999, Vol.23: 851-859
22. Phillips TW, Nguyen LT, Munro SD. Loosening of cementless femoral stems: a biomechanical analysis of immediate fixation with loading vertical, femur horizontal. *J Biomech*, 1991, Vol.24: 37-48
23. Baleani M, Cristofolini L, Toni A. Initial stability of a new hybrid fixation hip stem experimental measurement of implant-bone micromotion under torsional load in comparison with cemented and cementless stems. *J Biomed Mater Res*, 2000, Vol.50: 605-615
24. Total Hip Replacement. NIH Consens Statement, 1994, Sep 12-14, 12(5): 1-31

25. Cristofolini L, Viceconti M, Cappello A, Toni A. Mechanical validation of whole bone composite femur models. *J Biomechanics*, 1996 , Vol.29: 525-35
26. Doyle JF, Phillips JW. *Manual of experimental stress analysis*. Society for experimental mechanics, 1991, Vol.24
27. Monti L, Cristofolini L, Toni A, Ceroni RG. In vitro testing of the primary stability of the VerSys enhanced taper stem: a comparative study in intact and intraoperatively cracked femora. *Proc Instn Mech Engrs*, 2001, Vol.215 part H: 75-83
28. Cristofolini L. A critical analysis of stress shielding evaluation of hip prostheses. *Crit Rev Biomed Eng*, 1997, Vol.25: 409-483.

## **CHAPTER 3**

**CAN THE RASP BE USED TO PREDICT INTRA-  
OPERATIVELY THE PRIMARY STABILITY THAT CAN BE  
ACHIEVED BY PRESS-FITTING THE STEM IN  
CEMENTLESS HIP ARTHROPLASTY?**



This work will be submitted on *Clinical Biomechanics*. It is inserted as chapter 3 of the thesis, as it describes the tool that was adapted and validated to verify if it is possible to have a predictive information about the stem stability, when optimally press-fitted, by measuring the micromotion of the rasp.

### **3.1 Introduction**

Primary stability of cementless hip stems plays a crucial role in the long term success of the operation[1, 2]. The initial fixation of cementless hip stems relies on the achievement of a mechanical interlock of the prosthesis in the surrounding bone through proper rasping and press-fitting procedures, in order to limit stem-bone interface micromotion. This goal is achieved if the size of the implanted stem optimizes the proximal and distal fit-and-fill, thus maximizing the stem-bone contact area [3-5]. Surgeon's experience in planning the stem size to be implanted is fundamental for achieving good fixation. However, especially for complicated cases, there is still the risk that the stem size chosen reveals unsuitable[6, 7], resulting in an unstable implant.

Different approaches have been explored aiming to evaluate the extent of stability achieved during surgery. Some intra-operative devices have been developed to aid the surgeon in evaluating the extent of fixation of the stem just implanted[8-10]. Furthermore, several pre-operative subject-specific software packages have been implemented to help the surgeon plan the stem size and type, considering the femur anatomy and geometry of the specific patient [6, 7].

In the clinical practice, different techniques, such as X-ray, Computer Tomography, and Dual Energy X-ray Absorptiometry, are daily used to estimate the bone quality and anatomy of the femur. Pre-operative planning software packages, based on the clinical imaging techniques above, allow the surgeon to estimate the size of the stem that achieves the best fit-and-fill in the patient's femur. However, the final confirmation of the stem size chosen pre-operatively is always intra-operative. In case of pre-operative stem mis-sizing, intra-operative complications may occur. In this case, the surgeon could decide either to extract and replace the stem with the correct size, thus increasing the cost for the overall operation, as well as the operating time. Otherwise the surgeon may opt to yield to sub-optimal implantation, leading to an unpredictable clinical outcome. No system is currently available that allows

determining, during the rasping procedure, if the correct stem size has been chosen pre-operatively. An interview with two experienced surgeons at this institution confirmed that it could be extremely beneficial and helpful if the surgeons were provided with this type of real-time information.

The aim of the present investigation was to assess whether it is possible to have a predictive information on the primary stability of the planned stem, prior to its insertion. This was achieved in three steps:

- Developing an intra-operative tool able to measure the stability of the rasp in the femoral canal
- Confirming *in vitro* if the rasp stability is a good predictor of the maximum primary implant stability that can be achieved once the stem is optimally press-fitted.
- Assessing *in vivo* the feasibility of the intra-operative rasp stability assessment.

## 3.2 Materials and Methods

### 3.2.1 The intra-operative device

Torsional loads represent the most critical condition for primary stability[2, 11]. Therefore it was decided to evaluate the stability of the rasp by measuring the rasp-femur interface micromotion caused by the application of an external torque. An intra-operative rasp stability assessment device (RSAD) was developed (Fig.3.1), based on a wrench previously validated *in vitro*[8] and tested *in vivo* for assessing the stability of the stem.

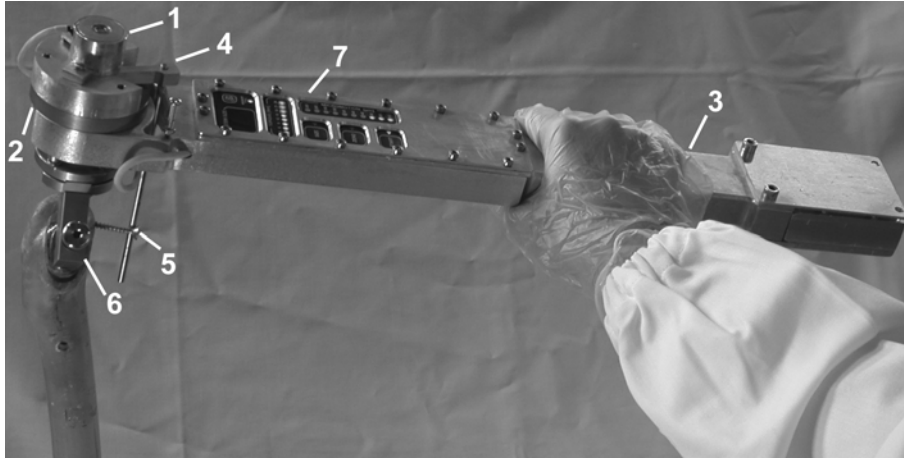


**Fig.3.1** Photo of the RSAD: the RVDT angular sensor (1) and the torsional load cell (2) are connected to the handle (3). The angular probe (4), jointed with the shaft, is in contact with the Kirschner nail (5). The probe (4) can move within an angular range of about 70° and is kept into contact with the nail by means of a returning spring. A precision conical tapered connector (6) provides a rigid connection with the stem. It is possible to set the device to right or left simply by unscrewing four screws and rotating the stem connector 180°. The electronics are hosted inside the handle. The surgeon interface (7) is visible on the handle top: the four buttons, the display and the two bi-coloured series of LEDs.

The RSAD consisted of:

- A connector to secure it to the rasp;
- A torsional load cell to measure the torque applied by the surgeon;
- An angular transducer to measure the relative rotation of the rasp with respect to a reference screw that was secured to the anterior bone surface;
- The electronics for signal conditioning;
- A handle to enable manual application of a torque

The angular readout was converted to the corresponding linear micromotion, through an appropriate calibration coefficient. Torque and micromotion data were acquired at 200Hz, saved on an internal memory and visualized in real time on the surgeon interface. The intrinsic accuracy of the RSAD was 0.04Nm for the torque and 20 micrometers for the micromotion.

### 3.2.2 In vitro validation

For the *in vitro* tests, three cadaveric fresh-frozen human femurs were selected based on Dual Energy X-ray Absorptiometry, in order to cover a wide range of variability in terms of bone quality (Tab. 3.1). Femurs with severe osteoporosis were excluded from the study, as recommended in the surgical practice for cementless hip stems. Additionally, two composite femurs (3103, Pacific Research, Vashon Island, WA, USA) were selected to represent ideal bone quality [12].

Specimen	Height (cm)	Weight (Kg)	Age (years)	Implant size
Donor's 1	178	75	52	15_left
Donor's 2	170	82	49	11_left
Donor's 3	152	64	56	13_right
Patient 1	145	44	51	11_right
Patient 2	170	75	77	15_right

**Tab. 3.1** Data on height, weight, age and implant size are here reported for each cadaveric specimen tested and for the two hip patients that were treated with the RSAD.

The femurs CT-scanned to perform specimen-specific pre-operative planning using the Hip-Op software[7]. During *in vitro* tests, the cadaveric femurs were moistened with cloths soaked with physiological solution. All femurs were implanted with an anatomical cementless hip stem made of titanium alloy (AncaFit, Wright Medical Technology, Arlington, TN, USA). The femurs were clamped distally in a vice with rubber pads. The femurs were first prepared for the implantation by an experienced hip surgeon (familiar with this type of cementless system), following the standard surgical technique. The end of the reaming procedure was defined following the standard surgical criteria: the femoral canal was considered optimal based on the experience of the surgeon, who performed a visual inspection of the motion of the rasp when loaded manually. Furthermore, the surgeon checked his assessment by comparing the depth of the rasp inserted in the femoral canal to the position planned pre-operatively. When rasping of the femoral canal was completed, the surgeon was asked to leave the last rasp used inside the femur, in its final position. Stability of the rasp was measured using the RSAD rasp in three repetitions. A torque of at least 8Nm was applied. During the measurements, the output of the device was blinded to avoid biasing the surgeon.

Then, the surgeon continued with standard stem implantation. Again, the surgeon defined the optimal stem press-fitting by manually loading the press-fitted stem and visually judging the extent of micromotion, as in the routine surgical practice. When stem stability was considered satisfactory based on the surgeon's experience, the surgeon applied the measurement device to the stem. Three measurement repetition were performed on the stem, applying a torque of 15Nm.

In addition, in order to assess if the optimal stem seating defined by the surgeon was indeed the most stable one, the stem was extracted and reinserted three additional times by a different operator, imposing different degrees of press-fitting. The stem stability was recorded for each new degree of press-fitting and compared with that indicated by the surgeon.

### **3.2.3 Preliminary in vivo verification**

In order to verify the clinical applicability of the RSAD just validated *in vitro*, and to verify if *in vitro* data correlated with *in vivo* ones, two *in vivo* sessions were carried out. In order to assess the independence of the methodology from the surgeon, the *in vitro* sessions were carried out at two different medical institutes, under the supervision of two experienced surgeons, implanting the same type of stem tested *in vitro* (AncaFit, Wright). Following the protocol used for the *in vitro* tests, they were asked to apply the intra-operative device first on the last rasp used to prepare the femoral canal, and then on the stem suitably press-fitted. The signals of the RSAD were recorded, however the RSAD was blinded during the clinical session to avoid any biasing of the surgeon. Thus, the rasping and press-fitting procedures were performed exactly as they would have been in the absence of the RSAD. The data recorded in the operating room were processed similarly to the *in vitro* tests.

### **3.2.4 Data processing and statistical analysis**

Torque and micromotion data were processed using custom-made software written in MatLab (7.0, The MathWorks Inc.). A second-order low-pass digital Butterworth filter (cut off frequency 10Hz) enabled to eliminate the high-frequency noise. Several parameters were

preliminarily calculated in order to assess the ones (RASP-PARAMETER and STEM-PARAMETER, respectively) which enabled the best rasp-stem correlation.

Correlation between the RASP-PARAMETER and the STEM-PARAMETER was assessed first considering only the *in vitro* sessions, then including also the series recorded in the operating room.

### 3.3 Results

The RSAD successfully measured rasp stability in all the test sessions. The standard surgical procedure was modified only for the introduction of the two stability-measurement sessions at the end of the reaming process. It was estimated that such additional operations would extend the operating time by 2 min, which is negligible with respect to the 75-80min-duration typical of a standard procedure[13, 14].

Micromotion measurements confirmed that the final stem position (which was deemed satisfactory by the surgeon) was sufficiently stable (<100micrometer at 15Nm)[2, 8, 11]. Furthermore, the stability achieved with the other degrees of press-fitting tested subsequently was similar or poorer to that achieved by the surgeon. This confirmed that the press-fitting recommended by the surgeon can be assumed as optimal possible stem press-fitting.

Observing the typical torque-micromotion curves for the rasp and the stem (Fig.3.2), it was possible to notice that:

- The rasp micromotion showed a highly non-linear trend, with a pronounced “knee”, corresponding to a sudden increase of the micromotion rate; the slope of the first part of the rasp curve ranged between 0.11Nm/micrometer and 1.16Nm/micrometer ( $R^2 \geq 0.88$ ) on all specimens. The second part of the curve (above the “knee”) was characterized by a almost-horizontal line. The slope change occurred between 2.1 – 7.2 Nm.
- The stem micromotion increased linearly in the tested range, with a slope ranging from 0.22Nm/micrometer to 0.51Nm/micrometer ( $R^2 \geq 0.93$ ) on all specimens.

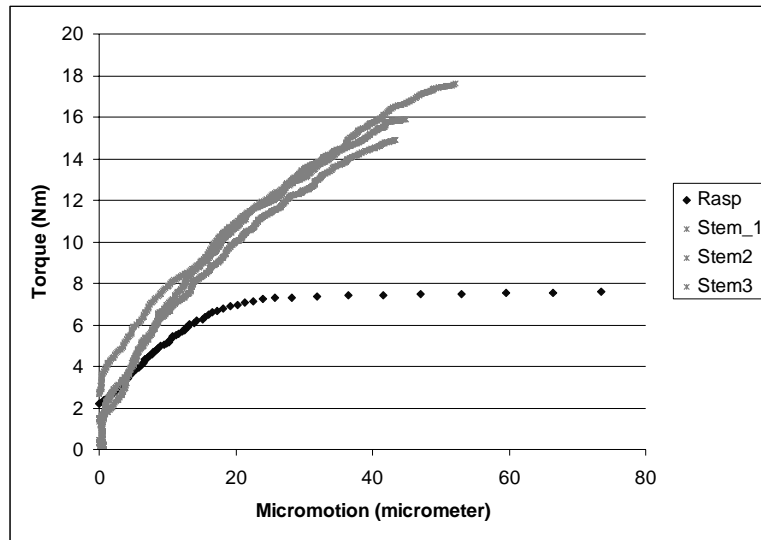


**Fig.3.2** Typical torque micromotion curve measured during the tests, for one specimen. It is possible to observe that the rasp shows a completely non linear behavior, while the stem behaves linearly in the three repetitions.

Among the various indicators preliminarily calculated, the ones that were more robust and better correlated were (Fig.3.2):

- RASP-PARAMETER: as the torque-micromotion curve for the rasp exhibited an uneven slope, the slope of the initial part was obtained. In order to identify the “knee” of the torque-micromotion curve in an operator-independent way, points were iteratively included starting from the lowest torque values; a linear regression analysis was performed at each step. The procedure was stopped when the  $R^2$  coefficient was maximized. The slope of the linear regression for such optimal set of points was assumed as an indicator for the rasp.
- STEM-PARAMETER: As the torque-micromotion curve for the stem stability assessment was highly linear [8], the slope of the linear regression from 0 to 15Nm was assumed as an indicator for the stem.

The RASP-PARAMETER and the STEM-PARAMETER were significantly correlated when the five *in vitro* test sessions were examined (correlation coefficient= 0.745; Fisher Test P-value= 0.0595, Fig.3.3a).

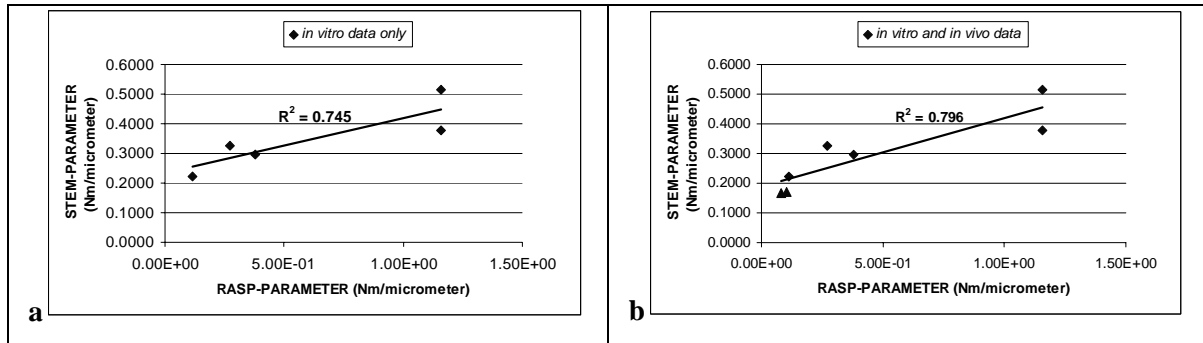


**Fig. 3.3** Result of the correlation analysis between rasp and stem parameters, considering the *in vitro* tests only (a) and both *in vitro* (small rhombs) and *in vivo* (triangles) data (b). The correlation indexes are reported: by adding the two points gathered in the *in vivo* sessions to the *in vitro* ones, the correlation further improved.

The preliminary verification of the protocol in the operating room ran smoothly, with nearly no interaction with the routine procedure. The measurement procedure with the RSAD on the rasp took about 2 minutes. The torque-micromotion curves both for the rasp and for the stem test were similar to those obtained from the *in vitro* specimens. The RASP-PARAMETER and STEM-PARAMETER were calculated also for the *in vivo* sessions. When the two points gathered in the *in vivo* sessions were added to the *in vitro* ones (plotted in Fig.3.3a), the correlation further improved, (correlation coefficient= 0.796, Fisher Test P-value= 0.0069, Fig.3.3b). This confirms that the *in vitro* and *in vivo* measurements belong to the same statistical distribution. It further confirms that the correlation analysis confirmed that the rasp indicator extracted from the *in vitro* trial was the best predictor of the stem stability.

### 3.4 Discussion

In order to provide predictive measurement of the maximum stability that can be achieved by a hip stem, an intra-operative tool (RSAD) was developed to measure the stability of the rasp, when a torsional load was applied. An *in vitro* trial was performed on both composite and fresh frozen cadaveric specimens in order to cover a wide range in terms of bone quality. The results were processed with the aim to find a parameter relative rasp torque-micromotion curve that could be used as a predictor of the stability of the stem, when suitably press-fitted.

The stem was characterized by a linear relation between torque and interface micromotion up to a torque of 20Nm (comparable to stair-climbing[2, 11]). Conversely, the acquisitions made by applying the device to the rasp revealed the presence of a highly non-linear trend: the torque-micromotion diagram for the rasp data was characterized by a first linear part followed by a pronounced “knee” that correspond to a sudden increase in the micromotion rate. That “knee” was probably due to the effect of the different function of the rasp with respect to the stem: the reaming instrument in fact features sharp-edged blades, while, for this study, it could be assumed that the stem has a uniform surface (only the surface material and finish is different between the proximal and distal part). The blades of the rasp are conceived to cut the surrounding bone. Thus the “knee” of the torque-micromotion curve of the rasp could be considered as a threshold, after which the blades of the rasp penetrate the trabecular bone. The second part of the torque-micromotion diagram relative to the rasp showed a consistent increase in the micromotion rate: once the force exerted by the rasp blades overcome the reaction forces of the bone, the torque necessary to rotate the rasp is significantly lower. It was found that the slope of the initial part of the rasp stability curve is the rasp-related indicator that best predict the maximum stability that can be achieved with the stem.

Previous preliminary tests on composite and embalmed cadaveric femurs[15], suggested that stem stability was correlated with rasp stability. From those tests the value of the torque at which the “knee” occurred seemed to be the best indicator of stem stability. However, subsequent tests made in different sessions revealed a great variability of the value of the torque corresponding to the “knee”, depending on the rasp blades and on the quality of the bone, and showed that the RASP-PARAMETER chosen here is more robust.

Preliminary results from replication of the presented protocol on two hip patients allowed to verify that the protocol validated *in vitro* could be easily implemented in the operating room. Moreover, they showed that the proposed indicator (RASP-PARAMETER) yields the same results *in vitro* and *in vivo*, independently of bone quality, different anatomy, and varying sharpness of the rasp blades. Moreover, it was possible to verify that the time for surgery did not increase significantly, nor the procedure got complicated.

As a limitation of the present investigation, the following issue should be highlighted: the present investigation was performed on a single prosthetic design. While it seems reasonable that similar results should be obtained for other anatomical cementless stems, the actual values of the RASP-PARAMETER and STEM-PARAMETER may vary.

In conclusion, an intra-operative procedure was developed, that measured the rasp micromotions in order to predict stem stability during the rasping phase. It enabled extracting reliable indications on the stability of the corresponding stem when optimally press-fitted, regardless to the user, to the patient specific bone quality and to the performance of the rasp.

## References

1. Maloney, W.J., Schmalzried, T., Harris, W. H., *Analysis of long-term cemented total hip arthroplasty retrievals*. Clin Orthop Relat Res, 2002(405): p. 70-8.
2. Schneider, E., Kinast, C., Eulenberger, J., Wyder, D., Eskilsson, G., Perren, S. M., *A comparative study of the initial stability of cementless hip prostheses*. Clin Orthop Relat Res, 1989(248): p. 200-9.
3. Engh CA., Bobyn.J.D., *The influence of stem size and extent of porous coating on femoral bone resorption after primary cementless hip arthroplasty*. Clin Orthop Relat Res, 1988. **231**: p. 7-28.
4. Gotze, C., Steens, W., Vieth, V., Poremba, C., Claes, L., Steinbeck, J., *Primary stability in cementless femoral stems: custom-made versus conventional femoral prosthesis*. Clin Biomech (Bristol, Avon), 2002. **17**(4): p. 267-73.
5. Otani T., Whiteside L.A., White S.E., McCarthy D.S., *Reaming technique of the femoral diaphysis in Cementless Total Hip Arthroplasty*. Clin Orthop Relat Res, 1995. **311**: p. 210-221.
6. Viceconti M, Lattanzi R., Zannoni C, Cappello A, *Effect of display modality on spatial accuracy of orthopaedic surgery pre-operative planning applications*. Med Inform Internet Med, 2002. **27**(1): p. 21-32.
7. Lattanzi R., Viceconti M., Zannoni C., Quadrani P., Toni A., *Hip-Op: an innovative software to plan total hip replacement surgery*. Med Inform Internet Med, 2002. **27**(2): p. 71-83.
8. Cristofolini, L., Varini E., Pelgrefi I., Cappello A., Toni A., *Device to measure intra-operatively the primary stability of cementless hip stems*. Med Eng Phys, 2006. **28**(5): p. 475-82.
9. Harris, W.H., Mulroy RD., Maloney WJ., Burke DW., Chandler HP., Zalenski EB., *Intraoperative measurement of rotational stability of femoral components of total hip arthroplasty*. Clin Orthop Relat Res, 1991(266): p. 119-26.
10. Jeacques, S.V.N., Pastrav C., Zahariuch A., Van der Perre G., *Analysis of the fixation quality of cementless hip prostheses using vibrational technique*. in ISMA. 2004.
11. Harman, M.K., Toni, A., Cristofolini, L., Viceconti, M., *Initial stability of uncemented hip stems: an in-vitro protocol to measure torsional interface motion*. Med Eng Phys, 1995. **17**(3): p. 163-71.
12. Cristofolini, L., Viceconti M., Cappello A., Toni A., *Mechanical validation of whole bone composite femur models*. J Biomech, 1996. **29**(4): p. 525-35.
13. Honl M, Dierk O., Gauck C, Carrero V, Lampe F, Dries S, Quante M, Schwieger K, Hille E, Morlock MM., *Comparison of Robotic-Assisted and Manual Implantation of a Primary Total Hip Replacement: A Prospective Study*. J Bone Joint Surg Am, 2003. **85-A**(8): p. 1470-1478.
14. Kalteis T, Handelm M., Bathis H, Perlick L, Tingart M, Grifka J., *Imageless navigation for insertion of the acetabular component in total hip arthroplasty. IS IT AS ACCURATE AS CT-BASED NAVIGATION?* J Bone Joint Surg Br, 2006. **88-B**(2): p. 163-167.

15. Varini E., Vandi M., Cristofolini L., Cappello A., Viceconti M. *PRIMARY HIP STEM MICROMOTION ASSESSMENT: CORRELATION BETWEEN RASP AND STEM STABILITY*. in *XX Conference of the International Society of Biomechanics*. 2005.

## **CHAPTER 4**

# **INTRA-OPERATIVE EVALUATION OF CEMENTLESS HIP IMPLANT STABILITY: A PROTOTYPE DEVICE BASED ON VIBRATION ANALYSIS**



The following chapter is part of a manuscript that is being published on *Medical Engineering and Physics*. It concerns the development and validation of a device based on the vibration analysis technique to measure the stability of hip prosthesis. The expected advantages of a vibration-based device are easier clinical use, smaller dimensions and minor overall cost with respect to other devices based on direct micromotion measurement.

## **4.1 Introduction**

Cementless hip implants are mechanically stabilized in the host bone during surgery by a press-fitting procedure. The primary mechanical stability achieved by these implants is critical for the long-term outcomes of the operation [1-5]. Various factors affect long-term stability and finally the outcome [5]. It is commonly accepted that one of these is the achievement of a good level of osteointegration between bone tissue and stem surface [5-8]. Osteointegration is possible if the relative stem/bone micromotion is below a certain threshold. In the literature different ranges can be found, from 30 to 150 micrometre [6,9]. In-vitro studies have shown that the largest values of shear micromovement at the stem/femur interface are measured when the torsional moment around the femur axis prevails [4,10-12]. Typical values of physiological torsional moment vary from 15 to 29 Nm [13-18]. The surgeon's experience in planning the type and the size of stem to be implanted is fundamental for achieving good fixation. However, even assuming a theoretically perfect choice, there is still the practical problem of correct positioning of the stem in the femur during surgery. In particular the level of press-fitting during stem insertion is critical. Excessive press-fit of the stem can cause femoral intra-operative fractures (incidence 3% - 28% after uncemented hip replacements [19-22]), thus leading to an unpredictable outcome of the operation. Conversely, if the surgeon does not press-fit enough the stem, the implant moves inside the femur, leading to the formation of a layer of fibrous tissue, thus resulting in the aseptic loosening of the prosthesis [23,24].

The direct intra-operative measurement of the stem-bone micromotion under a torsional load and its comparison with a stability threshold obtained from the literature [7,25] is a possible approach to solve the problem of stability assessment and assist the surgeon in achieving the optimal compromise. A device based on the direct assessment of implant stability was developed

first by Harris *et al.* in 1991 [7]. The method consisted of a torque wrench applied by the surgeon to an implanted stem. The surgeon could also evaluate the displacement between stem and femur, by judging visually the indication of a micrometer dial gauge in contact with the femur and fixed to the stem. In that study the accuracy and the repeatability of the method were not clearly assessed. Recently, a new intra-operative device has been validated [25]. The study describes an instrument, characterized by two highly accurate sensors able to measure in real time and with a good overall accuracy the extent of torque applied by the surgeon and the micromotion achieved at the stem-bone interface. While the system worked satisfactorily, during intra-operative testing the surgeons raised some concerns about the need for dedicated training to obtain accurate measurements.

Recently, a new approach has been explored for assessing stem stability intra-operatively. It is based on the study of the frequency pattern of the implant-bone system, by using vibration analysis. This method has been successfully used to investigate the mechanical properties of the bone and its application to evaluate the extent of fixation of dental implants has been explored [26-29], even if its validity in this field is still under discussion [30]. Several studies have been published recently on the stability assessment of hip implants by mechanical vibration analysis. Li *et al.* [31], in 1996, demonstrated the usefulness of vibration in the diagnosis of implant loosening by considering the amplitude response at all frequencies (within a certain range) and the spectral analysis of particular waveforms. Georgiou and Cunningham [32] performed a comparison of vibration testing and radiographs in patients with total hip replacement and found that the vibration testing method was 20% more sensitive with respect to radiographs and was able to diagnose 13% more patients. They used vibrations up to 1000Hz and discriminated successfully grossly unstable implants from highly stable ones. However, to detect early loosening the method seemed to have insufficient diagnostic sensitivity. Thus, more advanced techniques of excitation and signal analysis seem to be necessary to improve the sensitivity of the technique. Qi *et al.* [33] suggested exciting the implant-bone system with higher harmonics (at least 1000Hz or higher) being more sensitive to implant stability and indicative of interface failure. Confirmation of these results came from Jacques *et al.* [34], who combined experimental testing and simulated modal analysis. Their study demonstrated that the resonance frequency shift of the higher vibration modes of the implant-bone system was the most sensitive parameter to detect the stability of the prosthesis in the femur.

The aim of the present study was to develop and validate a prototype device based on the vibration analysis technique to measure intra-operatively the extent of implant stability. The expected advantages of a vibration-based device are easier clinical use, smaller dimensions and minor overall cost with respect to other devices based on direct micromotion measurement [25]. To do that, the frequency response function (FRF) of the bone-implant system has to be measured, while applying torque to the prosthesis. It is known that a femur implanted with a stable prosthesis behaves linearly, when it is subjected to a mechanical excitation. Grossly unstable implants, on the contrary, show a non-linear response. A system that is in the early stage of loosening, however, still behaves quite similarly to a linear system [34]. Thus, in these cases, using a method based on FRF study is preferred to a harmonic distortion method, which will have a low sensitivity [34]. The device was developed and preliminary tests were performed to set the software parameters and validate the protocol.

## **4.2 Materials and Methods**

### **4.2.1 Description of the prototype device**

#### Rationale

The aim of this work was to excite the stem-bone system to a selected range of frequencies and measure the frequency response function (FRF) before, during, and after the application of external torque. The torsional moment, in fact, causes the highest micromotion at the stem-bone interface [4,10-12]. For this reason the device should be composed of a handle - to be used by the surgeon to apply the torque - and a vibrating system. The direction of the input vibration should be tangential to a circle centred on the axis of the stem-bone system, to produce a torsional vibration (Fig.4.1). A torsional load cell should be connected to the handle from one side and to the stem from the other side through a custom-made connector. The magnitude to be monitored is the acceleration that can be acquired through an accelerometer in contact with the femur and directed tangentially, with reference to the system axis. Based on spectral analysis, the signal can be studied in terms of amplitude, frequency and phase at resonance.

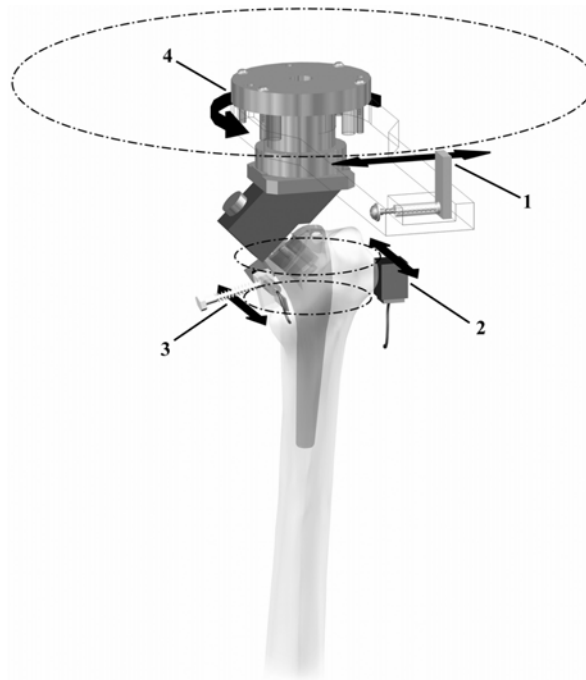


**Fig.4.1** Diagram showing: 1 – vibrating system (CMB); 2 – accelerometer; 3 – additional displacement transducer (LVDT); 4 – torsional load cell. The lines of action of such devices are tangent to circles centered on the stem axis.

At this stage, a laboratory prototype was implemented. However, the most critical components (excitation and measurement systems) were selected and designed for future incorporation in an intra-operative device.

For *in-vitro* validation, an additional sensor would provide a measurement of the micromotion at the stem-bone interface. Thus the results from the spectral analysis could be correlated with the implant stability.

### Transducers

An accelerometer (ADXL210, Analog Devices, measurement range  $\pm 10g$ ) is attached to the greater trochanter of the femur by a small box tightened with a screw, which is inserted in the cortical layer of the bone. The measurement axis of the accelerometer is directed tangentially with respect to the stem-femur axis (Fig.4.1).

A piezoelectric vibrator (CMB, standard part no.B3, Noliac, Denmark, max operating voltage  $\pm 100\text{V}$ , stroke  $\pm 85\text{micrometre}$ , blocking force  $7\text{N}$ , resonance frequency  $2350\text{Hz}$ , max operating temperature  $125^\circ\text{C}$ ) is placed at the external end of the handle and is appropriately powered by a custom-designed amplifier. The vibrator is accurately aligned to cause a tangential vibration of the stem-bone system. More precisely, it is inserted in a cavity machined inside the handle and fastened by a plastic tipped screw. The input signal to the vibrator enables the monitoring of the spectrum of the stem-bone system during the application of the external torque. Thus, the software-generated signal is made by a sum of sinusoidal waves with a fixed shift in frequency ( $\Delta f_{\text{IN}}$ ) and with constant amplitude. Each wave has a randomized phase shift so as to lower the overall amplitude of the signal. Finally, that signal is integrated twice, so as to force the system into constant acceleration. Thus, the transfer function of the stem-bone system is proportional to the spectrum of the accelerometer output.

Attached to the handle is a torsional load cell (Mod.TR11, Leane Int., Parma, Italy, range  $\pm 50\text{Nm}$ ) that measures the extent of the torque applied during the stability test. The other extremity of the load cell is linked rigidly to the prosthesis by an appropriate connector.

To compare the results of the FRF analysis with the actual stem-bone micromotion an additional sensor was used. To this end, a displacement transducer (LVDT Mod.D5/40G8, RDP Electronics, Wolverhampton, UK) is mounted onto a metal frame glued onto the femoral neck resection cut. The LVDT mobile core is kept in contact with an L-shaped aluminum slab glued onto the stem neck. To acquire all signals from the transducers, the system is equipped with an acquisition system (NI6221, National Instruments, U.S.A).

#### Data processing unit

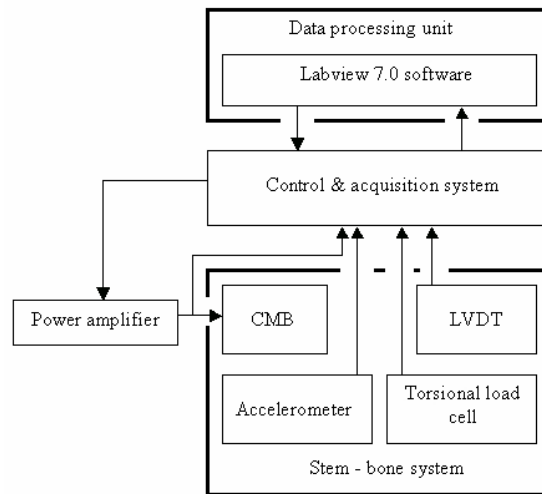


**Fig.4.2** Schedule of the system: CMB, LVDT, accelerometer and torsional load cell are part of the hardware unit; at the top the data processing unit is visible.

The processing unit (Fig.4.2) was developed by software Labview (version 7.0, National Instruments, U.S.A). It generates the control signal for the vibrator amplifier and controls the power of all transducers. Furthermore, the software allows the acquisition of all signals from the transducers and enables the visualization of the results to the user. This is useful, firstly to visualize in real-time the level of torque applied and the extent of micromotion achieved at the interface. Furthermore, at the end of the test, it plots versus time the torque, the implant-bone micromotion and the frequency that cause the highest resonance in the excitation range, in terms of amplitude and frequency of the acceleration signal and the phase of the same signal referred to the excitation signal. To do that, the Short Time Fast Fourier Transform (STFFT) technique was used, with rectangular time windows partly overlapped and with the overlap time selectable by the user. To improve the accuracy for the estimation of the frequency and amplitude at the selected resonance frequency of the system, an algorithm for quadratic interpolation, was used.

Finally, a user-friendly interface was required to set all the parameters for the generation and acquisition of the signals for and from the transducers and for the correct experimental timing.

### Operating procedure

After press-fitting the stem, the operator inserts the device by an appropriate connector. The operator sets the software parameters (see section 4.2.2) as desired. The software, at the beginning of the test, resets to zero all the sensors and generates the excitation signal for the

vibrating system. By pressing a button the acquisition of all the signals is started (excitation, output of the LVDT, output of the accelerometer, output of the torsional load cell). After that, the operator follows the procedure as indicated by the software: at the beginning of the test, during the BEFORE period, the excitation is turned on but the system must not be touched by the operator. After that, the operator applies a torque of up to 15 Nm in a specific period of time (TORQUE). The torque level was chosen at the lower-bound of the interval found in literature [13-18], to simplify intra-operative application while still applying a load that can detect stem instability. The operator follows the lighting up of two LEDs that indicate the correct timing for applying, maintaining and releasing the handle. The value of torque applied and the extent of micromotion achieved at the stem-bone interface are visualized in real-time on a display in order to allow the operator to reach the desired levels. After that, the operator must wait (AFTER), in order to allow the system to recover. Finally, the acquisition stops and the software starts processing the signals acquired, displaying and saving the results. This procedure enables the surgeon to make a decision whether to increase press-fitting or not.

#### **4.2.2 Setting the software parameters**

Preliminary in-vitro tests were carried out in order to set the software parameters with the aim of maximizing the sensitivity and specificity of the protocol and reducing the experimental time and the computational load. To do that, the prototype was mounted on a composite femur (Mod 3103, Pacific Res. Labs. Inc., Vashon Island, WA) implanted with a cementless stem (AnCaFit size 14, Wright Medical Technology, Arlington, TN, USA). Different degrees of press-fitting were considered. The femur was fixed distally with a clamp with vulcanized rubber pads interposed. In these early tests no torque was applied to the stem-bone system. The amplitude spectrum of the accelerometer signal was analyzed to:

- i) Define the frequency range of the excitation signal. The range must be wide enough to enable the detection, for the loaded system, of the frequency corresponding to the highest amplitude peak of the acceleration signal, and the shift of this frequency even up to several tens of hertz (unstable implants) (Fig.4.3). However, the band should include a limited number of components to increase the amplitude of each harmonic (because of the amplification unit, the overall amplitude of this signal must be limited). Finally, a good frequency resolution was

sought. A range of 0-2000Hz was scanned by exciting the system at single frequencies. A simplified setup was used with a femur implanted with different degrees of press-fitting.

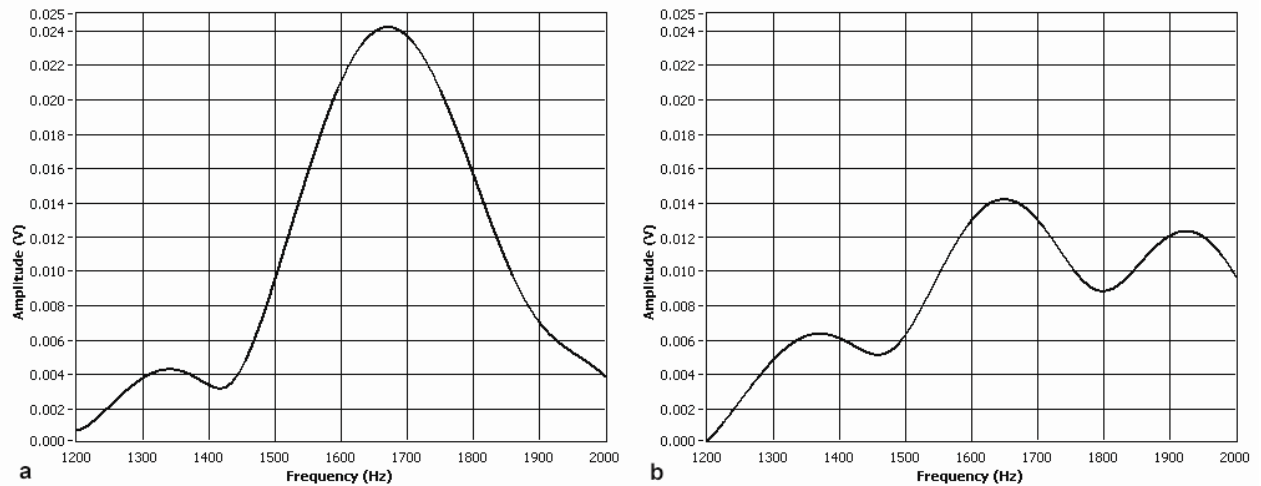


**Fig.4.3** Typical frequency response function (FRF) for a stable (a) and unstable implant (b).

- ii) Define the maximum amplitude of the first spectral component of the excitation signal to achieve good accuracy of the output spectrum and avoid exceeding the full scale of the accelerometer.
- iii) Set the parameters for the correct acquisition of the signal from the accelerometer; the sampling frequency, window length, and window overlap time were set to obtain readable graphs in the time domain and a frequency resolution ( $\Delta f_{\text{STFFT}}$ ) from the STFFT algorithm equal to the resolution of the input signal ( $\Delta f_{\text{IN}}$ ).

To optimize the protocol timing, other tests were performed by simulating the intended use of the device. Thus, during the tests, a torque of up to 15 Nm was applied.

- iv) Define correct timing for each step of the experimental protocol with reference to the operating procedure: at the beginning of the test, before the application of the torque, the excitation is turned on but the system is in a steady state (BEFORE). After that, for the torque application a specific period of time is defined (TORQUE). Finally, the AFTER period allows the system to recover.

### **4.2.3 In-vitro validation**

With the parameters obtained from the preliminary setting trial, the device was tested on four composite femurs implanted with a cementless stem and instrumented with the accelerometer and the additional LVDT. Each specimen during the tests was held distally through a clamp with rubber pads.

Repetitive tests were made with no torque applied, to evaluate the error made in the estimation of the resonance frequency and the amplitude at the resonance frequency in the BEFORE and AFTER periods of the operating procedure.

Furthermore, the above described protocol (see Section 4.2.1) was applied to all the implanted composite bones. All specimens were tested with at least 10 degrees of press-fitting. For loose implants a level of 15Nm of torque applied was not reached, because even with lower values the stem moved macroscopically (i.e. more than 1mm) in the femur.

The amplitude of the accelerometer signal, the shift of the frequency causing the highest resonance in the excitation band, calculated between the BEFORE period and AFTER period, and the output from the displacement transducer were considered for the data processing. In a typical displacement curve, certain points can be distinguished: maximum, permanent and elastic micromotion. The maximum is the highest value reached by the transducer, the permanent is the value registered in the AFTER period, both calculated with respect to the value acquired in the BEFORE period, and the elastic micromotion is the difference between the maximum and the permanent values.

## **4.3 Results**

The prototype device was successfully developed, following the initial guidelines (Fig.4.4).

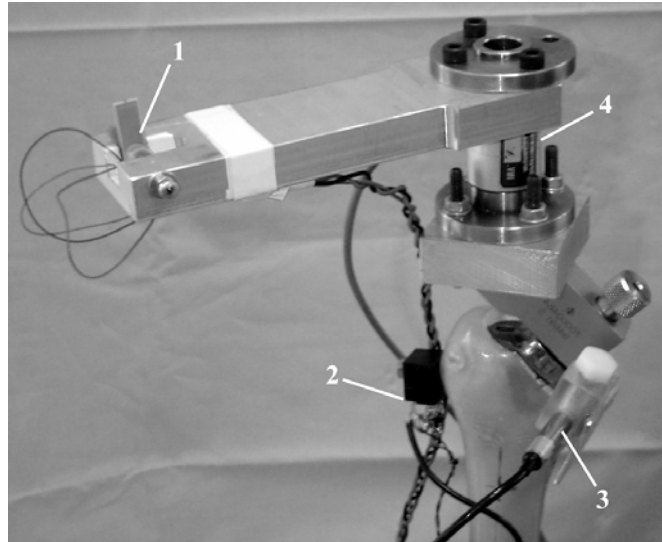


**Fig.4** Photograph of the prototype device: 1 - vibrator system (CMB); 2 – accelerometer; 3 – displacement transducer (LVDT); 4 – torsional load cell.

### 4.3.1 Parameter setting

From the preliminary tests without torque application, the following results were obtained:

- i) The test made exciting the system at single frequencies between 0Hz and 2000Hz showed that the frequency causing the highest amplitude peak was in the range 1400Hz-2000Hz. To take into account the shift of this frequency during loading, 1200Hz-2000Hz was defined as the optimal frequency band for the system excitation. This range allowed the detection of the resonance frequency causing the highest resonance of the stem-bone systems before, during, and after loading, considering different degrees of stability. The frequency resolution ( $\Delta f_{IN}$ ) was set as equal to 5Hz. Thus, 161 sinusoidal waves were overlapped to create the excitation signal.
- ii) The amplitude of the first spectral component (1200 Hz) of the excitation signal was set at 0.8V, which is the maximum value to avoid exceeding the full scale of the accelerometer. Thus, the overall amplitude of the excitation signal reached a value of about  $\pm 50V$ .
- iii) The sampling frequency was set at 62500 sample/s. In the STFFT algorithm, windows grouping 12500 samples were considered to obtain a frequency resolution ( $\Delta f_{STFFT}$ ) equal to that of the excitation signal ( $\Delta f_{IN}$ ). The window shift was set equal to 6250 samples.

- iv) For the protocol, it was decided to fix the duration of the BEFORE period at 2s and the AFTER period at 20s. These values allowed the operator to obtain correct information on the system in the steady states before and after the application of torque. Finally a duration of 10 seconds was chosen for the TORQUE period, in order to obtain a quasi-static loading condition.

### **4.3.2 In-vitro validation**

The results of the tests made without the application of external torque showed that the error on the estimation of the frequency causing the highest amplitude peak in the band 1200-2000Hz was less than 1Hz, thus less than 0.1% of its typical value. Fluctuations of each spectral component of the acceleration signal were less than 1% of the amplitude at the highest resonance.

Regarding the tests performed with the application of external torque, the amplitude and phase spectra showed, for all tests on the four composite femurs, the presence of a high-amplitude resonance frequency in the excitation band considered, more precisely in the range 1550-1700Hz. Furthermore in case of loose implants, in the excitation band more peaks with comparable amplitude were observed in the amplitude spectrum (Fig.4.3).

The frequency-time and amplitude-time plots of the acceleration signal at the highest resonance compared with the data from the LVDT transducer (Fig.4.5e,f), shows that in the case of quasi-stable implants the highest resonance frequency shifts to lower frequencies, while in the stable implant it is constant (Fig.4.5a,b). Furthermore, it seems that irregular changes of the peak at the resonance frequency during the torque application appear when high linear interface micromotions occur, thus in the case of quasi-stable implants (Fig.4.5c,d).

It was observed that generally, during the application of torque, both the frequency that causes the highest peak in the excitation band and the amplitude at that frequency decrease, especially for loose implants. This is mainly due to the damping effect caused by the hand of the operator while using the device.

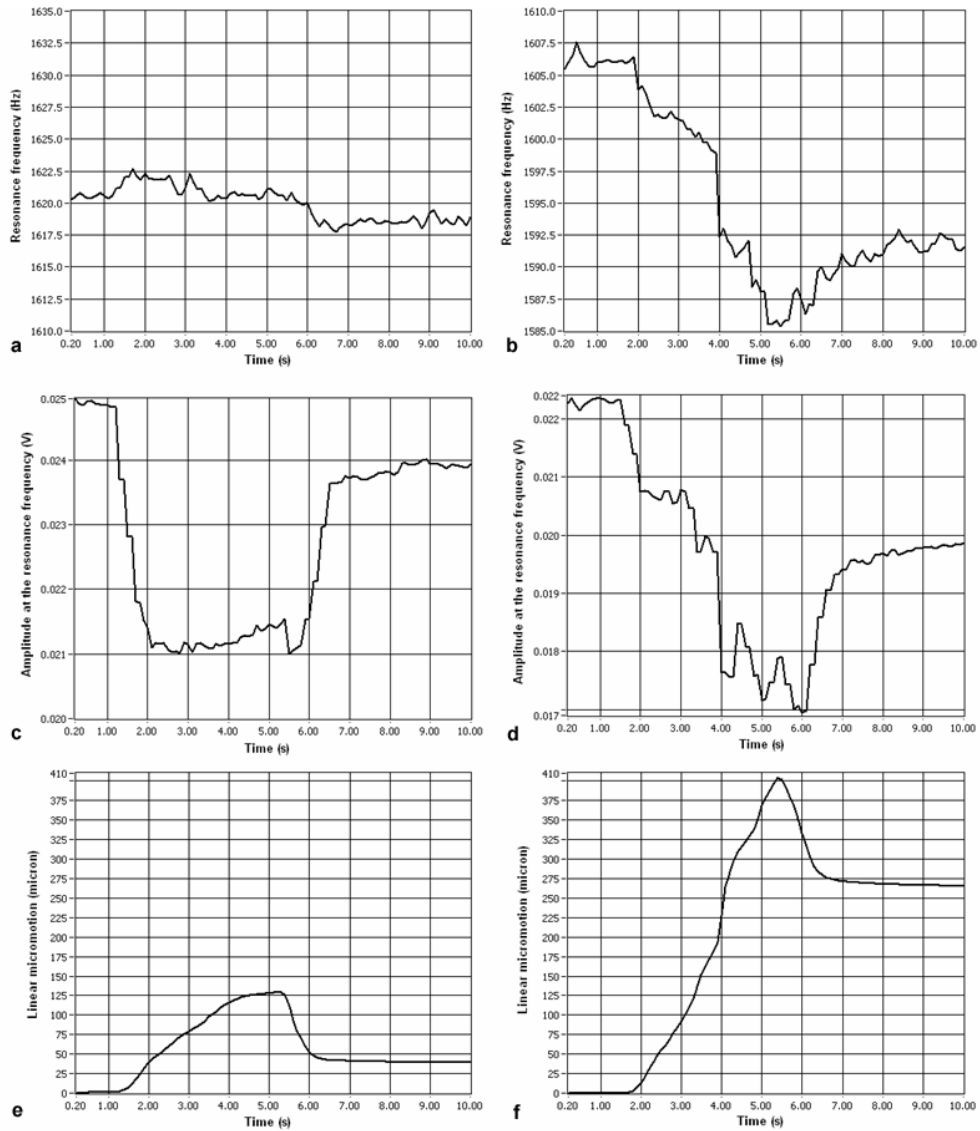


**Fig.4.5** Starting from the top, typical resonance frequency-time plots for a stable (a) and quasi-stable (b) implant are shown; in the central row are the corresponding amplitude-time graphs at the resonance frequency for the stable (c) and quasi-stable (d) case, and on the bottom, are the corresponding linear micromotion-time plots of the stable (e) and quasi-stable (f) implant.

By comparing the phase spectrum to the amplitude one, it seems that the stem-bone system in the excitation range, behaves as a minimum-phase system. Thus, it seems that the phase spectrum does not add information about the implant stability.

Based on the present results, in all the tested specimens a good correlation ( $R^2 \geq 0.90$ ) can be observed between the resonance frequency shift BEFORE-AFTER and the permanent

micromotion (Fig.4.6). However, the correlation line is characterized by a different slope for each specimen.

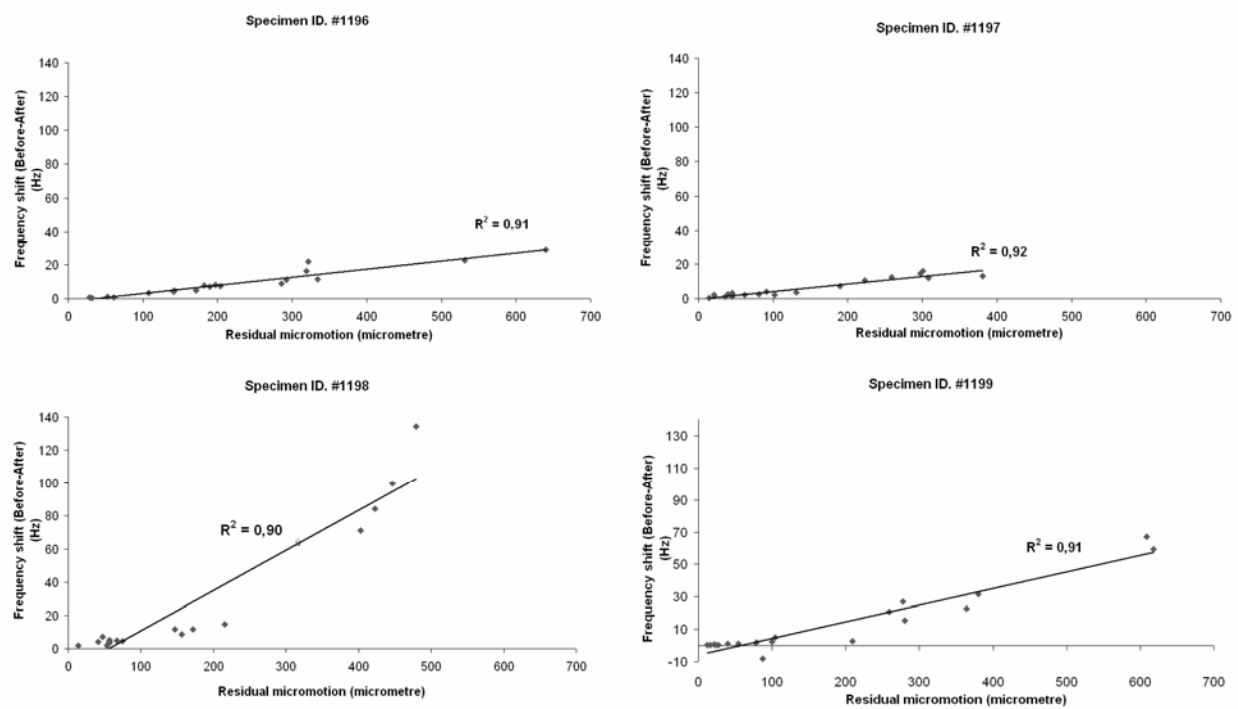


**Fig.6** Graphs of the resonance frequency shift vs residual interface micromotion for the four specimens tested. A regression line was computed for each specimen.

## 4.4 Discussion

The aim of the present investigation was the development of a prototype device, directly connected to the bone and the prosthesis, able to measure intra-operatively the extent of implant stability, by means of vibration analysis.

The technique used in the present work is currently of great interest. Vibrations have been successfully used to investigate the mechanical properties of the bone and its application to evaluate the extent of fixation of dental implants has been explored [26-29], even if its validity in the dental field is still under discussion [30]. More recently, the same technique has been used in orthopedics for the detection of hip implant stability [31-34]. Significant progress has been made, and it seems that a stable implant can be discriminated from a grossly unstable one by studying the harmonic content of the implant-bone system, when subjected to excitation. However, to help the surgeon evaluate the degree of fixation of an implant, it is necessary to detect also when the stability is not so good and the loosening not so evident. Therefore, computational studies have been carried out [33,34]. These studies have shown that to discriminate the quasi-stable cases, it necessary to study the high-frequency (above 1000Hz) response of the stem-bone system [33,34].

The device described in the present study was conceived to monitor the spectral content of the stem-bone system in the 1200-2000Hz range during the application of external torque and not only before or after that. The device, as in its current state, can not yet be actually considered as an intra-operative device. In fact, the power supply and amplification units must be miniaturized and the connections should be wireless. However, small-sized components were selected for the piezoelectric vibrator and the torsional load cell that can withstand autoclave and EtO sterilization. The accelerometer, being a low-cost sensor and having to be attached directly to the patient's body (through a Kirschner wire), could be a single-use device. The Authors' aim for the immediate future is to continue the development of the device towards intra-operative use. During the foreseen intra-operative use of the device, the surgeon, after "reading" the degree of implant stability, would complete the surgical procedure, if the stem were securely fixed. If the stem were not sufficiently stable, the surgeon would repeat the press-fitting procedure, and if necessary could decide to implant a different stem size.

The excitation band considered in this study was consistent with the results found in the literature; in fact, the input excitation is in a frequency range higher than 1000Hz as suggested by Jaecques S.V.N. *et al.* [34], but it is not included in the most sensitive band (higher than 2500Hz) as reported by Qi G. *et al.* [33], because of limitations imposed by the particular vibrating system. The CMB piezoelectric vibrator, in fact, has its own resonance of 2350Hz, thus it would be not suitable to exceed the limit of 2000Hz. Preliminary results from replication of the

protocol on four composite bones confirmed the suitability of the excitation frequency range chosen.

The in-vitro trial was carried out successfully. The device showed good repeatability in the generation of the excitation signal and high accuracy in the acquisition of the output signal from the accelerometer. The preliminary tests on the four specimens revealed the presence of one high-amplitude resonance frequency in the excitation range for stable implants, while for loose prostheses several resonance frequencies with comparable amplitudes were found in the excitation range. This result confirmed those found by Georgiou and Cunningham [32].

The preliminary results on the tested specimens confirmed the ability of this instrument to discriminate between different levels of stability. In particular, the magnitudes that showed the best correlation with the implant stability were the frequency and the amplitude at the highest peak in the amplitude spectrum of the system in the frequency range considered. Furthermore, it was observed that, even with permanent micromotion at the implant-bone interface typical of quasi-stable implants, the phase and amplitude spectra showed changes accurately detected by the device. Thus, it seems that the proposed device is able to evaluate the implant stability, discriminating between many levels of fixation: stable, loose and quasi-stable implants. However, it must be highlighted that inter-femur variability was not negligible, as the slope of the correlation graph was different for each specimen. Furthermore, it was noticed that if only low residual micromotions were considered (e.g. <500micrometre), the inter-specimen variability lowered significantly. This observation may be explained by considering that most of the tests were made at the borderline of stability, thus the cases showing high residual micromotions (>500 micrometre) were relatively few. Therefore an error on one of these tests had a great influence on the slope of the correlation line.

More tests, also involving human femurs, are needed to elucidate if inter-specimen variability would prevent from defining a single stability threshold that applies independently of bone geometry, bone quality, canal preparation, etc.

While it is not yet possible to quantify a threshold for discriminating between a stable and a quasi-stable implant in general, from the presented results it can be speculated that it would be of the order of a few hertz, probably less than 10Hz. In fact, based on the correlation between the frequency shift during loading and the residual micromotion, it seems that a shift higher than 5Hz corresponds to 150micrometre or more of permanent micromotion, which could be

considered a border value for the activation of the osteointegration process [3,6,8,9]. More tests on cadaveric specimens are needed to estimate this value accurately.

Conversely, the present results seem to indicate that the analysis of the phase spectrum does not add significant information to the analysis of the resonant frequency (amplitude and frequency shift), i.e. it behaves like a minimum-phase system. This is not in agreement with Qi *et al.* [33]: they reported that the phase angle analysis reveals more differences than the amplitude frequency. However, direct comparison between the present study and the one by Qi *et al.* [33] is not possible as: (i) Qi *et al.* present a merely numerical simulation; (ii) they modelled cemented fixation; (iii) either complete debonding or perfect bonding was simulated on a fraction of the stem surface.

The reported differences in the frequency responses of a stable and quasi-stable implant could be interpreted by considering the physical properties of the system. The resonance frequency and the corresponding amplitude depend both on the interface torsional stiffness and on the system inertia. Thus, the frequency and amplitude shifts observed during the external torque application (Fig.5) could be explained in terms of changes in the interface torsional stiffness. This interpretation is valid only for stable and quasi-stable implants. On the other hand, if the implant is largely unstable, it is no more necessary to accurately measure its degree of instability.

This study has some limitations:

- The device was tested on composite specimens, thus in order to confirm the obtained results more experimental tests are needed, both on composite and cadaveric specimens.
- The *in-vitro* tests performed, did not simulate all the surrounding tissues (muscles, tendons, ligaments, etc.) that are involved in the actual use of the device. Preliminary results indicate that the presence of such tissues would affect the amplitude of the acceleration signal (by up to 40%), due to the soft tissue damping effect. Conversely the resonance frequency is virtually unaffected (<2Hz variation) by soft tissues surrounding the bone [35].

To confirm and possibly improve the results, a more complete trial of *in-vitro* tests on composite and cadaveric femurs is now in progress [35], including simulation of surrounding soft tissues.

## **References**

1. Kapandji, A., Physiologie articulaire, In La Hanche, Librerie Maloine SA, 1982, Fascicule II.I.
2. Rydell, N.W., Forces acting on the femoral head prosthesis, *Acta Orthopaedica Scand*, 1966, 37 Suppl 88, pp.96-125.
3. Maloney, W.J., Jasty, M., Burke, D.W., O'Connor, D.O., Zalenski, E.B., Bragdon, C.R., Harris, W.H., Biomechanical and histologic investigation of uncemented total hip arthroplasties: A study of autopsy-retrieved femurs after in vivo cycling, *Clin Orthop Rel Res*, 1989, 249, pp.129-40.
4. Schneider, E., Kinast, C., Eulenberger, J., Wyder, D., Eskilsson, G., Perren, S.M., A comparative study of the initial stability of cementless hip prostheses, *Clin Orthop Rel Res*, 1989, 248, pp. 200-9.
5. Mjöberg, B., The theory of early loosening of hip prostheses, *Orthopedics*, 1997, 20 (12), pp.1169-75.
6. Søballe, K., Hydroxyapatite ceramic coating for bone implant fixation: Mechanical and histological studies in dogs, *Acta Orthop Scand*, 1993, Suppl 255, pp. 1-58.
7. Harris, W.H., Mulroy, R.D., Maloney, W.J., Burke, D.W., Chandler, H.P., Zalenski, E.B., Intraoperative measurement of rotational stability of femoral components of total hip arthroplasty, *Clin Orthop*, 1991, 266, pp. 119-126.
8. Brånemark, R., Ohnells, L.O., Skalak, R., Carlsson, L., Branemark, P.I., Biomechanical characterization of osteointegration: an experimental in-vivo investigation in the beagle dog, *J Orthop Res*, 1998, 16 (1), pp.61-9.
9. Pilliar, R.M., Lee, J.M., Maniopoulos, C., Observations on the effect of movement on bone ingrowth into porous-surfaced implants, *Clin Orthop Rel Res*, 1986, 208, pp. 108-113.
10. Harman, M.K, Toni, A., Cristofolini, L., Viceconti, M., Initial stability of uncemented hip stems: an in vitro protocol to measure torsional interface motion, *Med Eng Phys*, 1995, 17, pp. 163-171.
11. Callaghan, J.J., Fulghum, C.S., Lsisson, R.R., Stranne, S.K., The effect of femoral stem geometry on interface motion in uncemented porous-coated total hip prostheses: Comparison of straight-stem and curved-stem designs, *J Bone Joint Surg Am*, 1992, 74, pp. 839-848.

12. Nunn, D., Freeman, M.A., Tanner, K.E., Bonfield, W., Torsional stability of the femoral component of total hip arthroplasty: Response to an anteriorly applied load, *J Bone Joint Surg Am*, 1989, 71, pp. 452-5.
13. Heller, M.O., Bergmann, G., Deuretzbacher, G., Claes, L., Haas, N.P., Duda, G.N., Influence of femoral anteversion on proximal femoral loading: measurement and simulation in four patients, *Clin Biomech*, 2001, 16, pp. 644-649.
14. Bergmann, G., Graichen, F., Rohlmann, A., Is staircase walking a risk for the fixation of hip implants?, *J Biomech*, 1995, 28, pp. 535-53.
15. Hodge, W.A., Carlson, K.L., Fijan, R.S., Burgess, R.G., Riley, P.O., Harris, W.H., Mann, R.W., Contact pressures from an instrumented hip endoprosthesis, *J Bone Joint Surg*, 1989, 71-A, pp. 1378-86.
16. Kotzar, G.M., Davy, D.T., Goldberg, W.M., Heiple, K.G., Berilla, J., Brown, R.H., Burnstein, A.H., Telemeterized in vivo hip joint force data: a report on two patients after total hip surgery, *J Orthop Res*, 1991, 9, pp. 621-33.
17. Bergmann, G., Deuretzbacher, G., Heller, M., Graichen, F., Rohlmann, A., Strauss, J., Duda G.N., Hip contact forces and gait patterns from routine activities, *J Biomech*, 2001, 34, pp.859-71.
18. Heller, M.O., Bergmann, G., Deuretzbacher, G., Durselen, L., Pohl, M., Claes, L., Haas, N.P., Duda, G.N., Musculo-skeletal loading conditions at the hip during walking and stair climbing, *J Biomech*, 2001, 34, pp.883-93.
19. Schutzer, S.F., Grady-Beson, J., Jasty, M., O'Connor, D.O., Bragdon, C., Harris, W.H., Influence of intraoperative femoral fractures and cerclage wiring on bone ingrowth into canine porous coated femoral components, *J Arthroplasty*, 1995, 10, pp. 823-829.
20. Schwartz, J.T.J., Mayer, J.G., Engh, C.A., Femoral fractures during non-cemented total hip arthroplasty, *J Bone Joint Surg [Am]*, 1989, 71(8), pp. 1135-1142.
21. Otani, T., Witheside, L.A., Failure of cementless fixation of the femoral component in total hip arthroplasty, *Ortho Clin North Am*, 1992, 23, pp. 335-346.
22. Schmidt, A.H., Kyle, R.F., Periprosthetic fractures of the femur, *Ortho Clin North Am*, 2002, 33, pp. 143-152.

23. Goodman, S.B., The effects of micromotion and particulate materials on tissue differentiation: Bone chamber studies in rabbits, *Acta Orthop Scand*, 1994, Suppl.258, pp 1-43.
24. Ishiguro, N., Kojima, T., Ito, T., Saga, S., Anma, H., Kurokouchi, K., Iwahori, Y., Iwase, T., Iwata, H., Macrophage activation and migration in interface tissue around loosening total hip arthroplasty components, *J Biomed Mater Res*, 1997, 35, pp. 399-406.
25. Cristofolini, L., Varini, E., Pelgrefi, I., Cappello, A., Toni, A., Device to measure intra-operatively the primary stability of cementless hip stems, *Med Eng Phys*, 2006, 28(5), pp.475-82.
26. Lowet, G, Van Audekercke, R, Van der Perre, G, Geusens, P, Dequeker, J, Lammens, J., The relation between resonant frequencies and torsional stiffness of long bones in vitro. Validation of a simple beam model., *J Biomech*, 1993, 26(6), pp. 689-96.
27. Van Der Perre, G, Lowet, G., In vivo assessment of bone mechanical properties by vibration and ultrasonic wave propagation analysis, *Bone*, 1996, 18(1 Suppl), pp. 29S-35S.
28. Meredith, N., Shagaldi, F., Alleyne, D., Sennerby, L., Cawley, P., The application of resonance frequency measurements to study the stability of titanium implants during healing in the rabbit tibia, *Clin. Oral. Impl. Res.*, 1997, 8(3), pp. 234-243.
29. Friberg, B., Sennerby, L., Linden, B., Gröndahl, K., Lekholm, U., Stability measurements of one-stage Brånemark implants during healing in mandibles. A clinical resonance frequency analysis study, *Int. J. Oral Maxillofac. Surg.*, 1999, 28, pp. 266-272.
30. Koka, S., Commentary on resonance frequency analysis, *Int J Prosthodont*, 19(1), p.84.
31. Li, P.L.S., Jones, N.B., Gregg, P.J., Vibration analysis in the detection of total hip prosthetic loosening, *Med.Eng.Phys.*, 1996, 18(7), pp. 596-600.
32. Georgiou, A.P., Cunningham J.L., Accurate diagnosis of hip prosthetic loosening using a vibrational technique, *Clin Biomech*, 2001, 16, pp. 315-323.
33. Qi, G, Mouchon, W.P., Tan, T.E., How much can a vibrational diagnostic tool reveal in total hip arthroplasty loosening?, *Clin Biomech*, 2003, 18, pp. 444-458.
34. Jaecques, S.V.N., Pastrav, C., Zahariuc, A., Van der Perre, G., Analysis of the fixation quality of cementless hip prostheses using a vibrational technique, *Proc. International Conference on Noise and Vibration Engineering*, 2004, pp.443-456.

35. Varini, E., Lannocca, M., Bialoblocka, E., Cappello, A., Cristofolini, L., Primary stability assessment in hip arthroplasty: a device based on the vibrational technique, *J Biomech*, 2006, 39 Suppl. 1, p.S127.

## **CHAPTER 5**

### **IN VITRO MEASUREMENT OF THE FREQUENCY RESPONSE FUNCTION OF STEM-BONE SYSTEMS FOR THE EVALUATION OF IMPLANT STABILITY**



The topic of this section concerns the results of *in-vitro* tests performed both on composite and cadaveric specimens by using the device based on the vibration analysis technique described in the previous chapter. From the results it seems that the parameter that best correlate with the implant stability is the shift of the resonance frequency of the stem-bone system, measured on the system in the phases “before” and “after” the application of an external torque. This chapter is part of a paper that will be sent to the Journal of Sound and Vibrations.

## 5.1. Introduction

The vibration analysis technique is largely used to monitor structures integrity. In most cases, vibration-based methods can offer an effective and convenient way to detect cracks in a target object by monitoring changes in the resonant frequencies, in the mode shapes or in the damping factors [1-7]. Vibration analysis has been successfully introduced in the biomechanical field to investigate the mechanical properties of the bone [8,9]. Furthermore, a possible application to evaluate the extent of fixation of dental implants has been explored [10,11], even if its validity in this field is still under discussion [12].

Cementless hip implants are mechanically stabilized in the host bone during surgery by a press-fitting procedure. It is recognized that a prosthesis that is firmly fixed in the surrounding bone moves less than 150microns, if at least 15Nm of torsional load is applied. Thus, the stability of this prosthesis type relay on the achievement of a good mechanical interlock between stem and bone. As the primary mechanical stability achieved by these implants is critical for the long-term outcomes of the operation [13-15], in the biomechanical field there has been a lot of concerns about the development of reliable methods for measuring the degree of implant stability.

A first approach to solve that problem was explored in the latest years. It was based on the direct micromotion as a consequence of a torque application. The device was implemented and thoroughly validated. It featured good results, sufficient accuracy but quite complicated operation technique [16].

Recently, several studies have been published on the assessment of the stability of cementless hip implants by vibration analysis. The main findings could be listed as follows:

- the amplitude response at all frequencies (within a certain range) and the spectral analysis of particular waveforms could be successfully used to diagnose implant loosening [17];

- the vibration testing method was found 20% more sensitive with respect to radiographs and was demonstrated being able to diagnose 13% more patients with total hip arthroplasty [18];
- the implant-bone system should be excited with higher harmonics (at least 1000Hz or higher) being more sensitive to implant stability and indicative of interface failure [19];
- the resonance frequency shift of the higher vibration modes of the implant-bone system seems to be the most sensitive parameter to detect the stability of the prosthesis in the femur [20].

In summary, as indicated in previous studies by several authors, vibration-based methods have been largely explored with the aim to evaluate the stability of a cementless stem by means of a simple, accurate and cost-effective technique. These methods seem to be sensitive and accurate enough to evaluate the interface micromotion, even if a validation of those findings is still challenging.

The research reported in this paper refers to an in-vitro trial made both on composite and cadaveric specimens with the aim to demonstrate if it is possible to evaluate the extent of stability of a cementless prosthesis by using a device based on the vibration analysis technique. In particular, this work was devoted to validate the ability of a vibration-based method to discriminate between stable and quasi-stable implants, which represents the most critical decision for the surgeon during operation.

## 5.2. Simplified model of the system

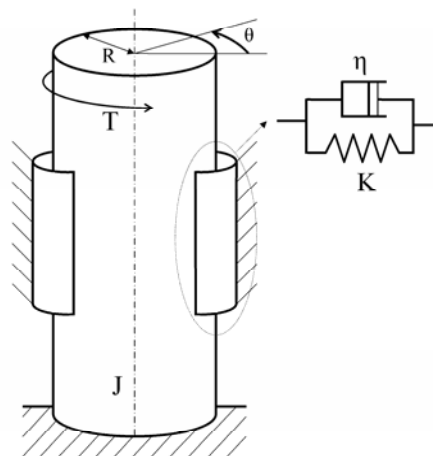


*Fig. 5.1 Schematic of the reference explanatory model.*

A simplified model of the stem-bone system could help understanding the main issues related to the device design (Fig.5.1). It is simply composed of a cylinder, representing the bone-prosthesis system, and a coupling that replicates the mechanical behaviour at the stem-femur interface. As the bone during the test was clamped distally in a vice, in the simplified model a fixed joint is provided as constrained condition for the cylinder. Furthermore, the cylinder is characterized by a moment of inertia  $J$  ( $\text{Nms}^2\text{rad}^{-1}$ ), with respect to the longitudinal axis of the femur. The interface between stem and bone was assumed to behave as a “spring-damper” complex, characterized by  $n$  ( $\text{Nms rad}^{-1}$ ), as coefficient of torsional viscosity, and  $K$  ( $\text{Nm rad}^{-1}$ ), as coefficient of torsional stiffness (Fig.5.1). If an external torsional excitation  $T$  ( $\text{Nm}$ ) is applied to the cylinder, the stem-bone system behaves as a II order system. In the Fourier domain, the transfer function of the system  $G(j\omega)$  involves the motion  $\theta(j\omega)$  of the stem with respect to the femur and the torque applied  $T(j\omega)$ . In particular, the resonance frequency and the amplitude at resonance are described as follows:

$$\omega_p = (K/J)^{1/2} \cdot (1 - \eta^2/2KJ)^{1/2} \quad [\text{rad/sec}]$$

$$|G(j\omega_p)| = (\eta/(KJ))^{1/2} \cdot (1 - \eta^2/4KJ)^{1/2}^{-1}$$

Different degrees of press-fitting of the stem into the femur correspond to different coefficient of torsional stiffness  $K$  at the interface. Thus, if a variation in  $K$  occurs, a shift in the resonance frequency and amplitude at resonance will be observed.

As several torsional modes of vibration characterize the stem-bone system, it was decided to study the one the features the highest amplitude in the excitation range. The acceleration  $a(t)$  was measured through an accelerometer placed in contact to the femur. The idea was to study the spectrum of the acceleration signal in terms of amplitude, frequency and phase, considering the highest resonance in the frequency range excited. It was thought that in this way it would be possible to gain information on the behaviour of the stem-bone interface during the application of an external torque.

## 5.3 In-vitro testing

### 5.3.1 The measurement device

The device is conceived to excite the bone-prosthesis system to a selected range of frequencies and measure the frequency response function (FRF) before, during, and after the application of external torque [16]. It is essentially made by a handle for the torque application, a torsional load cell that measure the amount of load applied to the system, an accelerometer and an exciter. The latter involves a piezoelectric vibrator (CMB, standard part no.B3, Noliac, Denmark, max operating voltage  $\pm 100V$ , stroke  $\pm 85\mu\text{m}$ , blocking force 7N, resonance frequency 2350Hz, max operating temperature  $125^\circ\text{C}$ ), which is placed at the external end of the handle. Attached to the greater trochanter of the bone is the accelerometer (ADXL210, Analog Devices, measurement range  $\pm 10g$ ). Both exciter and accelerometer are aligned so as to excite and measure, respectively, in the same direction tangential to an ideal circle centered on the bone-prosthesis axis (Fig.5.2). The input signal to the vibrator is software-generated to force the system into constant acceleration. This method allowed the transfer function of the system to be proportional to the spectrum of the accelerometer output. For this reason, the accelerometer output was studied in both time and frequency domains.

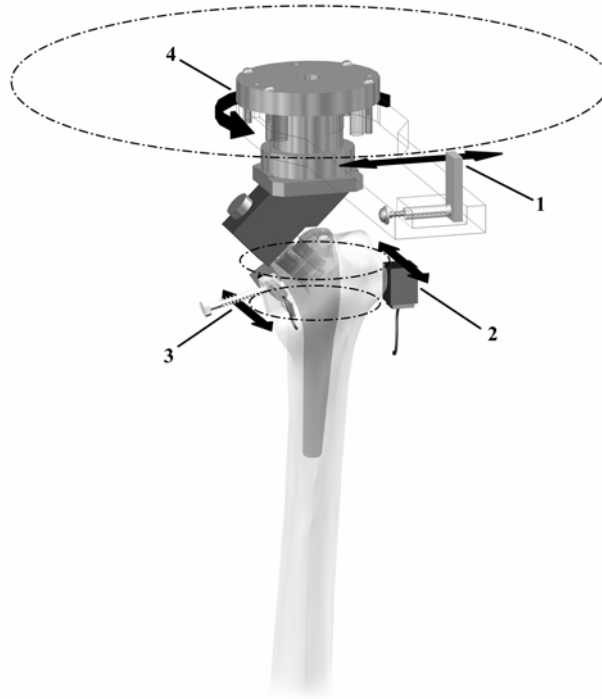


**Fig. 5.2** Diagram showing: 1 – vibrating system (CMB); 2 – accelerometer; 3 – additional displacement transducer (LVDT); 4 – torsional load cell. The lines of action of such devices are tangent to circles centered on the stem axis.

### 5.3.2 In-vitro testing protocol

Four fresh frozen cadaveric specimens were selected for testing, based on the Dual Energy X-ray Absorptiometry exam, in order to cover a wide range of variability in terms of bone quality. Additionally, one composite femur was added as control specimen. Those bones showing a high degree of osteoporosis were excluded from the experimentation, as it is recommended in the surgical practice for cementless implants.

Each specimen was CT-scanned so as to perform specimen-specific pre-operative planning using the Hip-Op software (Lattanzi R. et al, 2002). During in-vitro tests, the cadaveric specimens were moistened with cloths soaked with physiological solution. All the specimens were clamped distally in a vice with rubber pads. The femurs were first prepared for the implantation by an experienced hip surgeon (familiar with this type of cementless system), following the standard surgical technique.

By manually loading the press-fitted stem and visually judging the extent of micromotion, as in the routine surgical practice, the surgeon defined optimal the stem press-fitting. Thus, he stopped the implantation procedure and started measuring implant stability. Three measurement repetitions were performed, applying a torque up to 15Nm. Data were acquired (NI6221, National Instruments, U.S.A) and analyzed in both time and frequency domains.

In order to compare the results of the FRF analysis with the actual stem-bone micromotion an additional sensor was used. To this end, a displacement transducer (LVDT Mod.D5/40G8, RDP Electronics, Wolverhampton, UK) was mounted onto a metal frame glued onto the femoral neck resection cut. The LVDT mobile core was kept in contact with an L-shaped aluminum slab glued onto the stem neck.

The system was excited between 1200Hz and 2000Hz. This range allowed the detection of the resonance frequency causing the highest resonance of the stem-bone systems before, during, and after loading [16].

In addition, in order to assess if the optimal stem seating defined by the surgeon was indeed the most stable one, the stem was extracted and reinserted three additional times by a different operator, imposing different degrees of press-fitting. The stem stability was recorded for each new degree of press-fitting and compared with that indicated by the surgeon.

Correlation analysis between the evaluation of stability made through vibration assessment and the measured stem-bone micromotion (reference measurement) was performed.

### 5.3 Results

The tests were successfully carried out (Fig.5.3). The vibration system worked generally well and it was appreciated by the surgeon. The reference measurement of the linear micromotion at the stem-bone interface performed through the LVDT revealed being very useful in measuring the extent of stability of the prosthesis.

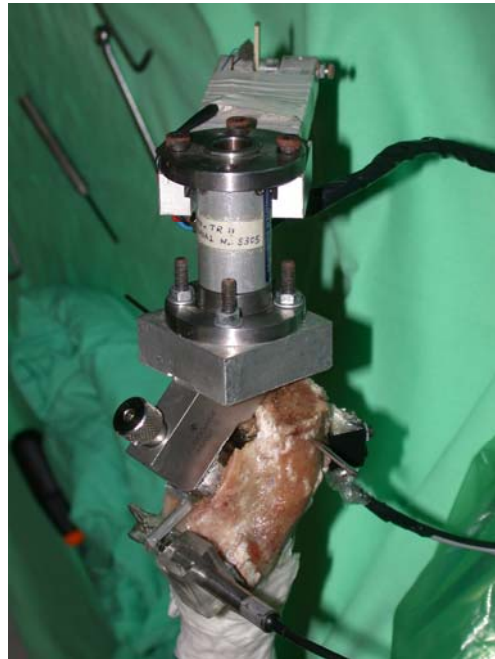


*Fig. 5.3 Photograph of the testing set up*

It was estimated that the time necessary for the measurement procedure would add about 4 minutes to the time for the standard surgical practice, considering the placement of each component, the measurement protocol and the final extraction of the device.

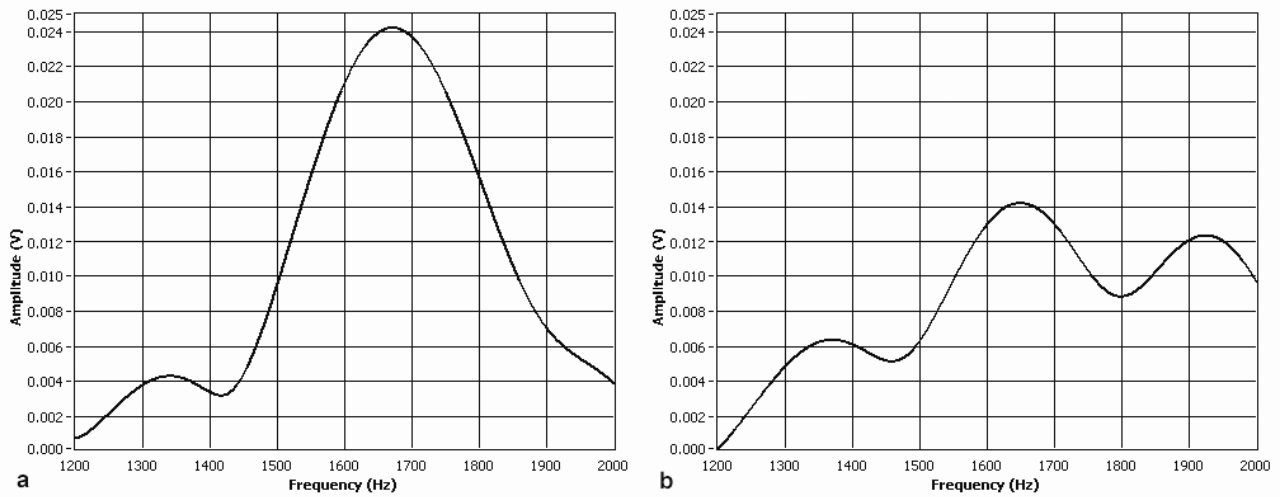


Fig. 5.4 Typical frequency response function of the system: stable (a) and unstable (b) case.

The typical spectrum of the acceleration signal showed the presence of a high amplitude peak in the excitation range considered (Fig.5.4). In particular, it was noticed that the peak shifted to lower frequencies as a result of the torque application. This behaviour was much more evident if the stem-femur coupling was not sufficiently secured. The acquisitions made on the specimens that were prepared and press-fitted by the surgeon to the extent he judged sufficient to realize a stable fixation, generally revealed a frequency shift significantly lower than the cases in which the stem were extracted and reinserted to different degrees of stability (Fig.5.5).

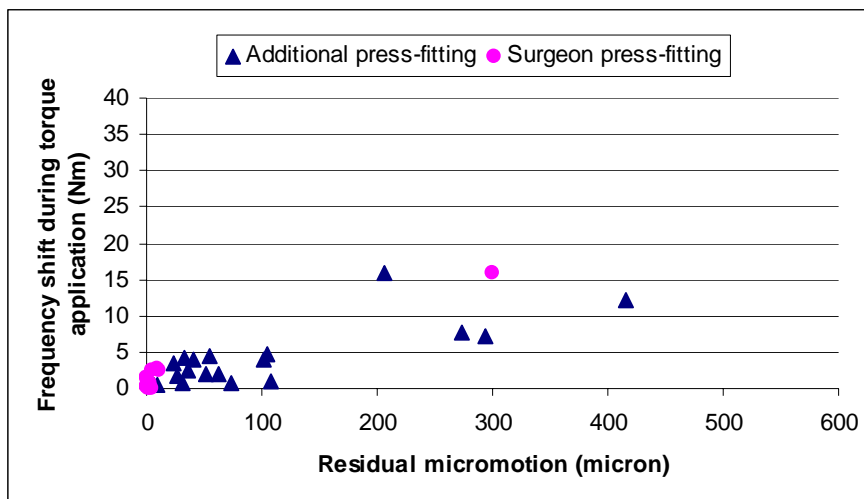
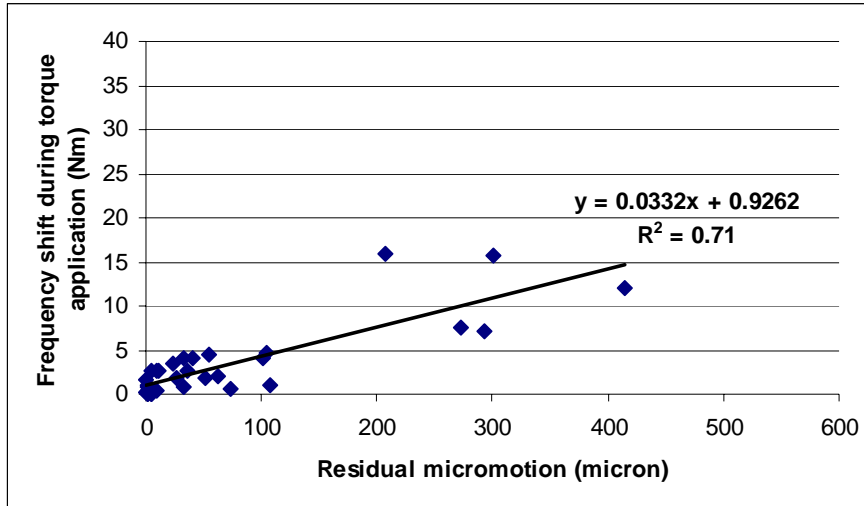


Fig. 5.5 Shift of the frequency of the highest peak in the excitation range plotted as a function of the interface micromotion measured through the reference LVDT: tests with press-fitting made by the surgeon are divided by the test with additional press-fitting.

By studying the linear correlation between the shift of the frequency of the highest peak in the amplitude spectrum within the excitation range and the corresponding linear interface micromotion, a correlation index equal to 0.70 was found (Fig.5.6).



**Fig. 6** Correlation graph: the shift of the frequency of the highest peak in the excitation range is plotted as a function of the interface micromotion measured through the reference LVDT. All data are represented.

Furthermore, it was noticed that if the frequency of the highest peak of the FRF in the excitation range, shifted less than 5Hz during torque application, then the residual micromotion after load removal was always less than 150 micron.

## 5.4 Discussion

This study was aimed at the validation of a device based on the vibration analysis technique. In particular, the goal was to discriminate between stable and quasi-stable implants by studying the frequency response function (FRF) of the implant-bone system, when excited to a selected range of frequencies.

The vibrating system was tested both on cadaveric and composite specimens. An additional LVDT sensor was used as reference measurement of implant stability. The results showed that the measurement system is accurate enough to detect different levels of implant stability. The shift of the highest amplitude peak of the FRF in the excitation range considering the system in the states before and after torque application, resulted the best indicator of prosthesis stability. This parameter was in fact highly correlated to the residual micromotion

at the interface between stem and bone. From the results, it was possible to estimate a stability threshold in terms of maximum shift of the frequency corresponding to the highest peak of the FRF in the excitation range: if this frequency after torque application shifted more than 5Hz, the system moved more than 150 microns. In that quasi-stable condition, the success of the stabilization process of the implant relay on the post-operative period.

These results confirmed the observations made during a preliminary trial of the system [16]. That preliminary in-vitro trial was performed on composite femurs only and revealed a slightly different threshold for discriminate stable from quasi-stable implants. Composite femurs, when subjected to high frequency mechanical excitation, behaved in a significantly different way with respect to cadaveric specimens. Therefore, the vibration data obtained from composite femurs seemed to be suitable to understand the overall behaviour of the system, but did not add information for the evaluation of a quantitative stability threshold.

As a limitation of the of the present study, the following issues must be considered:

- The presented data revealed the presence of few unstable cases; in particular, by observing the correlation graph (Fig.5.6) it is evident that the major percentage of data concentrated in the range of micromotion between few microns till 110micron, while 5 cases exceeded 150microns of interface micromotion and none was over 500microns. This could be considered a limitation of the study, even if the aim of the study was to discriminate between stable and quasi-stable implants, thus the unstable cases were of lower interest. Furthermore, it is evident that a well defined trend was observed and confirmed the preliminary study made on composite femurs [16].
- Finally, it must be said that the measurement system is still at a prototyping stage; thus it needs to be industrialized to reduce its dimensions and improve its performances.

Concluding, this study has demonstrated the great potentialities that a vibration based method could offer when used to evaluate the degree of stability of a cementless implant. The presented results showed that the system is accurate enough to discriminate between different levels of stability and that the shift of the highest peak in the excitation range during torque application is the best indicator of implant stability.

## References

1. R.Y. Liang, F.K. Choy, J.L. Hu, Detection of cracks in beam structures using measurements of natural frequencies, *Journal of the Franklin Institute—Engineering and Applied Mathematics* 328 (1991) 505–518.
2. S. Chinchalkar, Determination of crack location in beams using natural frequencies, *Journal of Sound and Vibration* 247 (2001) 417–429.
3. P.F. Rigos, A.D. Dimarogonas, Identification of crack location and magnitude in a cantilever beam from the vibration modes, *Journal of Sound and Vibration* 138 (1989) 381–388.
4. T.C. Tsai, Y.Z. Wang, Vibration analysis and diagnosis of a cracked shaft, *Journal of Sound and Vibration* 192 (1996) 607–620.
5. J.T. Kim, Y.S. Ryu, H.M. Cho, N. Stubbs, Damage identification in beam-type structures: frequency-based method vs. mode-shapebased method, *Engineering Structures* 25 (2003) 57–67.
6. C. Kyriazoglou, B.H. Le Page, F.J. Guild, Vibration damping for crack detection in composite laminates, *Composites, Part A—Applied Science and Manufacturing* 35 (2004) 945–953.
7. S.D. Panteliou, T.G. Chondros, V.C. Argyrakis, A.D. Dimarogonas, Damping factor as an indicator of crack severity, *Journal of Sound and Vibration* 241 (2001) 235–245.
8. Lowet, G, Van Audekercke, R, Van der Perre, G, Geusens, P, Dequeker, J, Lammens, J., The relation between resonant frequencies and torsional stiffness of long bones in vitro. Validation of a simple beam model., *J Biomech*, 1993, 26(6), pp. 689-96.
9. Van Der Perre, G, Lowet, G, In vivo assessment of bone mechanical properties by vibration and ultrasonic wave propagation analysis, *Bone*, 1996, 18(1 Suppl), pp. 29S-35S.
10. Meredith, N., Shagaldi, F., Alleyne, D., Sennerby, L., Cawley, P., The application of resonance frequency measurements to study the stability of titanium implants during healing in the rabbit tibia, *Clin. Oral. Impl. Res.*, 1997, 8(3), pp. 234-243.
11. Friberg, B., Sennerby, L., Linden, B., Gröndahl, K., Lekholm, U., Stability measurements of one-stage Brånemark implants during healing in mandibles. A clinical resonance frequency analysis study, *Int. J. Oral Maxillofac. Surg.*, 1999, 28, pp. 266-272.
12. Koka, S., Commentary on resonance frequency analysis, *Int J Prosthodont*, 19(1), p.84.
13. Maloney, W.J., Jasty, M., Burke, D.W., O'Connor, D.O., Zalenski, E.B., Bragdon, C.R., Harris, W.H., Biomechanical and histologic investigation of uncemented total hip

- arthroplasties: A study of autopsy-retrieved femurs after in vivo cycling, *Clin Orthop Rel Res*, 1989, 249, pp.129-40.
14. Schneider, E., Kinast, C., Eulenberger, J., Wyder, D., Eskilsson, G., Perren, S.M., A comparative study of the initial stability of cementless hip prostheses, *Clin Orthop Rel Res*, 1989, 248, pp. 200-9.
  15. Mjöberg, B., The theory of early loosening of hip prostheses, *Orthopedics*, 1997, 20 (12), pp.1169-75.
  16. Lannocca M., Varini E., Cappello A., Cristofolini L., Bialoblocka E., Intra-operative evaluation of cementless hip implant stability: a prototype device based on vibration analysis, *Med Ang Phys*, in press.
  17. Li, P.L.S., Jones, N.B., Gregg, P.J., Vibration analysis in the detection of total hip prosthetic loosening, *Med.Eng.Phys.*, 1996, 18(7), pp. 596-600.
  18. Georgiou, A.P., Cunningham J.L., Accurate diagnosis of hip prosthetic loosening using a vibrational technique, *Clin Biomech*, 2001, 16, pp. 315-323.
  19. Qi, G., Mouchon, W.P., Tan, T.E., How much can a vibrational diagnostic tool reveal in total hip arthroplasty loosening?, *Clin Biomech*, 2003, 18, pp. 444-458.
  20. Jaecques, S.V.N., Pastrav, C., Zahariuc, A., Van der Perre, G., Analysis of the fixation quality of cementless hip prostheses using a vibrational technique, *Proc. International Conference on Noise and Vibration Engineering*, 2004, pp.443-456.
  21. Cristofolini, L., Varini, E., Pelgrefi, I., Cappello, A., Toni, A., Device to measure intra-operatively the primary stability of cementless hip stems, *Med Eng Phys*, 2006, 28(5), pp.475-82.



## **CHAPTER 6**

# **PROPOSAL FOR AN IN VITRO METHOD FOR ASSESSING IMPLANT-BONE MICROMOTIONS IN RESURFACING IMPLANTS UNDER DIFFERENT LOADING CONDITIONS**



This chapter reports a manuscript which is ‘in revision’ under the *Journal of Engineering and Medicine*. It concerns the development of an in-vitro protocol to measure the extent of micromotion between bone and a resurfacing prosthesis. The aim of this work was to assess if it could be useful to develop an intra-operative device to measure during surgery the stability achieved. The protocol included testing the instrumented specimens under a wide range of loading conditions, including a final failure test.

## 6.1 Introduction

Hip-resurfacing was used in the earliest attempts to treat hip osteoarthritis (Smith-Petersen, 1978), but the initial encouraging outcomes soon revealed unacceptable failure rates (Freeman and Bradley, 1983; Head, 1984; Howie et al., 1990; Jolley et al., 1982). However, when properly used, proximal resurfacing can be expected to better restore the functional anatomy (head centre) of the affected hip joint. In addition, hip-resurfacing designs allow the surgeons to preserve more bone tissue, providing easier revision procedures (Amstutz et al., 2004; Daniel et al., 2004; Howie, et al., 1990; Mont et al., 2001) if compared to the standard technique. For these reasons, the resurfacing technique, properly revised, was re-proposed in more recent designs. It has been reintroduced in the surgical practice (McMinn et al., 1996; Wagner and Wagner, 1996), as a beneficial solution even for active patients (key indications are correct bony anatomy and quality), becoming fairly popular in some countries in the last few years.

Preliminary short-term clinical results for this new type of hip prostheses are encouraging (Back et al., 2005; Daniel, et al., 2004; Treacy et al., 2005). A potentially concerning failure scenario in the short-term is aseptic loosening (in addition to neck-fractures, which can account for up to half of the failures (out of 400implants) (Amstutz, et al., 2004); in some cases extensive radiolucency was observed around the short femoral stem, probably indicative of early loosening. (Howie et al., 2005) performed a randomised clinical trial, which resulted in several failures, including a number of early femoral component loosening.

The primary stability obtained with a prosthetic device is recognised to play a critical role in aseptic loosening (Malchau H., 2000). Additionally, early micromotion is known as a potential predictor of failure (Kärrholm, 2000). Thus, each new design should be subjected to

pre-clinical tests specifically designed to assess its stability under physiological loads. The assessment of primary stability *in-vitro* is a quite well-established procedure for conventional hip replacements (Britton and Prendergast, 2005; Cristofolini et al., 2003; Harman et al., 1995; Monti et al., 1999). However, to the authors' knowledge, no protocol has been proposed to test the stability of hip resurfacing.

Knowing that implant-bone micromotion is a reliable indicator of implant primary stability and that early micro-motion is a potential predictor of long-term outcome, the aims of this work were,:

- 1) To develop a new procedure for the pre-clinical evaluation of micromotion in hip-resurfacing with the following features:
  - Such protocol should be able to explore implant micromotions under different loading scenarios covering the physiological range.
  - The set-up must be adaptable to different prosthetic designs
- 2) Assess the ability of the protocol to measure implant micromotion in the elastic region (sub-critical load values).
- 3) Assess its suitability to evaluate the implant micromotions up to failure, to elucidate the failure mechanism.

## 6.2 Materials and Methods

### 6.2.1 Micromotion measurements

The implanted specimens were instrumented with two high-precision waterproof spring-preloaded LVDTs (D5/40AW, RDP, UK, accuracy: 1micron), to measure bone-prosthesis micromotion, following a protocol derived from previous experience (Cristofolini, et al., 2003).

In order to measure the maximum gap-opening and shear-slippage micromotions, the LVDTs were positioned where these micromotions reached the respective peak values in a preliminary FE study (Taddei et al., 2005)(Fig.6.1):

- GAP-opening was measured between the most medial point of the rim of the prosthetic components and the adjacent bone.

- SHEAR-slippage was measured between the bone and the prosthesis on the posterior side. Relative position of the two transducers was scaled by the head diameter.

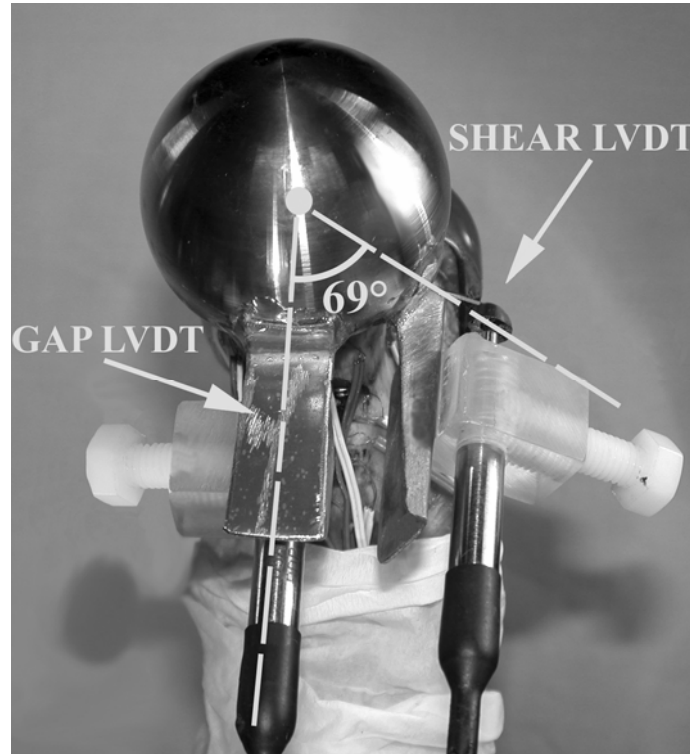


**Fig.6.1** Medial view of the proximal implanted femur: the two LVDTs were accurately aligned so as to lie in the plane of the edge of the prosthesis, with the line of action respectively in a radial direction, for the LVDT measuring GAP micromotion, and in a tangential direction, for the one measuring SHEAR micromotion. To allow consistent positioning with different head sizes, relative position of the two transducers was calculated considering a polar reference system centered on the head center, thus angular distance was constant through specimens ( $69^\circ$ ). The body of the transducers was connected with a small fixture to the lowest point of the prosthesis (respectively at the medial and posterior sides) and close to the prosthesis rim. The moving part of the LVDTs were instrumented with a  $\phi 2\text{mm}$  spherical tip in contact with a metal plate (L-shaped for the SHEAR LVDT) glued onto the bone with the surface perpendicular to the axis of the LVDT.

The frame of the LVDTs were mounted by means of custom adjusted fixtures and bi-component epoxy glue. The setup and the assembling technique for the transducers were optimized using the first set of three femurs (implanted with three different prosthetic designs, see below).

The LVDT signals were logged in a multi-channel unit (34970A, Agilent-Technologies, USA) together with load and position signals from the testing machine. Continuous recording

from the LVDTs allowed measuring the inducible micromotion (which was recovered within seconds after unloading) and permanent migration (not recovered after load removal).

### 6.2.2 Mechanical in-vitro testing

A set of five loading conditions (Taddei, et al., 2005) was selected to cover the physiological range of maximum hip-reaction angles recorded in hip patients (Bergmann et al., 2001) during a wide range of activities (including level walking at different speeds, single-leg-stance, stair-climbing and -descending, standing-up from seated position), and generate bending in different planes, axial loading, and torsion. These configurations (1-5 in Fig.6.2) do not represent any specific motor task but they correspond to the extreme directions of the resultant hip joint force in the frontal and sagittal planes. With the aim to explore the effect of different loading conditions on the head-neck region, it was decided not to include the action of any muscle, that would mainly affect the distal femur (Cristofolini et al., 1995) (Cristofolini et al., 2006).



**Fig.6.2** The load cases simulated on a right femur (lateral view on the left, posterior view on the right): Angles define only the relative position of the femur specimens under the testing machine, needed to obtain the correct in-vitro loading, and do not correspond to any specific anatomical

*position. Load cases 1-5 were applied in the non-destructive tests. Load case F was used to simulate spontaneous head-neck fractures.*

The femurs were mounted on the load-cell of the testing machine (8502, Instron, Canton, MA, USA). A system of cross-rails was provided to avoid application of undesired horizontal force components. In order to measure initial implant stability, a quasi-static scenario was preferred, rather than fatigue testing. Load was applied in 25s and was held for 30s to allow settling and repeatable measurements (Cristofolini, 1997). The load was sufficiently low (75% BW) to allow repeated loading without bone/cement damage (based on FEM (Taddei, et al., 2005)).

Additionally, configuration 2 and 4 (Fig.6.2) were replicated by applying the full load in six equal increments, where the load was held for 25s after each ramp. Micromotions were recorded during the whole loading time and for 90s after load removal, checking system linearity and quantifying viscoelastic phenomena.

Five measurement repetitions were taken for each loading configuration, with the specimen being allowed to recover at least five minutes between replicates. The whole loading set-up was dismantled and realigned between replicates.

Finally, a failure test was performed to evaluate micromotion till the instant prior to implant failure (Cristofolini, et al., 2006). An additional loading scenario was thus designed (load case F in Fig.6.2) to replicate the loading associated with the highest risk of spontaneous fractures. A preliminary FE study (Taddei, et al., 2005) explored under which condition (among the motor tasks reported by Bergmann (Bergmann, et al., 2001) stresses are highest in the head-neck region. This study showed that the most suitable scenario was when the force was at 8° in the frontal plane. The load rate was set so as to cause fracture in 2-4s from load application.

### **6.2.3 Specimens**

A total of five fresh frozen human cadaveric femurs, were obtained from the International Institute for the Advancement of Medicine (IIAM, Jessup, PA, USA), excluding donors with musculoskeletal pathologies. Donor data were:

- Sex: 5 males.
- Age: average 62.4years, range 51-80years.
- Height: average 176.2cm, range 175-178cm.
- Weight: average 99.8kg, range 75-164kg.
- Head diameter: average 50.6mm, range 48.0-54.4mm.

A visual inspection and radiographic assessment (including DEXA and CT scanning) confirmed the absence of abnormalities, defects, or damage. The femurs were wrapped in cloth soaked with physiological solution and stored at -25°C when not in use, and constantly moistened by means of wet clothes during testing.

The femurs were prepared with a set of reference axes to allow for reproducible alignment throughout the test, following a validated protocol (Cristofolini, 1997; Ruff and Hayes, 1983). The femoral condyles were potted in a steel box with dental cement.

Implantations were carried out by experienced surgeons following the prescribed surgical techniques. A first set of two specimens was used for optimizing the testing set-up and LVDT fixtures, and to verify that the method could be adapted to different resurfacing designs. They were implanted with the following devices (one each):

- Conserve Plus (Wright Medical Technology Inc., Arlington, Tennessee, USA): this was tested as part of another study (Taddei F.).
- BHR resurfacing prosthesis (Midland Medical Technologies, Birmingham, UK).

Once the method was consolidated, the remaining three specimens were used to assess the repeatability of the method. Thus, they were implanted with BHR prosthesis (sizes 46, 50).

#### **6.2.4 Statistics**

Micromotion data were preliminary screened with the Chauvenet criterion for outliers. Linearity was checked. Finally data were processed statistically to assess:

- Correlation between the two measurement locations (GAP and SHEAR): Correlation Analysis
- The significance of loading scenario: One-factor ANOVA.

## 6.3 Results

The results below cover the series of 3 specimens tested once the protocol was consolidated (assessing protocol repeatability). The results from the preliminary test are not reported due to the slightly different testing set-up.

### 6.3.1 Micromotion during non-destructive testing

Micromotion measurements were successfully performed on all the implanted specimens for all the loading conditions. The recorded values were in the predicted direction (Taddei, et al., 2005), consistent with the direction of the applied load, both in GAP-opening and in SHEAR-sliding. Load-micromotion linearity was good ( $R^2 \geq 0.98$ ), confirming the linear behavior of the measurement system and the bone. GAP and SHEAR micromotions were highly correlated (Correlation coefficient=0.765, Fisher Test P-value<0.0001).

All the displacement readouts were very low (always lower than 20 micron) with the reduced-load simulation (Fig.6.3). Measurement repeatability was good in all specimens: variability between repeats on the same specimen, under the same loading condition, ranged from less than 1micron to 3.7micron, depending on specimen and loading condition. Inter-specimen variability for the same loading scenario ranged between 1.6micron and 5.3micron.

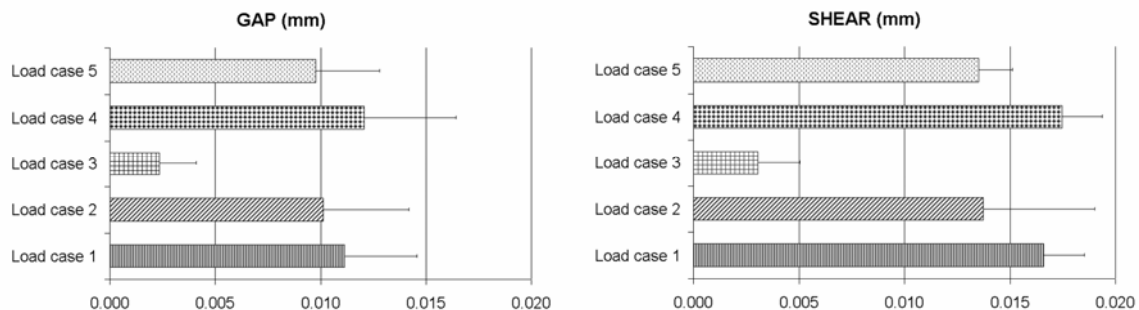


**Fig.6.3** GAP and SHEAR micromotions under load for the five loading conditions (different directions of the hip joint force) tested non-destructively: Average between BHR specimens  $\pm$  standard deviation.

The peak values under load for each loading condition were slightly different. Due to the high repeatability, the effect of the loading scenario on micromotions was statistically significant for the GAP measurement direction (ANOVA: P-value=0.048) and almost significant for the SHEAR direction (ANOVA: P-value=0.073).

The permanent micromotions after load removal never exceeded 7 micron for both the LVDT measuring GAP and the one measuring SHEAR micromotion for all the tested specimens under all loading conditions. These values (comparable to the accuracy of the measurement system) were not considered for the statistical analysis.

### 6.3.2 Micromotion during destructive testing

Tests to failure were successfully carried out. Micromotions were acquired during the whole test. In all cases, a non-linear trend was observed in the last instants prior to failure (Fig.6.4), showing that the measurement system is capable to track the failure pattern. Bone-prosthesis maximum micromotion recorded at failure ranged between 123 and 218micron medially (gap-opening), and between 169 and 599micron posteriorly (shear-sliding).

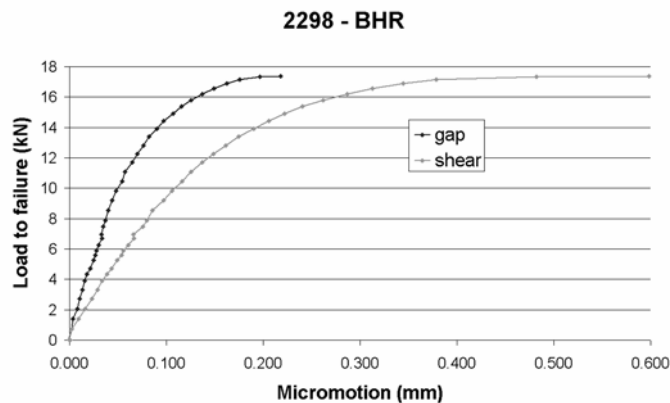


**Fig.6.4** Typical load-micromotion curve for a BHR implant, when loaded to failure: the two lines correspond to the two transducers recording gap opening (medially) and shear sliding (posterior side).

## 6.4 Discussion

A new procedure was developed to measure micromotion *in-vitro* in resurfacing implants with the following features. The protocol was first tuned on two different designs implanted in cadaveric femurs. Its repeatability and reproducibility were then assessed on three more human cadaveric femurs, implanted with a BHR resurfacing prostheses. The protocol included different loading scenarios to explore micromotions in the physiological range.

The flexibility of the protocol was demonstrated by applying it to two different prosthetic designs, and to different head sizes during the preliminary tests.

Micromotions were successfully measured in the elastic range (low load values). Also, micromotions were tracked until specimen failure, obtaining different patterns in relation to the implant type.

The implant micromotion under load caused gap-opening in the medial region, and shear-sliding in the posterior one. This confirms that this protocol is capable of assessing the two main components of relative micromotion, in the areas where they reach the maximum value (Taddei, et al., 2005). The values measured under load for the tested prosthesis, both for peak and permanent micromotions are comparable with those found for cemented hip prostheses (Cristofolini, et al., 2003).

The failure tests confirmed that the protocol allowed measuring the prosthesis micromotion up to failure, being able to discriminate the elastic region from the non-linear trend typical of the instants prior to failure.

Comparison of the present results against clinical outcome is favourable: experimentally measured micromotions were small; RSA studies indicated small or non-significant migrations during the first year (Glyn-Jones et al., 2004; McMinn and Pynsent, 2002).

As no other *in-vitro* study has been published on micromotion of resurfacing implants, this procedure can be reasonably compared only with the protocols for conventional stemmed prostheses (Baleani et al., 2000; Buhler et al., 1997; Gotze et al., 2002; Harman, et al., 1995; Monti, et al., 1999). The accuracy of such validated protocols ranges from a fraction of a micron to several micron. The accuracy of the present protocol was equal to the precision of the transducers, which was better than one micron. Linearity and repeatability were checked and showed values consistent with those reported in other *in-vitro* tests (Monti, et al., 1999).

Furthermore, *in-vitro* protocols for total hip replacement usually measure micromotions when the specimen is subjected to a torsional load (alone or with axial components). In the present investigation, five different loading configurations were considered in order to cover the physiological range of maximum hip-reaction angles recorded in hip patients (Bergmann, et al., 2001; Taddei, et al., 2005). This guarantees that, even if highest micromotions occur for different loading directions, its highest value is detected by the procedure proposed.

As the test protocol includes assessment of the fracture mode, cadaveric specimens must be used (composite femurs are unsuitable for fracture tests (Cristofolini et al., 1996)). As cadaveric specimens cannot withstand several loading cycles without non-physiological damage, this study was limited to few loading cycles. However, it can be assumed that this setup could be modified to include several loading cycles (if fracture test is given up) by using composite femur models. Such protocol has already successfully been implemented for standard hip stems (Cristofolini, et al., 2003).

In conclusion, a protocol has been developed (based on previous exploratory FE studies) and thoroughly validated, confirming its ability to measure the largest micromotions occurring at the bone-prosthesis interface in a number of loading scenarios covering the physiological range, including when the specimen was brought to failure.

## **References**

- Amstutz, H.C., Beaulé, P.E., Dorey, F.J., Le Duff, M.J., Campbell, P.A., Gruen, T.A., 2004. Metal-on-metal hybrid surface arthroplasty: two to six-year follow-up study. *J Bone Joint Surg Am* 86-A, 28-39.
- Back, D.L., Dalziel, R., Young, D., Shimmin, A., 2005. Early results of primary Birmingham hip resurfacings. An independent prospective study of the first 230 hips. *J Bone Joint Surg Br* 87, 324-329.
- Baleani, M., Cristofolini, L., Toni, A., 2000. Initial stability of a new hybrid fixation hip stem: experimental measurement of implant-bone micromotion under torsional load in comparison with cemented and cementless stems. *J Biomed Mater Res* 50, 605-615.
- Bergmann, G., Deuretzbacher, G., Heller, M., Graichen, F., Rohlmann, A., Strauss, J., Duda, G.N., 2001. Hip contact forces and gait patterns from routine activities. *J Biomech* 34, 859-871.
- Britton, J.R., Prendergast, P.J., 2005. Preclinical testing of femoral hip components: an experimental investigation with four prostheses. *J Biomech Eng* 127, 872-880.
- Buhler, D.W., Berlemann, U., Lippuner, K., Jaeger, P., Nolte, L.P., 1997. Three-dimensional primary stability of cementless femoral stems. *Clin Biomech (Bristol, Avon)* 12, 75-86.
- Cristofolini, L., 1997. A critical analysis of stress shielding evaluation of hip prostheses. *Crit Rev Biomed Eng* 25, 409-483.
- Cristofolini, L., Pallini, F., Schileo, E., Juszczak, M., Varini, E., Martelli, S., Taddei, F., Biomechanical testing of the proximal femoral epiphysis: intact and implanted condition. 2006, 8th Biennial ASME Conference of Engineering Systems Design and analysis, Torino (Italy),
- Cristofolini, L., Teutonico, A.S., Monti, L., Cappello, A., Toni, A., 2003. Comparative in vitro study on the long term performance of cemented hip stems: validation of a protocol to discriminate between "good" and "bad" designs. *J Biomech* 36, 1603-1615.
- Cristofolini, L., Viceconti, M., Cappello, A., Toni, A., 1996. Mechanical validation of whole bone composite femur models. *J Biomech* 29, 525-535.

Cristofolini, L., Viceconti, M., Toni, A., Giunti, A., 1995. Influence of thigh muscles on the axial strains in a proximal femur during early stance in gait. *J Biomech* 28, 617-624.

Daniel, J., Pynsent, P.B., McMinn, D.J., 2004. Metal-on-metal resurfacing of the hip in patients under the age of 55 years with osteoarthritis. *J Bone Joint Surg Br* 86, 177-184.

Freeman, M.A., Bradley, G.W., 1983. ICLH surface replacement of the hip. An analysis of the first 10 years. *J Bone Joint Surg Br* 65, 405-411.

Glyn-Jones, S., Gill, H.S., McLardy-Smith, P., Murray, D., 2004. Roentgen stereophotogrammetric analysis of the Birmingham hip resurfacing arthroplasty. *J Bone Joint Surg Br*. 86-B, 172-176.

Gotze, C., Steens, W., Vieth, V., Poremba, C., Claes, L., Steinbeck, J., 2002. Primary stability in cementless femoral stems: custom-made versus conventional femoral prosthesis. *Clin Biomech (Bristol, Avon)* 17, 267-273.

Harman, M.K., Toni, A., Cristofolini, L., Viceconti, M., 1995. Initial stability of uncemented hip stems: an in-vitro protocol to measure torsional interface motion. *Med Eng Phys* 17, 163-171.

Head, W.C., 1984. Total articular resurfacing arthroplasty. Analysis of component failure in sixty-seven hips. *J Bone Joint Surg Am* 66, 28-34.

Howie, D.W., Campbell, D., McGee, M., Cornish, B.L., 1990. Wagner resurfacing hip arthroplasty. The results of one hundred consecutive arthroplasties after eight to ten years. *J Bone Joint Surg Am* 72, 708-714.

Howie, D.W., McGee, M.A., Costi, K., Graves, S.E., 2005. Metal-on-metal resurfacing versus total hip replacement-the value of a randomized clinical trial. *Orthop Clin North Am* 36, 195-201, ix.

Jolley, M.N., Salvati, E.A., Brown, G.C., 1982. Early results and complications of surface replacement of the hip. *J Bone Joint Surg Am* 64, 366-377.

Kärrholm, J., Nivbrant, B., Thanner, J., Anderberg, C., Börlin, N., Herberts, P., Malchau, H, Radiostereometric evaluation of hip implant design and surface finish. Micromotion of cemented femoral stems. 2000, 67th Annual Meeting of the American Academy of Orthopaedic Surgeons, Orlando, USA,

Malchau H., H.P., Söderman P., Odén A., Prognosis of total hip replacement. Update and validation of results from the Swedish National Hip Arthroplasty Registry 1979-1998. 2000, 67th Annual Meeting of the American Academy of Orthopaedic Surgeons, Orlando, Florida, USA,

McMinn, D., Pynsent, P., Surgical aspects of hip resurfacing. 2002, Transactions of the IMechE International Conference: Engineers & surgeons joined at the hip. Refining future strategies in total hip replacement, London,

McMinn, D., Treacy, R., Lin, K., Pynsent, P., 1996. Metal on metal surface replacement of the hip. Experience of the McMinn prosthesis. Clin Orthop Relat Res S89-98.

Mont, M.A., Rajadhyaksha, A.D., Hungerford, D.S., 2001. Outcomes of limited femoral resurfacing arthroplasty compared with total hip arthroplasty for osteonecrosis of the femoral head. J Arthroplasty 16, 134-139.

Monti, L., Cristofolini, L., Viceconti, M., 1999. Methods for quantitative analysis of the primary stability in uncemented hip prostheses. Artif Organs 23, 851-859.

Ruff, C.B., Hayes, W.C., 1983. Cross-sectional geometry of Pecos Pueblo femora and tibiae—a biomechanical investigation: II. Sex, age, side differences. Am J Phys Anthropol 60, 383-400.

Smith-Petersen, M.N., 1978. The classic: Evolution of mould arthroplasty of the hip joint by M. N. Smith-Petersen, J. Bone Joint Surg. 30B:L:59, 1948. Clin Orthop Relat Res 5-11.

Taddei, F., Cristofolini, L., Martelli, S., Gill, H.S., Viceconti, M., 2005. Subject-specific finite element models of long bones: An in vitro evaluation of the overall accuracy. J Biomech (in press).

Taddei F., V.E., Gill H.S., Cristofolini L., Viceconti M., A combined experimental and finite element study on load transfer and micromotions of a resurfacing hip prosthesis. To be submitted to J Biomechanics

Treacy, R.B., McBryde, C.W., Pynsent, P.B., 2005. Birmingham hip resurfacing arthroplasty. A minimum follow-up of five years. J Bone Joint Surg Br 87, 167-170.

Wagner, M., Wagner, H., 1996. Preliminary results of uncemented metal on metal stemmed and resurfacing hip replacement arthroplasty. Clin Orthop Relat Res S78-88.



## ***Conclusions***

The research activity carried out during the three years of Ph.D Course in Bioengineering was motivated by a great interest in the orthopaedic topics and a great will to work for providing the surgeons with accurate, reliable and ready-to-use tools that could make easier their activity. A deep analysis of the reference Literature, a great support from the experience held by the Laboratorio di Tecnologia Medica (Istituti Ortopedici Rizzoli, Bologna) and the Laboratorio di Bioingegneria (DEIS Department – University of Bologna) and a deep personal engagement, allowed me to carried out the research work I just reported.

Although total hip replacement is considered a successful procedure, there are still some issues that must be considered and solved in order to prevent intra-operative complications that could compromise the success of the surgery thus causing discomfort, pain and potential risk for the patient. One of these issues concerns the evaluation of the primary stability intra-operatively.

The aim of the studies here presented was to develop intra-operative tools that could help the surgeon evaluating the degree of primary stability achieved by press-fitting the stem, during total hip replacement surgery. Different devices have been developed and fully validated.

The first device is based on the direct measurement of the relative stem-bone micromotion under torsional load. It was successfully validated and calibrated. It showed a good overall accuracy that was deemed sufficient by two surgeons. It is being now tested in the clinical setting; the preliminary results are extremely positive.

An additional tool was developed by modify an existing device for the application on the rasp. It showed that it seem possible to predict the stability of a stem, in optimally press-fitting condition, by measuring the micromotion under torsional load of the last rasp used by the surgeon to prepare the femoral canal. This information is really useful for the surgeon to check if the pre-operative planning was correct, thus avoiding intra-operative complications that would increase the risks for the patient.

The vibration analysis technique was used as basic principle for another device. It was fully validated *in-vitro* and it needs now to be industrialized in order to fulfill the requirements to

enter in the clinical setting. The great advantages of this vibration-based device are easier clinical use, smaller dimensions and minor overall cost with respect to other devices based on direct micromotion measurement.

The tool developed for *in-vitro* evaluation of the stability of resurfacing prosthesis demonstrated that an intra-operative tool is not necessary for that kind of prosthesis, as the micromotion recorded were extremely low, thus not critical for the stabilization process. However, the *in-vitro* tool validated to test the stability can be successfully applied for assessing resurfacing implants pre-clinically.

Two experienced surgeons were asked to evaluate the validated devices from a clinical point of view: both seemed really satisfied by the advantages that each device allowed and deemed useful and efficient their use in the clinical setting. A clinical trial was planned and it is now running under their supervision.

## **Acknowledgements**

I'd like to thank the *Laboratorio di Tecnologia Medica* – Istituti Ortopedici Rizzoli – Bologna - Italy, where I carried out most of the work here presented, as well as the *Laboratorio di Bioingegneria* – University of Bologna - Italy. Some of this work formed part of a project financed by the European Commission: ISAC project (Intra-operative Stability Assessment Console) IST-1999-20226. Thanks are due also to Stryker for co-funding part of this work.



## **APPENDIX A**

### **STEM DAMAGE DURING IMPLANTATION OF MODULAR HIP PRSTHESIS**





This additional study was published on *Artificial Organs* 2006, Jul 30(7):564-7. It was performed during the first part of my research work, when validating the device based on the direct measurement of implant stability. Based on a specific commercial design (AnCAFit, Wright-Cremascoli Ortho, France), the aim of this work was to assess if stem-holders of modular prostheses can induce any stem damage, and if so to identify the features which provide minimal damage. Two different stem-holder connector designs were investigated.

## **INTRODUCTION**

The possibility of adapting the geometry of the prosthesis to the joint morphology of the patient provides more flexibility during primary surgery and simplified revision procedures (1,2). This is particularly useful when the hip anatomy is badly affected as in DDH or in post-traumatic arthritis (3) and when a mini approach is used (4). In recent years modular stems are increasingly used in total hip replacement. This kind of prosthesis is generally assembled by taper locks that show a low rate of disassembly and interface failure (2,5). For instance, the AnCAFit (Wright-Cremascoli Ortho, France) modular hip prosthesis features a modular neck (that allows selection of different lengths and angles) that is press-fitted in a cavity in the stem.

Several problems have been clearly identified with implant modularity. Evidence of corrosion and fretting at the modular junction have been observed (1,6,8). Periprosthetic osteolysis is frequently observed in association with wear and fretting debris (8). Nevertheless, many new designs have been recently introduced in the market. While their biomechanical performance has been thoroughly investigated, much less attention has been paid to the problems related to the implantation technique.

The tool-kit used for the implantation of this kind of femoral components is made of instruments (like stem-holders) characterised by special connectors to be inserted in the modular cavities. The coupling geometry must be precise and the connector has to be rigid enough to withstand and transfer the high loads exerted during stem press fitting. A poorly designed connector or badly handled instrument can damage the surface of the coupling (Fig.1a), so that it could compromise the precision coupling with the neck, modifying the pressure distribution at the coupling interface and damaging the finish and roughness of the matching surfaces. Surface finish is crucial in achieving optimal coupling of taper connectors and minimizing fretting and surface damage (9). All these factors could promote the

generation of possible sites of fretting and associated production of potentially harmful debris (5,9).

This work is aimed to assess if stem-holders can induce any stem damage, and if so to identify the connector features which provide minimal damage to the stem. It is suspected that when such stem-holders are handled during surgery, loads applied manually or when press-fitting the stem (with hammer blows) could induce undesired contacts and damage to the stem.

### **MATERIALS AND METHODS**

All the tests were conducted on five cementless modular neck stems (AnCAFit, stem sizes 11-16). Two different types of stem-holder connector (Wright-Cremascoli Ortho) were tested in order to quantify the amount of damage. Both are designed to be inserted in the stem housing for the modular neck, and both are characterized by the same rectangular section with the larger flat sides linked by circular connections. Connector A (Fig.1b) has a coupling  $4.1^\circ$  tapered end made of solid Ti6Al4V alloy that perfectly fills the stem neck housing. It also features a screw made of AISI316L steel that fits the threaded hole placed in the central part at the bottom of the stem slot to fasten the connector to the prosthesis. Connector B (Fig.1c) has a different coupling geometry characterized by a constant section, where only the distal part is stably in contact with the stem slot. Its structure is made of AISI316L steel. It has four cylindrical inserts made of polytetrafluoroethylene (PTFE) at the edges between the larger sides and the circular sides of the section. The screw mechanism to safely fasten the connector to the stem is the same as connector A.

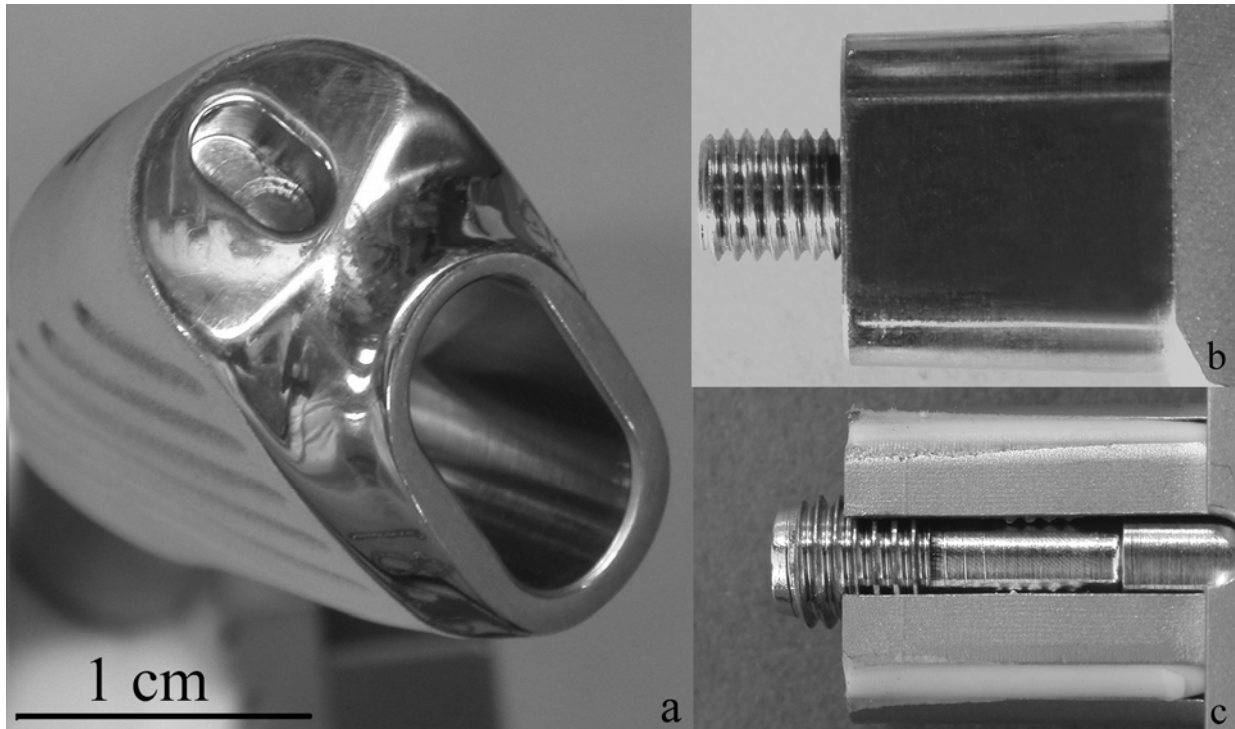


**Fig 1.** Photographs of the stem cavity, which houses the modular neck (a), of connector A (b) and connector B (c): the two connectors are similar, except that B does not feature the taper angle of A (the same of the stem cavity), and has four PTFE inserts at the corners.

#### *Inspection of surface damage*

The analyses were performed on the whole surface of the stem slot in order to explore the surface texture. A stereoscopic microscope (Nikon SMZ-2T, Japan) was used with a digital camera (Nikon Coolpix 995, Japan) to record any scratches, incisions and any other kind of damage. A piece of graph paper was acquired in each image to provide for dimensional scaling. The magnification used (10X - 30X) for the analysis was sufficient to detect damage with a dimension at least equal to the spacing of the machining ridges (about 100 micron).

Before each test and between each phase of the following protocol, the stems were thoroughly ultrasound clean-washed:

- A first surface inspection was performed on each stem cavity in its original condition, in order to record the initial damage caused by manufacturing.
- Then, a simulation of possible surgeon manoeuvres to completely press fit the stem into a femur was ran: the stem was first clamped in a vice with rubber pads; connector A was inserted in the stem cavity and properly fastened by the dedicated screw. Ten axial hammer blows (hammer weight: 500gr) were applied. Additionally, calibrated loads were applied

by means of a handle linked to the connector to reach 15-20 Nm of torque (ten repeats). This type of load was agreed with three experienced surgeons to simulate the worst possible clinical scenario. The torque was applied in order to simulate possible further applications for intra-op stability measurements (10).

- The stem and the connector surfaces were inspected with the same protocol.
- After microscopic inspection and documentation of the damage caused by connector A, the same stem was used for testing connector B, following the same procedure. As a preliminary study indicated that surface damage caused by connector A was minimal, the very same specimens were tested with both connectors, so as to allow paired comparisons using modularities that were machined with exactly the same tolerance.
- Thus, the damage caused by the use of connector B was quantified analysing the added damage with respect to the one observed after the use of connector A.

#### *Effectiveness of the PTFE inserts*

One more test was performed on connector B: the metal part of this connector is supposed not to come in contact with the stem while used by the surgeon, because of the four PTFE inserts. It was suspected that the inserts could get squeezed under load, allowing the sharp metallic connector edges to touch the stem slot surface. By measuring the stem-connector electrical conductivity it was possible to assess if there was contact between the two metallic surfaces. For this test connector B was carefully inserted in one stem cavity, the connector screw was removed. A multimeter (Mod. 27, Fluke) was used to measure stem-neck insulation while an axial force and a torque were applied manually.

## **RESULTS**

#### *Inspection of surface damage*

The microscopic analyses revealed the presence of damage caused by manufacturing. This is normally small in dimension (single scratches, less than 1 mm long), very localized, with a random direction. The handling damage, on the contrary, was caused by the compression of the machining ridges, mainly along the stem slot axis. After the use of connector A and B respectively, the stems revealed additional damage if compared to the preliminary results. The damage induced by connector B was more extensive (more numerous, longer and deeper scars), and different in pattern if compared to the one caused by connector A (Tab. 1).

**Tab.1** Damage caused by the use of the two different connector geometries.

<b>STEM DAMAGE</b>		
<u>Location and type</u>	<u>Presence after connector A</u>	<u>Presence after connector B</u>
Central part of the anterior or posterior flat side: areas with contact damage (machining grooves dent)	Average per stem: <b>0.8 counts</b>	Average per stem: <b>2.3 counts</b>
Between the circular and the rectilinear sides: slight line in axial direction, along half the cavity depth.	Average per stem: <b>1.0 counts</b>	Average per stem: <b>2.8 counts</b>
Ends of the rectilinear sides: Twin slight lines (Fig.2a) in axial direction along the cavity depth.	<b>None</b>	Average per stem: <b>0.8 counts</b>
Central part of the anterior or posterior flat side: oblique scratch possibly induced by connector screw during insertion	Average per stem: <b>0.5 counts</b>	<b>None</b>
Between the circular and the rectilinear sides: PTFE residue trapped in the machining grooves.	<b>None</b>	<b>In 2 stems</b>
Bottom of the cavity: circular damage.	<b>None</b>	Average per stem: <b>4 counts</b>

## CONNECTOR DAMAGE

<u>Location and type</u>	<u>Connector A</u>	<u>Connector B</u>
On the rims along the PTFE inserts and the distal sharp corners: damage on the connector (Fig.2b)	None	Observed after the first test with the connector

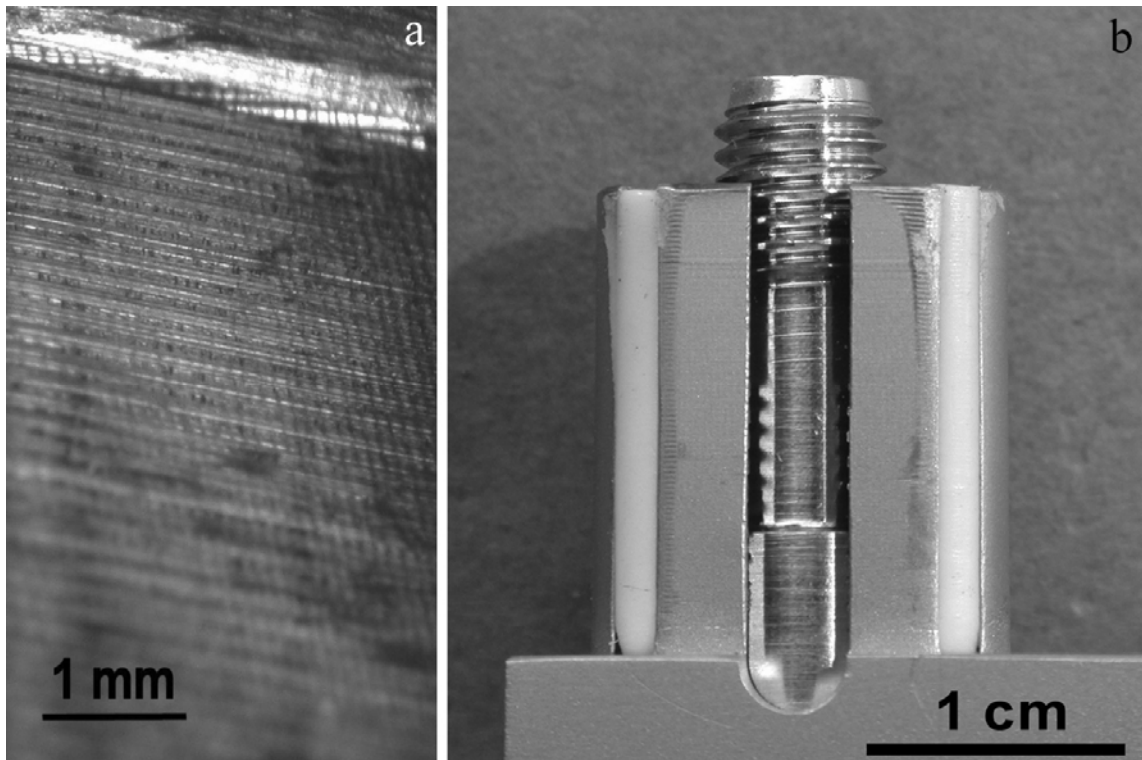


**Fig 2.** Example of damage caused by the use of connector B: a couple of slight lines observed in some stem and placed at the ends of the rectilinear sides (a) and the damage observed on connector B after the first mechanical simulation on a stem (b).

### *Effectiveness of the PTFE inserts*

The resistance measured by the multimeter when the load was applied on connector B dropped to smaller than 1 Ohm (PTFE electrical insulation was larger than 30 MOhm). This test showed that even with a small axial force or a torque applied, the metal part of connector B gets in direct contact with the stem.

## **DISCUSSION**

Based on the results obtained, the following general conclusions can be drawn and should be considered when designing and handling modular prostheses:

1. Stem-holders can produce surface damage independently of connector design. If these surgical devices are intended to be matched with the stem modularity, they could produce a possibly dangerous damage of the coupling surfaces.
2. The damage observed, could compromise the correct coupling between the two parts, leading to the generation of debris as produced by fretting (5). It is known, in fact, that the fretting process is strongly influenced by the distribution of pressure between the surfaces at the fretting interface and also by the surface roughness and finish (9). Changing of at least one of these factors could possibly have a strong effect in terms of fretting damage (1,6,7,8).

While it is not possible to quantify the amount of debris that could be produced because of the damaged coupled surfaces, the outcome is potentially extremely detrimental. In fact, as a result, the metallic wear generated by fretting could lead to different complications, which could compromise the long term outcome of the operation (8).

Our experimental results suggest that much more attention must be paid to the stem-holders used with modular prosthesis: a robust design should be sought, so that unexpected loads will not result in undesirable stem damage. Additionally, the surgeons should limit, if possible, a direct hammering of the stem-holder that could damage the matching surfaces of modular components and possibly lead to increased fretting.

## **References**

1. Bobynd JD, Tanzer M, Krygier JJ, Dujovne AR, Brooks CE, Concerns with modularity in total hip arthroplasty. *Clin Orthop Relat Res* 1994; 298: 27-36.
2. Cameron HU, Orthopaedic crossfire--Stem modularity is unnecessary in revision total hip arthroplasty: In opposition. *J Arthroplasty* 2003; 18(3 suppl 1): 101-103.
3. Noble PC, Kamaric E, Sugano N, Matsubara M, Harada Y, Ohzono K, Paravic V, Three-dimensional shape of the dysplastic femur: implications for THR. *Clin Orthop Relat Res* 2003; 417: 27-40.
4. Kennon RE, Keggi JM, Wetmore RS, Zatorski LE, Huo MH, Keggi KJ, Total hip arthroplasty through a minimally invasive anterior surgical approach. *J Bone Joint Surg Am* 2003; 85-A(suppl 4): 39-48.
5. Baleani M, Viceconti M, Walcholz K, Toni A, Metallic wear debris in dual modular hip arthroplasty. *Chir. Organi Mov* 1997; 82(3): 231-238.
6. Collier JP, Mayor MB, Jensen RE, Surprenant VA, Surprenant HP, McNamar JL, Belec L, Mechanisms of failure of modular prostheses. *Clin Orthop Relat Res* 1992; 285: 129-139.
7. Urban RM, Tomlinson MJ, Hall DJ, Jacobs JJ, Accumulation in liver and spleen of metal particles generated at nonbearing surfaces in hip arthroplasty. *J Arthroplasty* 2004; 19(8 suppl 3): 94-101.
8. Cook SD, Manley MT, Kester MA, Dong NG, Torsional resistance and wear of a modular sleeve-stem hip system. *Clin Mater* 1993; 12(3): 153-158.
9. Collins JA, Failure of materials in mechanical design. Analysis, prediction, prevention. New York: ed. Wiley-Interscience, 1993.
10. Cristofolini L., Varini E, Pelgreffi I., Cappello A., Toni A, Device to measure intra-operatively the primary stability of cementless hip stems. *Med Eng Phys* (in press).

## **APPENDIX B**

### **ON THE BIOMECHANICAL STABILITY OF STRAIGHT CONICAL HIP STEM**



# On the biomechanical stability of cementless straight conical hip stems

M Viceconti\*, A Pancanti, E Varini, F Traina, and L Cristofolini

Laboratorio di Tecnologia Medica, Rizzoli Orthopaedic Institute, Bologna, Italy

The manuscript was received on 25 October 2004 and was accepted after revision for publication on 12 July 2005.

DOI: 10.1243/09544119H06904

**Abstract:** The aim of the present study was to investigate *in vitro* the effect of deficient bone–implant contact on the primary stability of a straight conical stem. Various possible deficient contact patterns were derived from surgical simulations. The effect of stair climbing loads on the bone–implant micromotion was firstly investigated using a finite element model and then an *in vitro* test aimed at assessing primary stability. It was found that if the surface features are prevented from biting dense bone in a few small but critical regions, stem primary stability is completely lost. These results suggest that the surface features used in the axisymmetric stem under investigation can be too sensitive to deficient contact conditions, and thus should be augmented with additional antirotational fins. Preliminary tests showed that a stem with the addition of such fins presents good primary stability in all tested conditions.

**Keywords:** hip prosthesis, primary stability, surface features

## 1 INTRODUCTION

Cementless hip stems should be designed so as to ensure maximum primary stability, i.e. the minimum bone–implant micromovements induced by external loads soon after the operation. In this sense, the idea of designing a straight conical stem (Fig. 1) with a circular cross-section may appear unwise.

However, straight conical stems seem to have various surgical advantages, such as a simpler surgical technique, easier positioning, better fitting in very small and/or tubular anatomies, and simple correction of the retroversion without additional modularity [1, 2]. In order to compensate for this inherent geometric instability, all these designs present superficial features such as ribs, grooves, flares, and pegs, aimed to increase as much as possible the interlocking of the stem with the host bone, so as to increase the primary stability. Under ideal conditions these features provide very good biomechanical stability to the stem [3]. Indeed, even small features, such as pegs biting spongy bone to a depth of few millimetres, have been experimentally shown to provide

a significant improvement in primary stability of cementless devices [4, 5].

It is, however, unclear what level of primary stability these implants can ensure under less-than-optimal conditions. Although these stems are commonly considered easier to implant, surgical errors can also happen with these implants. The choice of an undersized stem, known to produce subsidence or a varus–valgus misalignment [6–8], is also a reported complication of conical stems [1]. Anatomical deformities in the host femur may prevent the contact between the implant surface and the host bone in certain regions [9]. Excessive reaming, which sometimes occurs in patients affected by osteoporosis, may also produce a lack of contact in certain regions.

The present study aims to investigate *in vitro* the effect that deficiencies in the bone–implant contact may have on the primary stability of a straight conical stem and to find solutions that may reduce this effect.

## 2 MATERIALS AND METHODS

The study was conducted on an axisymmetric cementless stem (hereafter called the ‘standard

\*Corresponding author: Laboratorio di Tecnologia Medica, Rizzoli Orthopaedic Institute, Via di Barbiano 1/10, Bologna, 40136, Italy. Email: viceconti@tecnio.ior.it



**Fig. 1** Examples of straight conical cementless stems (from left to right): Easy stem (Hit-Medica, Italy), stabilized by longitudinal slots; Cone stem (Centerpulse, Swiss), stabilized by longitudinal fins

stem') that is commercially available (Easy stem, Hit-Medica, Italy). This monolithic stem presents a conical shape in the portion that fits into the proximal and metaphyseal regions and a cylindrical shape in the diaphyseal region. The entire surface is covered with longitudinal slots; in the proximal (conical) portion they consist of short grooves while in the distal (cylindrical) portion long flares are present (Fig. 1). They are intended to increase the rotational stability of the stem. The distal cylindrical portion is split longitudinally. The stem has been routinely implanted in a few Italian hospitals since 1988. In order to separate the effect of the antirotational slots, some tests were conducted with a special version of the stem (hereafter called the 'smooth stem') manufactured with a smooth surface (Fig. 2). A third version of the Easy stem (hereafter called the 'finned stem') with the addition of two large lateral antirotational fins (Fig. 2), was prepared in order to evaluate the improvement that this would provide in critical conditions.

The stems were implanted in synthetic replicas of human femurs specifically designed for biomechanical tests (small size, mod. 3103, Pacific Research Labs, Vashon Island, Washington, USA). Their shape and mechanical properties accurately match those of human bones [10]. These synthetic femurs have



**Fig. 2** Versions of the cementless stem under testing: standard version (left); smooth stem without slots (centre); stem with lateral antirotational fins (right)

been extensively used in this type of *in vitro* studies [11] because they keep the interspecimen variability within reasonable limits. Indeed, they have been successfully used in primary stability studies [12–16]. While the absolute value of micromotion found with these models might not be the same as that found in cadaveric specimens, there is a general consensus that they can be used, with some caution, in comparative tests [12–16]. It has recently been shown that their behaviour in terms of primary stability when compared to cadaveric bone is not very different. Moreover, they predictably tend to slightly overestimate stem stability [17].

A skilled surgeon who routinely uses this type of prosthesis implanted the stems using the same set of instruments used in clinical practice. The femoral neck was resected with an L-shaped double cut (Fig. 3). The femur was firstly drilled with a cylindrical reamer, having a diameter of 12 mm, equal to that of the distal cylindrical portion of the stem. The final reaming was performed manually with a shaped conical reamer, which left the femur ready for press-fitting the stem.

A finite element model (FEM) of the synthetic bone implanted with the Easy stem was developed. Two separate experiments were used to validate the model predictions of the bone–implant relative micromotion. In the first experiment measurements were taken of the micromotion of the standard stem perfectly fitted into the host bone. These measurements were compared to the predictions obtained with the model assuming all slots are in contact with the counterfacing bone. In the second experiment measurements were taken of the micromotion of the smooth stem, and these measurements were compared with the predictions of the model obtained assuming that no slot is in contact with the host bone. Once validated in these two extreme conditions, the finite element model was used to

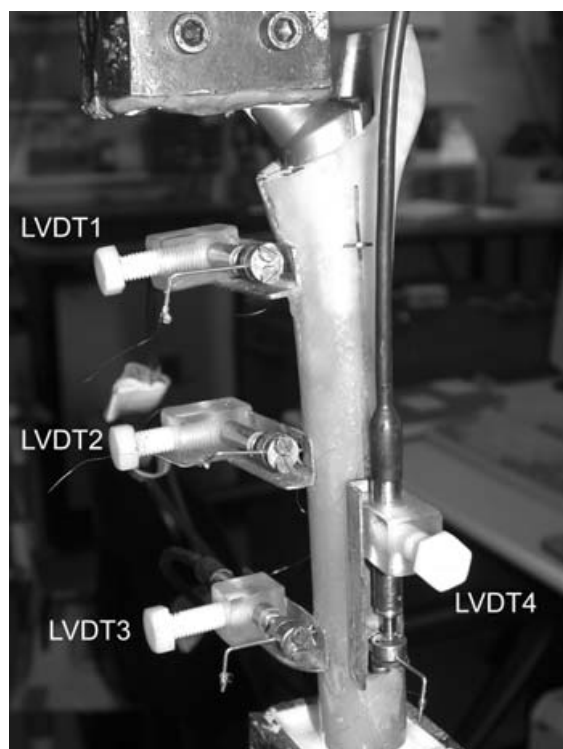


**Fig. 3** Experimental set-up used for the primary stability tests. The block of acrylic cement enclosing the stem neck is used to apply the torsion load in a repeatable way, while the four linear variable differential transducers (LVDTs) continuously record the bone–implant micromotion

investigate the effect of the deficient contact condition on the primary stability of the Easy stem, e.g. partial contact between the slots and the host bone. Of the many configurations investigated using the FEM, three were physically replicated in implanted specimens; also the measurements of these intermediate configurations were found to be in good agreement with the model predictions. Lastly, in order to reduce the sensitivity of the stem primary stability to deficient contact conditions, the finite element model was used to investigate the effect of additional antirotational elements. One particular configuration that included two large fins in the lateral-proximal region (finned stem) was manufactured, and its primary stability was assessed experimentally. Once again the model predictions were confirmed by these measurements.

### 2.1 *In vitro* assessment of the primary stability

A femur-aligned reference system was marked [18] on each femur to facilitate a repeatable procedure in all steps of the specimens' preparation and for improving cross-comparison against the FEM models.

After implantation, one thousand loading cycles (Fig. 3) were applied to each specimen following a previously validated protocol [16].

Each loading cycle was intended to reproduce the peak load applied to the head of the prosthesis when climbing up a stair, while the number of cycles represented an estimate of patient activity for the first three postoperative months [19]. An axial load was applied with a sinusoidal waveform (cycling between 275 and 1683 N) synchronous with the torsional moment (cycling between 5 and 26.2 N m) (Fig. 4).

Due to the presence of a lever arm in the medio-lateral direction, the axial load also generated a bending moment in the frontal plane (cycling between 3.8 and 23.2 N m). These load values were derived from the literature [20] for a body weight of 550 N, which is reasonable for the small size of the femora used in the present investigation. A recovery time of 7.5 s was allowed between two consecutive loading cycles. This was found in a previous study of the same type of synthetic bones to be an excellent compromise between the need for a long resting interval, to allow for recovery of viscoelastic phenomena, and the need to reduce the testing time [16]. The femora were mounted on a biaxial servo-hydraulic testing machine (858 MiniBionix, MTS Corp., Minneapolis, Minnesota, USA). The loading set-up (Fig. 4) was designed to apply the required load components while avoiding overconstraints. Proximally, the load was applied through a system of cross-rails, which guaranteed that only a vertical force would be applied. The femur was held between two perpendicular hinges to ensure that no other moments than the desired ones were transmitted.

An extensometer (632.06H-20, MTS Corp.) was used to measure the proximal-to-distal axial sinking of the stem within the femoral canal. Four LVDTs (D5/40G8, RDP Electronics, UK) were used to measure the relative bone–stem interface shear motion caused by rotation of the stem about the longitudinal axis of the femoral shaft. A set-up was studied to anchor the sensors at a negligible but controllable distance from the bone–implant interface [16]. For all the sensors, the measurement error is less than 4  $\mu\text{m}$  in the range of the micromovements of interest [16].

The output of the sensors was used to obtain the maximum elastic motion (i.e. the amount of relative slippage at the interface that is recovered after load release) and the permanent migration (i.e. the amount of relative slippage at the interface that is not recovered after the load release and which accumulates cycle after cycle). When the stems were excessively loose (with the micromotion exceeding

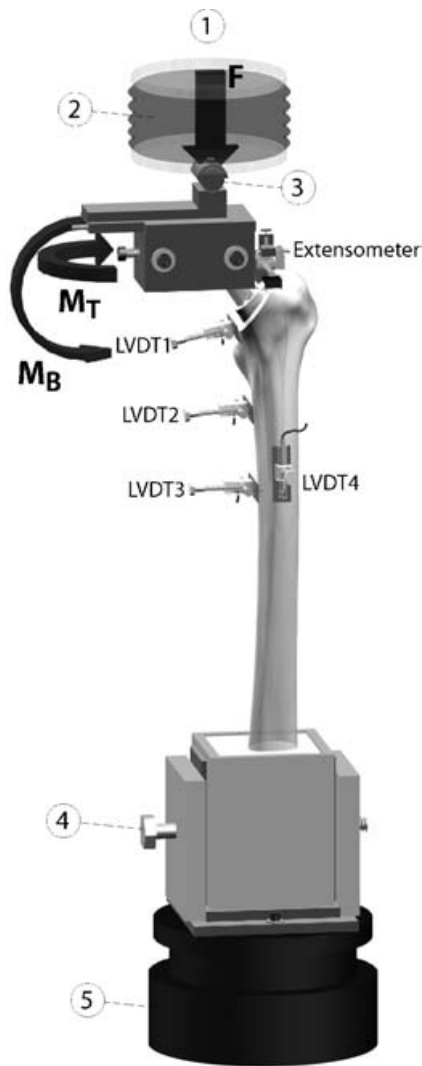


**Fig. 4** Schematic of the experimental set-up used for the primary stability tests. The block of acrylic cement enclosing the stem neck is used to apply the torsion load in a repeatable way, while the four LVDTs and the extensometer continuously record the bone–implant micromotion. The axial force ( $F$ ), the bending moment ( $M_B$ ) and the torsional moment ( $M_T$ ) are applied by the biaxial actuator (1). A system of cross-rails (2) and perpendicular hinges (3, 4) avoid transmission of any other load component than the designed ones. A biaxial load cell is mounted under the specimen measuring the loads applied

1 mm), the test was stopped before completion of one thousand cycles.

## 2.2 Development of the finite element model

The finite element model was created starting from computer aided design (CAD) models of the Easy stem and of the standardised femur, a freely available

three-dimensional model of the synthetic bone used in the experiments [21]. Using CAD software (UG v.17, Unigraphics Solutions, USA) the surgical modifications to the femur and the position of the stem with respect to the host bone were replicated consistently with those observed in the specimens used in the experiments. The solids were properly partitioned and then meshed into a structured hexahedral mesh composed of eight-node isoparametric ‘brick’ elements (Fig. 5) using a pre-processing software package (Hyperworks, Altair, USA). The resulting mesh was composed of 9699 elements and 8142 nodes, for a total of 24 426 unconstrained degrees of freedom.

The exact interface mechanics produced by the stem slot when they bite into the bone material could not be modelled in detail in a full-scale model such as the one used here. Thus, the stem was modelled as a smooth geometry in frictional contact with the counterfacing bone surface. Contact was modelled using face-to-face contact elements with an augmented Lagrangian formulation, penetration monitoring at Gauss points, and convergence monitoring on the square norm of the force vector. The interface was modelled assuming that each point of the metaphyseal region of the stem is in contact with some

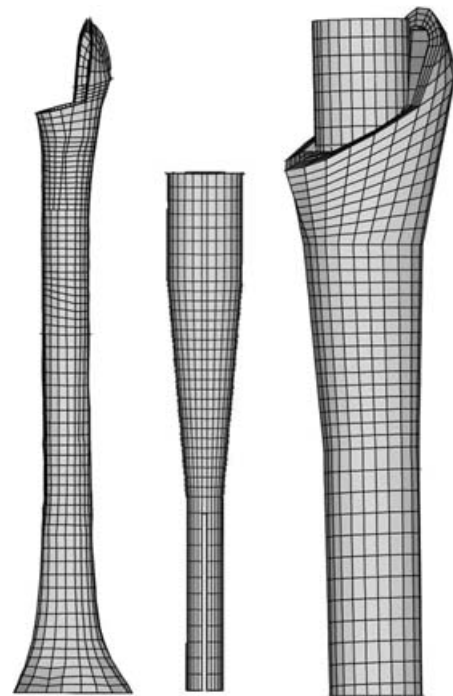


**Fig. 5** Finite element mesh used in the study: mesh of the operated femur (left), mesh of the stem (centre), and the complete model (right). The stem neck is replaced by an extension of the cylindrical portion where the torsional and flexural moments were applied

bone tissue, in agreement with the fact that the synthetic bones used in the experiments have the epiphysis and the metaphysis entirely filled with the polyurethane foam used to mimic cancellous bone. Thus, no gaps were present between the bone and stem in the underformed configuration. At convergence the model always presented an intermesh penetration of less than 1  $\mu\text{m}$ . The micromotion was defined as the change in distance between two paired Gauss points; this includes detachment of the stem from the bone and tangential sliding of the stem surface with respect to the bone surface. This quantity appears to be more relevant for osseointegration than specific components such as tangential micromotion; the single bone bridge that spans across the interface is equally disrupted both by detachment and by tangential sliding. What really matters is the change in distance between the two points that are paired in the undeformed configuration.

The mechanical effect of the slots was lumped into a set of nearly 500 springs that connected the stem surface and the counterfacing bone surface. A high stiffness was used to model the condition of the slot engaged with the bone, while a low stiffness modelled the condition of the unengaged slot. Each spring spanned from a node of the stem mesh to a node of the bone mesh; due to the mapped nature of the two meshes, these surface nodes were coincident and the remaining length of each spring was nil. Thus, the springs opposed each change in distance between the two nodes, including that due to rotation of the stem with respect to the bone. The stiffness of the springs was identified by comparing the micromotion predicted by the model with that measured in the experiments with the smooth stem and with the slotted stem. Optimal agreement was obtained for spring stiffnesses of respectively  $>108$  N/mm (slotted stem) and  $<1$  N/mm (smooth stem).

In order to validate these modelling assumptions, the model was solved under boundary conditions replicating those imposed in the *in vitro* tests. For the version of the stem with the anti-rotational slots the micromotion found experimentally was almost zero (ranging between 1 and 11  $\mu\text{m}$ ). The finite element model predicted a micromotion pattern that differed from the experimental measurements by  $3 \pm 1.5$   $\mu\text{m}$ , with a maximum difference of 4  $\mu\text{m}$ . When the model was configured to simulate a contact condition in which none of the slots was biting the counterfacing bone, the simulation was stopped for exceeding the micromotion limit ( $>400$   $\mu\text{m}$ , equivalent to approximately a rotation of  $2.5^\circ$ ) when the load was below 5 N m. By comparison, in the

experimental tests on the smooth stem the micromotion transducers went out of range when the stem rotated by  $10^\circ$  under the action of a torque of only 18.9 N m. On the basis of these two results it was concluded that the finite element model was able to predict with acceptable accuracy the primary stability of the Easy cementless stems for a wide range of interface conditions both with and without the antirotational slots.

### 2.3 Definition of the deficient contact conditions

Once validated, the FEM was used to explore the effect of deficient contact conditions (e.g. the presence of an area where the slots were not engaged into the bone) with primary stability of the Easy stem. The implantation of the Easy stem in various patients was simulated using computer tomography (CT) based surgical planning software (Hip-Op v1.4, B3C, Italy). The software computes the fraction of the implant surface in contact with dense cortical bone, with less dense spongy bone, and with bone marrow. The contact patterns varied from patient to patient, but it was nevertheless possible to identify two regions where the antirotational slots were always biting dense bone: the proximal medial posterior and the distal medial anterior. An exploratory analysis on multiple FEMs reproducing various contact patterns confirmed that these two were the regions where the lack of contact would reduce the primary stability of the stem more drastically.

On the basis of these observations it was assumed that these two locations are those where a lack of bone-implant contact (presence of gap) would affect the implant stability more severely. Three conditions of deficient contact were considered, assuming the same location but a different extension of the gap region: mildly defective, where it is assumed that only 24 per cent of the total implant surface is not in direct contact with bone tissue; moderately defective, where the gap region is assumed to be 37 per cent of the implant surface; severely defective, where the extension of the gap region is assumed to be 65 per cent of the implant surface. These three conditions were then replicated *in vitro* by filling selected slots in the gap region with talc-filled unsaturated polyester putty of the type used in car body shops (Mod. 140 Grifo, I.C.R., Reggio Emilia, Italy), which prevented penetration of the slot's rim into the surface of the reamed bone cavity (Fig. 6).

### 2.4 Design of additional antirotational elements

Various solutions to increase primary stability of the stem under deficient contact conditions were investi-



**Fig. 6** Anterior and posterior views of the stem specimen prepared to mimic the mildly defective condition (see the text for details). The filler material is visible in the anterior-distal slots and in the posterior-proximal slots

gated using the FEM. After some preliminary studies, attention was focused on to the placement of lateral antirotational fins in the proximal-lateral region of the stem. These fins, because of their large surface, are less sensitive to the presence of small gaps at the interface. Furthermore, their position allows the surgeon visually to inspect whether they are engaged with the bone or not. Thus, a scenario of complete disengagement is much more unlikely than for the surface slots. Different fin positions and dimensions were examined. Among the possible solutions, the one with two fins oriented towards the postero-lateral and the antero-lateral quadrants was selected. The FEMs confirmed that this modification was, among those considered, the one that improved primary stability the most. This solution was implemented in a prototype stem and tested *in vitro*.

### 3 RESULTS

The stem tended to migrate in the first stages of the test with few sudden steps (50–300  $\mu\text{m}$ ). This trend tended to settle after the first few hundred cycles. Once settled, the peak inducible micromotion of the Easy stem measured *in vitro* in the direction of rotation under normal interface conditions averaged

15  $\mu\text{m}$  (the range of three specimens was 2–33  $\mu\text{m}$ ). The peak inducible micromotion in the axial direction averaged 5  $\mu\text{m}$  (range of 3–8  $\mu\text{m}$ ). The FEM predicted a peak tangential micromotion of 11  $\mu\text{m}$ .

When some slots were modelled as unengaged in the critical regions the FEM predicted a dramatic increase in the relative micromotion. This prediction was confirmed by the experiments; when the mildly defective condition was replicated in the experimental set-up, the measured micromotion reached the limit value of 1 mm under the action of only 70 per cent of the maximum torque during the first loading cycle. This was accompanied by marked axial sinking (up to 330  $\mu\text{m}$ ). This condition was further worsened when more severe interface conditions were simulated *in vitro*.

If the constraints that simulated the presence of two antirotational fins located in the lateral aspect of the implant are included in the FEM with the mildly defective interface condition, the predicted micromotion is reduced to a peak value of 12  $\mu\text{m}$ . Similar values were found in the experimental test when the finned prototype was used: the peak inducible micromotion of the Easy stem measured *in vitro* in the direction of rotation was always smaller than 4  $\mu\text{m}$  (lower than the precision of the measurement system). Migrations in any direction were significantly smaller than in the original scenario (always smaller than 50  $\mu\text{m}$  after 1000 cycles, with no sudden events).

### 4 DISCUSSION

The aim of the study was to investigate *in vitro* the effect of deficient bone–implant contact on primary stability of a straight conical stem and to explore possible design modifications that could reduce this negative effect. Various possible deficient contact patterns were derived from surgical simulations. The effect of stair climbing loads on the bone–implant micromotion was firstly investigated using a finite element model and then an *in vitro* test aimed at assessing primary stability. It was found that if the surface features are prevented from biting dense bone in a few small but critical regions, stem primary stability is completely lost. This was sufficient to prevent the engagement of the surface slots in only 24 per cent of the interface area and to see an extremely stable stem becoming grossly loosened.

These results suggest that the surface features used in the stem under investigation are too sensitive in deficient contact conditions, and thus should be augmented with additional antirotational fins.

Preliminary tests showed that a stem with the addition of such fins presents good primary stability in all tested conditions.

Among the limitations of this study is the use of a synthetic replica of a human bone for primary stability measurements. The composite bones on average underestimate the micromotion induced by a given load because they tend to behave as best-quality bone tissue. On the other hand, if the same tests were performed on cadaver bone a very large variability would be observed, which would not be reduced even if the number of replications were increased drastically. In addition, the main result of this study, which is the sensitivity of stability of this stem to deficient contact patterns, would not be altered by the use of cadaver bones.

The results reported here are in principle only valid for the type of stem considered in this study. However, many of the observations are probably valid for all those stems that are axisymmetric and rely on surface features to achieve primary stability.

Another limitation is the very simple modelling strategy used to describe this bone-implant interface. While it cannot be used for any possible investigation on the interface, this representation was found adequate to describe stabilization of the stem against the bone. Thus, this should be considered as the simplest among the models that were found to be adequate.

## ACKNOWLEDGEMENTS

The authors would like to thank Luigi Lena for the illustrations, and Mauro Ansaloni and Roberta Fognani for their support during the experiments. The study was partially supported by the European Commission through the project Pre-Hip contract IST-1999-56408. Hit-Medica, the company that produces and commercializes the Easy stem, was partner in the Pre-Hip project and provided the specimens used in this study.

## REFERENCES

- 1 Kim, Y. Y., Kim, B. J., Ko, H. S., Sung, Y. B., Kim, S. K., and Shim, J. C. Total hip reconstruction in the anatomically distorted hip. Cemented versus hybrid total hip arthroplasty. *Arch. Orthop. Trauma Surg.*, 1998, **117**(1-2), 8-14.
- 2 Wagner, H. and Wagner, M. Cone prosthesis for the hip joint. *Arch. Orthop. Trauma. Surg.*, 2000, **120**(1-2), 88-95.
- 3 Buhler, D. W., Berlemann, U., Lippuner, K., Jaeger, P., and Nolte, L. P. Three-dimensional primary stability of cementless femoral stems. *Clin. Biomechanics*, 1997, **12**(2), 75-86.
- 4 Natarajan, R. and Andriacchi, T. P. The influence of displacement incompatibilities on bone ingrowth in porous tibial components. In 34th Annual Meeting, Orthopaedic Research Society, 1988, p. 331.
- 5 Giori, N. J., Beaupre, G. S., and Carter, D. R. The influence of fixation peg design on the shear stability of prosthetic implants. *J. Orthop. Res.*, 1990, **8**(6), 892-898.
- 6 Stulberg, B. N., Singer, R., Goldner, J., and Stulberg, J. Uncemented total hip arthroplasty in osteonecrosis: a 2- to 10-year evaluation. *Clin. Orthop.*, 1997, (334), 116-123.
- 7 Keisu, K. S., Mathiesen, E. B., and Lindgren, J. U. The uncemented fully textured Lord hip prosthesis: a 10- to 15-year followup study. *Clin. Orthop.*, 2001, (382), 133-142.
- 8 Eingartner, C., Volkmann, R., Winter, E., Maurer, F., Sauer, G., Weller, S., and Weise, K. Results of an uncemented straight femoral shaft prosthesis after 9 years of follow-up. *J. Arthroplasty*, 2000, **15**(4), 440-447.
- 9 Noble, P. C., Alexander, J. W., Lindahl, L. J., Yew, D. T., Granberry, W. M., and Tullos, H. S. The anatomic basis of femoral component design. *Clin. Orthop.*, 1988, (235), 148-165.
- 10 Cristofolini, L., Viceconti, M., Cappello, A., and Toni, A. Mechanical validation of whole bone composite femur models. *J. Biomechanics*, 1996, **29**(4), 525-535.
- 11 Cristofolini, L. A critical analysis of stress shielding evaluation of hip prostheses. *Critical Rev. Biomed. Engng*, 1997, **24**(4-5), 409-483.
- 12 Bianco, P. T., Bechtold, J. E., Kyle, R. E., and Gustilo, R. B. Synthetic composite femurs for use in evaluation of torsional stability of cementless femoral prosthesis. In ASME Biomechanics Symposium, 1989, pp. 297-300.
- 13 McKellop, H., Ebrahimzadeh, E., Niederer, P. G., and Sarmiento, A. Comparison of the stability of press-fit hip prosthesis femoral stems using a synthetic model femur. *J. Orthop. Res.*, 1991, **9**(2), 297-305.
- 14 Otani, T., Whiteside, L. A., White, S. E., and McCarthy, D. S. Effects of femoral component material properties on cementless fixation in total hip arthroplasty. A comparison study between carbon composite, titanium alloy, and stainless steel. *J. Arthroplasty*, 1993, **8**(1), 67-74.
- 15 Harman, M. K., Toni, A., Cristofolini, L., and Viceconti, M. Initial stability of uncemented hip stems: an *in-vitro* protocol to measure torsional interface motion. *Med. Engng Physics*, 1995, **17**(3), 163-171.
- 16 Monti, L., Cristofolini, L., and Viceconti, M. Methods for quantitative analysis of the primary stability in uncemented hip prostheses. *Artif. Organs*, 1999, **23**(9), 851-859.
- 17 Varini, E., Cristofolini, L., Cappello, A., and Toni, A. Primary stability of cementless hip stems:

- intraoperatively recorded micromotions. In 14th Conference of the European Society of Biomechanics, Den Bosch, The Netherlands, 2004, p. 229.
- 18 Ruff, C. B. and Hayes, W. C.** Cross-sectional geometry of Pecos Pueblo femora and tibiae – a biomechanical investigation: I. Method and general patterns of variation. *Am. J. Phys. Anthropol.*, 1983, **60**(3), 359–381.
- 19 McLeod, P. C., Kettelkamp, D. B., Srinivasan, V., and Henderson, O. L.** Measurements of repetitive activities of the knee. *J. Biomechanics*, 1975, **8**(6), 369–373.
- 20 Bergmann, G., Graichen, F., and Rohmann, A.** Is staircase walking a risk for the fixation of hip implants? *J. Biomechanics*, 1995, **28**(5), 535–553.
- 21 Viceconti, M., Casali, M., Massari, B., Cristofolini, L., Bassini, S., and Toni, A.** The ‘standardized femur program’ proposal for a reference geometry to be used for the creation of finite element models of the femur. *J. Biomechanics*, 1996, **29**(9), 1241.

## **APPENDIX C**

### **PREDICTING THE SUBJECT-SPECIFIC PRIMARY STABILITY OF CEMENTLESS IMPLANTS DURING PRE- OPERATIVE PLANNING: PRELIMINARY VALIDATION OF SUBJECT-SPECIFIC FINITE ELEMENT MODELS**





ELSEVIER

Journal of Biomechanics ■ (■■■■) ■■■-■■■

**JOURNAL  
OF  
BIOMECHANICS**
[www.elsevier.com/locate/jbiomech](http://www.elsevier.com/locate/jbiomech)  
[www.JBiomech.com](http://www.JBiomech.com)

# Predicting the subject-specific primary stability of cementless implants during pre-operative planning: Preliminary validation of subject-specific finite-element models

B. Reggiani<sup>a,\*</sup>, L. Cristofolini<sup>a,c</sup>, E. Varini<sup>b,c</sup>, M. Viceconti<sup>c</sup>

<sup>a</sup>DIEM—Dipartimento di Ingegneria delle Costruzioni Meccaniche, Nucleari, Aeronautiche e di Metallurgia, Università degli Studi di Bologna, Viale Risorgimento 2, 40136, Bologna, Italy

<sup>b</sup>DEIS—Dipartimento di Elettronica, Informatica e Sistemistica, Università degli Studi di Bologna, Viale Risorgimento 2, 40136, Bologna, Italy

<sup>c</sup>Laboratorio di Tecnologia Medica, Istituti Ortopedici Rizzoli, Via di Barbiano 1/10, 40136, Bologna, Italy

Accepted 30 October 2006

## Abstract

Pre-operative planning help the surgeon in taking the proper clinical decision. The ultimate goal of this work is to develop numerical models that allow the surgeon to estimate the primary stability *during* the pre-operative planning session. The present study was aimed to validate finite-element (FE) models accounting for patient and prosthetic size and position as planned by the surgeon. For this purpose, the FE model of a cadaveric femur was generated starting from the CT scan and the anatomical position of a cementless stem derived by a skilled surgeon using a pre-operative CT-based planning simulation software. In-vitro experimental measurements were used as benchmark problem to validate the bone–implant relative micromotions predicted by the patient-specific FE model. A maximum torque in internal rotation of 11.4 Nm was applied to the proximal part of the hip stem. The error on the maximum predicted micromotion was 12% of the peak micromotion measured experimentally. The average error over the entire range of applied torques was only 7% of peak measurement. Hence, the present study confirms that it is possible to accurately predict the level of primary stability achieved for cementless stems using numerical models that account for patient specificity and surgical variability.

© 2006 Elsevier Ltd. All rights reserved.

**Keywords:** Pre-operative planning; Subject-specific FE model; Primary stability; Micromotion; Cementless stem

## 1. Introduction

The most common reason for the aseptic loosening of cementless hip prostheses is the lack of primary stability (Maloney et al., 1989; Manes et al., 1996; Philips et al., 1990; Sugiyama et al., 1989). Excessive relative micromotion at the bone–implant interface may inhibit the bony in-growth and the secondary long-term fixation (Burke et al., 1991; Søballe et al., 1993) ultimately promoting the failure of the implant (Pilliar et al., 1986; Schneider et al., 1989a). To achieve a good level of primary stability the surgical technique plays a fundamental role. An inaccurate implant size and/or position, creating a potentially unstable condition, may result in the formation of a fibrous tissue

layer around the prosthesis deteriorating the mechanical characteristics of the interface. Hence, knowing the amount of relative micromotion that the physiological loads will induce at the bone–implant interface would be an essential information for the surgeon while he or she is planning a cementless total hip replacement.

In the last few years, computer-based protocols of pre-clinical evaluation of joint prostheses have remarkably improved and finite-element (FE) method has become a widely used tool by researchers in assessing the level of achieved primary stability. This is an attractive opportunity to train the surgeon to reliably assess operative planning.

Contrary to experimental methods, fully validated FE models can provide a complete map of the interface micromotions (Dammak et al., 1997; Tissakht et al., 1995) showing the location of the peak value. A number of

\*Corresponding author. Tel.: +39 051 2093437; fax: +39 051 2093412.  
E-mail address: [barbara.reggiani@mail.ing.unibo.it](mailto:barbara.reggiani@mail.ing.unibo.it) (B. Reggiani).

studies have extensively analysed the interface modelling parameters (Bernakiewicz and Viceconti, 2002; Viceconti et al., 2000) and the level of accuracy needed to predict the primary stability of cementless hip implants was established (Viceconti et al., 2000). Similar works were carried out for the pelvic component (Spears et al., 2001). The impact of inaccurate implant positioning on various biomechanical indicators has been investigated (Viceconti et al., 2004b). A statistical FE analysis recently demonstrated over a simulated population of 1000 cases that a mismatch up to 1 mm between the stem and the host bone at random locations of the interface is sufficient to produce a grossly loosened stem in 2% of the patients, while for another 3–5% the high level of predicted micromotion is likely to prevent any substantial osseointegration (Viceconti et al., 2006). These figures are surprisingly close to the failure rate for aseptic loosening reported in the most recent outcome reports (Stea et al., 2002; Various authors, 2003).

From these results it appears important to make sure that the prosthetic component perfectly fits the host bone, in order to further improve the clinical outcomes of cementless total hip replacement. However, even using one of the most sophisticated CT-based pre-operative planning software (Lattanzi et al., 2002) the repeatability of the anatomy-based implant sizing for the same patient by the same surgeon is worse than 1 mm (Viceconti et al., 2003). We may conclude that the surgeon needs to know not only the anatomical information but also the functional/biomechanical information in order to take the proper clinical decision; in this case the surgeon needs to know the primary stability of the cementless component.

This need can be addressed in two ways. Intra-operatively, using adequate measurement tools (Cristofolini et al., 2006; Varini et al., 2004). Pre-operatively, using numerical simulation models able to estimate the primary stability that the planned prosthetic size, placed in the planned position, will have under physiological loads.

The ultimate goal of this research work is to develop such numerical methods designed in a way that allows the surgeon to estimate the primary stability *during* the pre-operative planning session, possibly in an interactive environment that allows the surgeon to explore various configurations and pick the best one. Specifically, this paper focuses on the development and validation of patient-specific FE models created using the CT-scan data and the planned position.

FE models predicting bone stresses and strains of specific patients can be generated starting from the same CT scan that some surgeons use to plan the operation (Taddei et al., 2003). These patient-specific modelling protocols provide the automation, accuracy, robustness and generality required by clinical applications (Viceconti et al., 2004a). However, in authors' knowledge, the possibility to develop an implanted model starting from a pre-operative CT scan and a CT-based pre-operative planning defining the stem position has never been explored.

The general goal of this research activity is to develop methods that provide a rough estimate of the primary stability while the surgeon is planning. The present paper demonstrates that subject-specific FE models are accurate enough in the prediction of primary stability to be used as *references* in the validation of the less-accurate but faster methods.

## 2. Materials and methods

The 3D solid model of an intact cadaveric femur (specimen lab code #78) was generated from the CT dataset using a previously validated procedure (Viceconti et al., 1999). In a previous study (Taddei et al., 2006) it has been shown that the sensitivity of stress and strain predictions are affected by the uncertainties related to the femur geometry and the bone density for less than 9%. A linear convergence test on seven unstructured meshes with increasing refinement levels, consisting of parabolic tetrahedral elements, was developed to ensure the numerical accuracy of the model. The percentage error in energy norm and the differences in terms of stress, strain and displacement were less than 2.2%. The model that guaranteed the best compromise among computational time and accuracy was therefore chosen. In addition, the 95% confidence interval of the strain energy error distribution, 0.002J, was found close to the values previously reported for models derived from data collected in vivo (Viceconti et al., 2004a). An anatomic cementless hip stem (AncaFit, Cremascoli-Wright, Italy) was positioned in space inside the femur by a skilled surgeon using a simulation pre-operative CT based software (Hip-Op, B3C, Italy). Surgical parameters and hip stem geometry were then imported within the FE model resulting in 30,841 tetrahedral elements (Fig. 1).

A post-hoc indicator (Zienkiewicz and Zhu, 1987) was also computed for the FE model of the implanted femur. Since the error estimation

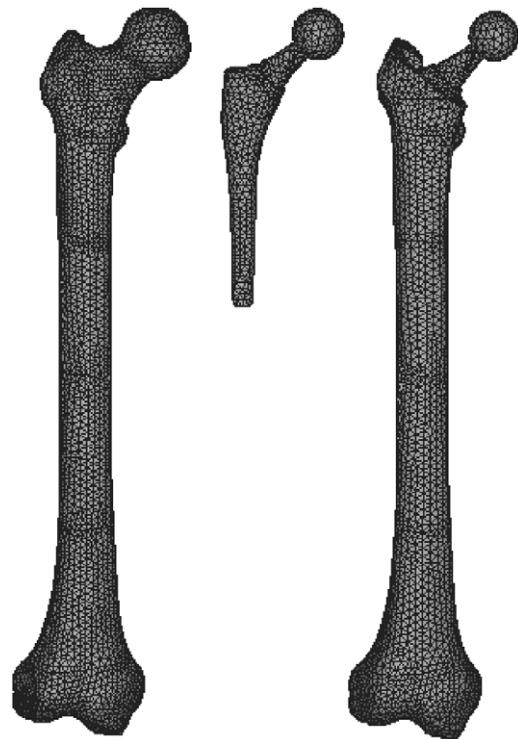


Fig. 1. Finite-element meshes of the femur considered in the present study. From left to right: the intact femur, the implanted prosthesis (AncaFit) and the implanted femur.

cannot be applied to inhomogeneous material and for contact problem, an homogeneous elastic modulus of 10,000 MPa was assigned to the femur and the always-bonded contact was set for the bone–implant contact. The maximum error for the femur was found to be 11% while for the prosthesis it was 7%.

The isotropic and linear properties of cortical and cancellous bone were considered. Mineral density was derived from the CT Hounsfield units using a linear calibration equation (Kalender, 1992) here computed for the specific patient:  $\rho = 0.8082HU - 5.6409$ . Elastic modulus  $E$  was related to mineral density  $\rho$  in the form of power relationship (Keller, 1994):

$$E = 10.5\rho^{2.57}.$$

Both mineral density and elastic modulus were then mapped onto each element of the generated mesh using in-house shareware software Bonemat (Taddei et al., 2004). The resulting range of elastic modulus was  $E = 9.25\text{--}25101$  MPa and  $\rho = 0.046\text{--}1.46$  g/cm<sup>3</sup> for the mineral density. A map of the aforementioned properties is showed in Fig. 2. The stem implant was made of titanium alloy ( $E = 105,000$  MPa;  $\nu = 0.3$ ).

Frictional contact was modelled at the bone–implant interface by means of asymmetric face-to-face contact elements. These are most accurate when compared to experimental measurements and allow accounting for large sliding (Hefzy and Singh, 1997; Mann et al., 1995; Viceconti et al., 2000). The coefficient of friction was set to 0.3 (Viceconti et al., 2000). A sensitivity analysis of the predicted micromotion at the calcar level over the variations of the coefficient of friction value within the range of uncertainty (0.1–0.5) produced differences of less than 35  $\mu\text{m}$ . An augmented Lagrangian approach with a full Newton–Raphson iterative scheme on residual force, combined with line search technique, was chosen to solve the contact problem. For force convergence, 1% tolerance based on Euclidean  $L_2$  norm was used. The peak compenetration was monitored, since it must be very small to get a good level of numerical accuracy. Setting a contact normal stiffness of 9000 N/mm involved a peak

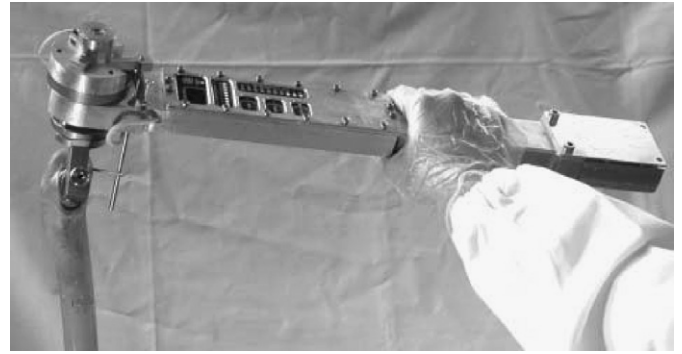


Fig. 3. Intra-operative Stability Assessment Console (ISAC).

compenetration of 3.2  $\mu\text{m}$  which is smaller than the previously reported values (Viceconti et al., 2000).

In the last few years, a large amount of devices and protocols have been developed to predict the primary stability of hip stems (Harris et al., 1991; Monti et al., 1999). These methods have been developed to pre-clinically validate new prosthetic designs. In this context, however, we considered more adequate to use as reference measurements those obtained from an intra-operative device for the assessment of the primary stability (Cristofolini et al., 2006; Varini et al., 2004). In-vitro measurements taken with the Intra-operative Stability Assessment Console (ISAC) (Fig. 3) were used as reference to validate the predictions obtained from the patient-specific FE models. The device mainly consists of two transducers with high accuracy, a torsional load cell and a RVDT angular sensor measuring, respectively, the torque applied and the stem-bone rotation. All the components are rigidly connected to minimize the effects of non-torsional load components. A handle, hosting all electronics, allows the surgeon to apply the torque whilst a series of leads gives information on the entity of the torque applied and on the level of implant stability. Tangential micromotion is measured at the calcar level.

To this purpose, the boundary conditions of the experimental set-up were replicated into the model. A maximum internal rotation of 11.4 Nm was applied to the proximal part of the hip stem and data recorded every 0.5 Nm (22 sub-steps). The distal-most femoral diaphysis was constrained (Fig. 4). Due to limitations of the original software control in the ISAC System at the time when the measurements were carried out, the device started to control for torque above 1.21 Nm. Thus experimental data acquisition was not available for the first fraction of the applied torque.

The procedure used to compute the bone–implant relative micromotion is described elsewhere (Pancanti et al., 2003). A monitoring element was selected to carry out the comparison at the same location where the micromotion sensor was located in the experiment set-up, e.g., the calcar level.

Two indicators were selected to judge the quality of the model: the root mean square (RMS) error and the peak error of predicted micromotion with respect to experimental measurements. The slope of the curves, opportunely partitioned, was also compared. Additionally, non-linear behaviour of experimental micromotion over the applied torque was investigated. To this purpose, two additional cadaver femur specimens (lab codes #82, #993) were tested to state the generality of this observed non-linearity. Since the experimental curve presented, within a range of torque values, a marked non-linearity, the slope of the torque–micromotion curve between the measured and the predicted values was compared not only globally but also over the four spans that go from 0–1.2, 1.2–2, 2–7.6 and 7.6–11.4 Nm.

### 3. Results

At an applied torque of 11.4 Nm the ISAC System measured 171  $\mu\text{m}$  and the FE model predicted 150  $\mu\text{m}$ .

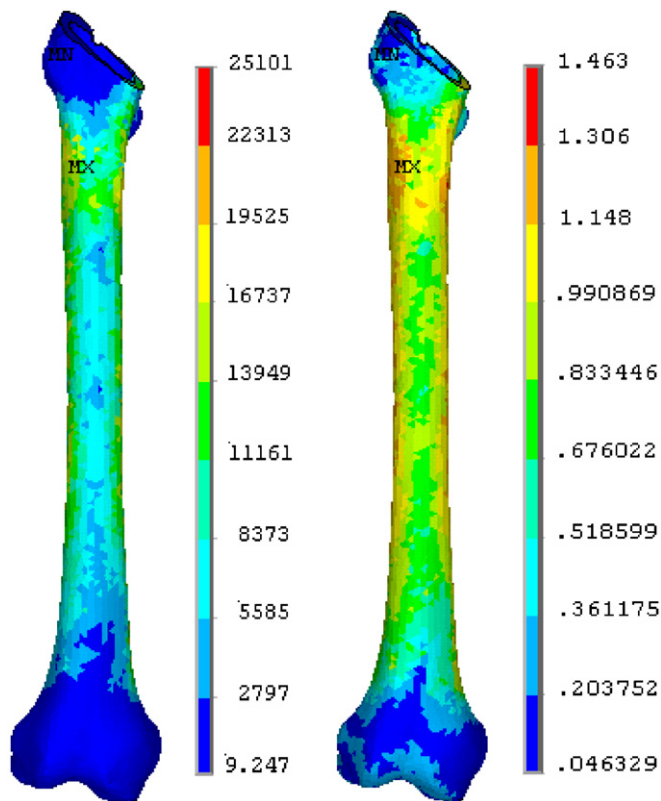


Fig. 2. Distribution of the mapped material properties on the finite-element model of the femur used in the present study: modulus of elasticity (MPa) (left) and mineral density (g/cm<sup>3</sup>) (right).



Fig. 4. Boundary conditions applied on the finite-element model of the femur. The light area is the constrained region. The arrow represents the internal rotation imposed to the stem of the prosthesis.

When compared over the entire loading range 0–11.4 Nm, the model predicted the sliding micromotion measured experimentally with an average (RMS) error of 12  $\mu\text{m}$  and a peak error of 21  $\mu\text{m}$  (Fig. 5).

The torque–micromotion curve predicted by the model was linear, with only a minimal non-linearity in the predicted micromotion between 9 and 10 Nm. Conversely, the experimental curve showed a marked non-linear relationship between torque and micromotion in the range 1–7 Nm and a linear relationship for higher values of torque. This non-linearity was not incidental; the same non-linear behaviour was observed in the other two specimens analysed (Fig. 6).

There was a good agreement between the slope of the experimental and the numerical curve in the two extreme regions (errors of 10% and 12%, respectively, in the first and last portions, Table 1).

Conversely, the intermediate region of the curves showed a significant discrepancy of the slope. However,

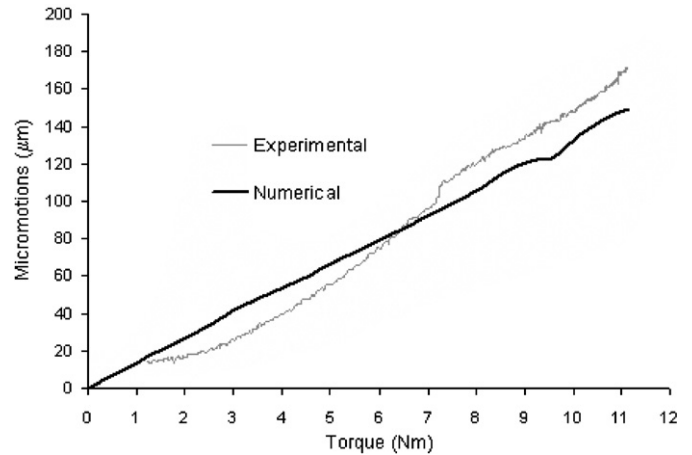


Fig. 5. The experimental micromotions compared to those predicted by the numerical finite element model over the entire range of the applied torque 0–11.4 Nm.

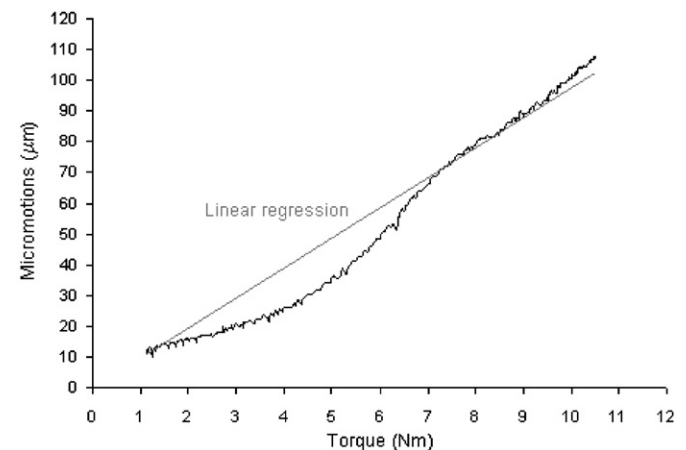
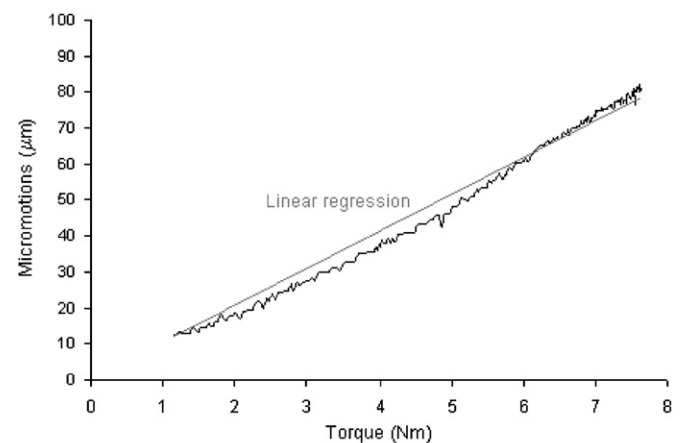


Fig. 6. The experimental micromotions over the applied torque for the other two femurs tested (specimen lab code #82, top, and #993 at the bottom) here used to state the generality of the non-linearity observed. The comparison with the reported slope of the linear regression led to better understand the magnitude of the non-linearity.

the overall difference between the slope of the linear regression of the experimental data and the FE predictions was less than 9%.

Table 1  
Slope of the experimental and numerical curves for the four analysed spans

Range of torque (Nm)	Slope ( $\mu\text{m}/\text{Nm}$ )		
	Experimental	Numerical	% error
0.0–1.2	13.4	12	10
1.2–2.0	4.6	11.8	157
2.0–7.6	18.5	13	30
7.6–11.4	15.7	13.8	12

The relative percentage error is also shown.

#### 4. Discussion and conclusion

The present work was aimed to develop patient-specific FE models of the proximal femur implanted with a cementless anatomical stem and to verify the accuracy with which these models predict the bone–implant relative micromotion. For this purpose, the FE model of a cadaver femur, implanted with an anatomic cementless hip stem (AncaFit), was developed, deriving the anatomy and the material properties from the CT scan of the patient's hip region. The implant position inside the femur was derived from the pre-operative plan that a skilled surgeon performed using a pre-operative planning CT-based software. The comparison of the micromotion at the calcar level as predicted by the numerical model with experimental measurements over the entire range of the applied load was thus carried out.

Good agreement, both in terms of average and peak value, was observed between predicted versus experimental micromotion. The error on the maximum predicted micromotion was only 12% of peak micromotion measured experimentally. The average error over the entire range of applied torques was only 7% of peak measurement.

Also the model predicted the slope of the torque–micromotion curve very close to that measured experimentally. The small discrepancy observed was ascribable to the non-linearity of the experimental micromotion that was not predicted by the model (that incorporated only linear-elastic materials). To preserve the study from the analysis of a singularity, other two specimens were tested, producing the same pattern of the micromotion over the applied torque.

Direct comparison of the reported results with previous studies from the literature is difficult since, to the authors' knowledge, this is the first attempt to predict the relative bone–implant micromotion by means of FE models without considering an average patient. Additionally, the applied boundary conditions aimed to replicate the specific experimental set-up of the ISAC System were not previously simulated.

The errors found for the predicted micromotion are comparable to those reported in studies with synthetic

femurs and clearly acceptable for most applications (Viceconti et al., 2000).

The micromotion measurements are taken on a physical specimen, in which the stem position with respect to the bone may differ by some millimetres from the one the surgeon planned using the Hip-Op software, and that was modelled in the FE model. In addition, the stem in reality is press-fitted into the reamed canal, a condition that is not considered in the numerical simulation. With respect to the stem position, we re-created the FE model defining the stem position this time from a post-implant CT scan, and found a difference of only 20  $\mu\text{m}$  between the two models, although the stem position differed by more than a millimetre. This suggests that while there is a sensitivity of the predicted stability over the real stem position achieved during surgery, the planned position is already a sufficiently accurate estimate to evaluate the primary stability. With respect to the press-fit, a previous validation study showed that the main effect of press-fit is to regularise the contact interface, and if this is assumed in ideal conditions in the model, the mechanical effect of press-fit can be neglected while retaining a very good level of accuracy (Viceconti et al., 2000).

A torsional load, such as that applied by the ISAC set-up on the hip stem, and replicated into the FE model, has been found to be the most critical for the primary stability in terms of induced micromotion in a number of experimental and numerical studies (Callaghan et al., 1992; Davy et al., 1988; Gustilo et al., 1989; Harman et al., 1995; Harris et al., 1991; Ishiguro et al., 1997; Kotzar et al., 1991; Maloney et al., 1989; Martens et al., 1980; Mjoberg et al., 1984; Nistor et al., 1991; Nunn et al., 1989; Philips et al., 1991; Schneider et al., 1989b; Sugiyama et al., 1989). From these, in vitro tests performed to measure the primary stability of cementless prostheses have shown that the highest values of micromotion at the bone–stem interface arise when torsional moment, in the range of 15–29 Nm, around the femur axis prevails (Bergmann et al., 1995). A smaller value of torque is applied to the ISAC device, as well as to the FE model, to account for the fact that patients apply reduced loads in the immediate post-operative period (Monti et al., 1999).

The main limit of the present study is that only one bone was tested. Nevertheless, as previously mentioned, to the knowledge of the authors, any previous study reports a validation of the relative bone–implant micromotion predictions of a FE model against a controlled experiment in vitro. In this study or in previous related studies conducted by our group we explored the sensitivity of the prediction accuracy to almost all factors related to the surgeon, to the patient, or to the modelling methods, always finding that the results, at least for this prosthetic model, are only mildly sensitive to these factors; because of this we tend to conclude that the present validation should stand true even if it is obtained on a single specimen.

A further limit is the assumption of the bone material as perfectly elastic. This simplified constitutive equation

prevents the model from replicating the post-elastic behaviour that is likely to occur. While the inclusion of an elasto-plastic material model would be relatively simple, to date the literature is still controversial on the definition of the yield and the ultimate strength values for both the cortical and the cancellous bone (Keaveny 2001; Ostrowska and Scigala, 2005). This is probably why also in most other numerical studies bone is assumed to be perfectly elastic (El' Sheikh et al., 2003; Senapati and Pal, 2002; Simões and Marques, 2005; Viceconti et al., 2000, 2001, 2004a, 2006).

Even with these limitations the present study confirms that it is possible to create a patient-specific FE model using a pre-operative CT scan and a CT-based pre-operative planning of the stem size and position, which can predict the primary stability of a cementless stem with an accuracy sufficient to draw clinically relevant conclusion. It is thus confirmed that this type of model can be used as a secondary reference for the validation of less accurate predictive models able to provide a gross estimate of primary stability interactively during pre-operative planning.

### Acknowledgements

The authors would like to thank Mauro Ansaloni, Marco Vandi and Alberto Pancanti for the support during this study.

### References

- Bergmann, G., Graichen, F., Rohlmann, A., 1995. Is staircase walking a risk for the fixation of hip implants? *Journal of Biomechanics* 28, 535–553.
- Bernakiewicz, M., Viceconti, M., 2002. The role of parameter identification in finite element contact analyses with reference to orthopaedic biomechanics applications. *Journal of Biomechanics* 35, 61–67.
- Burke, D.W., O'Connor, D.O., Zalenski, E.B., Jasty, M., Harris, W.H., 1991. Micromotion of cemented and uncemented femoral components. *Journal of Bone and Joint Surgery* 73B, 33–37.
- Callaghan, J.J., Fulghum, C.S., Glisson, R.R., Stranne, S.K., 1992. The effect of femoral stem geometry on interface motion in uncemented porous-coated total hip prostheses: comparison of straight-stem and curved-stem designs. *Journal of Bone and Joint Surgery—American Volume* 62, 839–848.
- Cristofolini, L., Varini, E., Pelgreffi, I., Cappello, A., Toni, A., 2006. Device to measure intra-operatively the primary stability of cementless hip stem. *Medical Engineering & Physics* 28, 475–482.
- Dammak, M., Shirazi-Adl, A., Zukor, D.J., 1997. Analysis of cementless implants using interface nonlinear friction-experimental and finite element studies. *Journal of Biomechanics* 30, 121–129.
- Davy, D.T., Kotzar, G.M., Brown, R.H., Heiple, K.G., Goldberg, V.M., Heiple, K.G.J., Berilla, J., Burstein, A.H., 1988. Telemetric force measurements across the hip after total arthroplasty. *Journal of Bone and Joint Surgery* 70 (A), 45–50.
- El' Sheikh, H.F., MacDonald, B.J., Hashmi, M.S.J., 2003. Finite element simulation of the hip joint during stumbling: a comparison between static and dynamic loading. *Journal of Materials Processing Technology* 143–144, 249–255.
- Gustilo, R.B., Bechtold, J.E., Giacchetto, J., Kyle, R.F., 1989. Rationale experience and results of long-stem femoral prosthesis. *Clinical Orthopaedics and Related Research* 249, 159–168.
- Harman, M.K., Toni, A., Cristofolini, L., Viceconti, M., 1995. Initial stability of uncemented hip stems: an in vitro protocol to measure torsional interface motion. *Medical Engineering Physics* 17, 163–171.
- Harris, W.H., Mulroy Jr., R.D., Maloney, W.J., Burke, D.W., Chandler, H.P., Zalenski, E.B., 1991. Intraoperative measurement of rotational stability of femoral components of total hip arthroplasty. *Clinical Orthopaedics and Related Research* 266, 119–126.
- Hefzy, M.S., Singh, S.P., 1997. Comparison between two techniques for modelling interface conditions in a porous coated hip endoprosthesis. *Medical Engineering and Physics* 19, 50–62.
- Ishiguro, N., Kojima, T., Ito, T., Saga, S., Anma, H., Kurokouchi, K., Iwashori, Y., Iwase, T., Iwata, H., 1997. Macrophage activation and migration in interface tissue around loosening total hip arthroplasty components. *Journal of Biomedical Materials Research* 35, 339–406.
- Kalender, W.A., 1992. A phantom for standardisation and quality control in spinal bone mineral measurement by QCT and DXA: design considerations and specifications. *Medical Physics* 19, 583–586.
- Keller, T.S., 1994. Predicting the compressive mechanical behaviour of bone. *Journal of Biomechanics* 27 (9), 1159–1168.
- Keaveny, T.M., 2001. Strength of trabecular bone. In: Cowin, S.C. (Ed.), *Bone Mechanics Handbook*, second ed. CRC Press, Boca Raton, FL, pp. 16–25.
- Kotzar, G.M., Davy, D.T., Goldberg, V.M., Heiple, K.G., Berilla, J., Heiple, K.G.J., Brown, R.H., Burstein, A.H., 1991. Telemeterized in vivo hip joint force data: a report on two patients after total hip surgery. *Journal of Orthopaedics Research* 9, 621–633.
- Lattanzi, R., Viceconti, M., Zannoni, C., Quadrani, P., Toni, A., 2002. Hip-Op: an innovative software to plan total hip replacement surgery. *Medical Informatics and the Internet in Medicine* 27 (2), 71–83.
- Maloney, W.J., Jasty, M., Burke, D.W., O'Connor, D.O., Zalenski, E.B., Bragdon, C., Harris, W.H., 1989. Biomechanical and histologic investigation of cemented total hip arthroplasties. A study of autopsy-retrieved femurs after in vivo cycling. *Clinical Orthopaedics and Related Research* 249, 129–140.
- Manes, E., Arancione, V., Andreoli, E., Celli, V., Erasmo, R., 1996. Incidenza delle revisioni dopo 20 anni. *Atti II Convegno Internazionale "Attualità e prospettive nella protesi d'anca-i reimpianti"*. Maggio, Roma, pp. 16–17.
- Mann, K., Bartel, D., Wright, T., Burstein, A., 1995. Coulomb frictional interfaces in modeling cemented total hip replacements: a more realistic model. *Journal of Biomechanics* 28, 1067–1078.
- Martens, M., Van Audekercke, R., De meester, P., Mulier, J.C., 1980. The mechanical characteristics of the long bones of the lower extremity in torsional loading. *Journal of Biomechanics* 13, 667–676.
- Mjoberg, B., Hansson, L.I., Selvik, G., 1984. Instability of total hip prosthesis at rotational stress: a roentgen stereophotogrammetric study. *Acta Orthopaedica Scandinavica* 55, 504–506.
- Monti, L., Cristofolini, L., Viceconti, M., 1999. Methods for quantitative analysis of the primary stability in uncemented hip prostheses. *Artificial Organs* 23 (9), 851–859.
- Nistor, L., Blaha, J.D., Kjellstrom, U., Selvik, G., 1991. In vivo measurements of relative motion between an uncemented femoral hip component and the femur by roentgen stereophotogrammetric analysis. *Clinical Orthopaedics and Related Research* 269, 220–227.
- Nunn, D., Freeman, M.A., Tanner, K.E., Bonfield, W., 1989. Torsional stability of the femoral component of hip arthroplasty: response to an anteriorly applied load. *Journal of Bone and Joint Surgery* 71, 452–455.
- Ostrowska, A., Scigala, K., 2005. The influence of in vitro factors on the bone properties values determination. In: *Proceeding of the Fourth Annual Meeting of Youth Symposium on Experimental Solid Mechanics*, Castrocaro Terme, Italy, pp. 93–94.
- Pancanti, A., Bernakiewicz, M., Viceconti, M., 2003. The primary stability of cementless stem varies between subjects as much as between activities. *Journal of Biomechanics* 36, 777–785.
- Philips, T.W., Messieh, S.S., McDonald, P.D., 1990. Femoral stem fixation in hip replacement. A biomechanical comparison of

- cementless and cemented prostheses. *Journal of Bone and Joint Surgery* 72 (3), 431–434.
- Phillips, T.W., Nguyen, L.T., Munro, S.D., 1991. Loosening of cementless femoral stems: a biomechanical analysis of immediate fixation with loading vertical, femur horizontal. *Journal of Biomechanics* 24, 37–48.
- Pilliar, R.M., Lee, J.M., Maniopoulos, C., 1986. Observations on the effect of movement on bone ingrowth into porous-surfaced implants. *Clinical Orthopaedics and Related Research* 208, 108–113.
- Schneider, E., Eulenberger, J., Steiner, W., Wyder, D., Friedman, R.J., Perren, S.M., 1989a. Experimental method for the in vitro testing of the initial stability of cementless hip prostheses. *Journal of Biomechanics* 22 (6–7), 735–744.
- Schneider, E., Kinast, C., Eulenberger, J., Wyder, D., Eskilsson, G., Perren, S.M., 1989b. A comparative study of the initial stability of cementless hip prosthesis. *Clinical Orthopaedics and Related Research* 248, 200–210.
- Senapati, S.K., Pal, S., 2002. UHMWPE–alumina ceramic composite, an improved prosthesis materials for an artificial cemented hip joint. *Trends in Biomaterial Artificial Organs* 16 (1), 5–7.
- Simões, J.A., Marques, A.T., 2005. Design of a composite hip femoral prosthesis. *Materials and Design* 26, 391–401.
- Søballe, K., Hansen, E.S., Brockstedt-Rasmussen, H., Bunger, C., 1993. Hydroxyapatite coating converts fibrous tissue to bone around loaded implants. *Journal of Bone and Joint Surgery* 75 (2), 270–278.
- Spears, I.R., Pfeleiderer, M., Schneider, E., Hille, E., Morlock, M.M., 2001. The effect of interfacial parameters on cup-bone relative micromotions. A finite element investigation. *Journal of Biomechanics* 34 (1), 113–120.
- Stea, S., Bordini, B., Sudanese, A., Toni, A., 2002. Registration of hip prostheses at the Rizzoli Institute. 11 years' experience. *Acta Orthopaedica Scandinavica Supplement* 73 (305), 40–44(5).
- Sugiyama, H., Whiteside, L.A., Kaiser, A.D., 1989. Examination of rotational fixation of the femoral component in total hip arthroplasty. A mechanical study of micromovement and acoustic emission. *Clinical Orthopaedics and Related Research* 249, 122–128.
- Taddei, F., Viceconti, M., Manfrini, M., Toni, A., 2003. Mechanical strength of a femoral reconstruction in paediatric oncology: a finite element study. *Proceedings of the Institution of Mechanical Engineers Part H—Journal of Engineering in Medicine* 217 (2), 111–119.
- Taddei, F., Pancanti, A., Viceconti, M., 2004. An improved method for the automatic mapping of computed tomography numbers onto finite element models. *Journal of Medical Engineering and Physics* 26, 61–69.
- Taddei, F., Martelli, S., Reggiani, B., Cristofolini, L., Viceconti, M., 2006. Finite-element modeling of bones from CT data: sensitivity to geometry and material uncertainties. *IEEE Transactions on Biomedical Engineering* 53 (11), 2194–2200.
- Tissakht, M., Eskandari, H., Ahmed, A.M., 1995. Micromotion analysis of the fixation of total knee tibial component. *Computers and Structures* 56, 365–375.
- Varini, E., Cristofolini, L., Cappello, A., Toni, A., 2004. Primary stability of cementless hip stems: intraoperatively recorded micromotions. In: *Proceedings of the 14th Annual Meeting of the European Society of Biomechanics, s' Hertogenbosch, the Netherlands, July 4–7, Poster #229*.
- Various authors, 2003. Annual Report 2003. The Swedish National Hip Arthroplasty Register.
- Viceconti, M., Zannoni, C., Testi, D., Cappello, A., 1999. A new method for the automatic mesh generation of bone segments from CT data. *Journal of Medical Engineering Technology* 23, 77–81.
- Viceconti, M., Muccini, R., Bernakiewicz, M., Baleani, M., Cristofolini, L., 2000. Large-sliding contact elements accurately predict levels of bone–implant micromotion relevant to osseointegration. *Journal of Biomechanics* 33, 1611–1618.
- Viceconti, M., Cristofolini, L., Baleani, M., Toni, A., 2001. Pre-clinical validation of a new partially cemented femoral prosthesis by synergetic use of numerical and experimental methods. *Journal of Biomechanics* 34, 723–731.
- Viceconti, M., Lattanzi, R., Antonietti, B., Paderni, S., Olmi, R., Sudanese, A., Toni, A., 2003. CT-based surgical planning software improves the accuracy of total hip replacement preoperative planning. *Medical Engineering and Physics* 25 (5), 371–377.
- Viceconti, M., Davinelli, M., Taddei, F., Cappello, A., 2004a. Automatic generation of accurate subject-specific bone finite element models to be used in clinical studies. *Journal of Biomechanics* 37, 1597–1605.
- Viceconti, M., Chiarini, A., Testi, D., Taddei, F., Bordini, B., Traina, F., Toni, A., 2004b. New aspects and approaches in pre-operative planning of hip reconstruction: a computer simulation. *Langenbecks Archives of Surgery* 389 (5), 400–404.
- Viceconti, M., Brusi, G., Pancanti, A., Cristofolini, L., 2006. Primary stability of an anatomical cementless hip stem: a statistical analysis. *Journal of Biomechanics* 39 (7), 1169–1179.
- Zienkiewicz, O.C., Zhu, J.Z., 1987. A simple error estimator and adaptive procedure for practical engineering analysis. *International Journal for Numerical Methods in Engineering* 24, 337–357.